Title

A screen for Listeria monocytogenes hemolytic activity mutants reveals HPF, a homolog of Hibernation Promoting Factor, which is essential for ribosomal hibernation and important for competitive fitness in vitro and in vivo.

Author

Kline, Benjamin Craft

Publication Date

2012

Peer reviewed|Thesis/dissertation

A screen for *Listeria monocytogenes* hemolytic activity mutants reveals HPF, a homolog of Hibernation Promoting Factor, which is essential for ribosomal hibernation and important for competitive fitness *in vitro* and *in vivo*

by

Benjamin Craft Kline

A dissertation submitted in partial satisfaction of the

requirements for the degree of

Doctor of Philosophy

in

Molecular and Cell Biology

in the

Graduate Division

of the

University of California, Berkeley

Committee in charge:

Professor Daniel A. Portnoy, Chair
Professor Arash Komeili
Professor Hiroshi Nikaido
Professor David Zusman

Spring 2012

Abstract

A screen for *Listeria monocytogenes* hemolytic activity mutants reveals HPF, a homolog of Hibernation Promoting Factor, which is essential for ribosomal hibernation and important for competitive fitness *in vitro* and *in vivo*.

by

Benjamin Craft Kline

Doctor of Philosophy in Molecular and Cell Biology

University of California, Berkeley

Professor Daniel A. Portnoy, Chair

Listeria monocytogenes is an opportunistic, potentially deadly, foodborne pathogen of humans and other vertebrates. Resistance to stressful conditions such as low pH, high salt, and refrigeration temperatures makes *L. monocytogenes* ideally suited to thrive on food sources, promoting transmission. A set of conserved virulence factors promotes establishment of infection once *L. monocytogenes* enters the host. In this work, we sought to better understand both the pathogenesis and the biology of *L. monocytogenes* by investigating factors involved both in virulence and in tolerance to sub-optimal growth conditions.

Listeriolysin O (LLO) is an essential virulence factor that allows *L. monocytogenes* to escape from the host phagosome into the cytosol. LLO is regulated on multiple levels to compartmentalize its function and prevent loss of virulence caused by host cell toxicity. To gain new information on the various mechanisms of LLO regulation, we performed a transposon mutagenesis screen for *L. monocytogenes* mutants in LLO production and activity. This screen identified PrsA2, a peptidyl-prolyl isomerase that we showed was important for *L. monocytogenes* virulence based on its contribution to re-folding of virulence factors following secretion. PrsA2 was shown to be important for folding and activity of LLO, and its deletion reduced bacterial virulence by 10^5-fold in a mouse model of infection. This work was published in the *Journal of Bacteriology*.

A *L. monocytogenes* homolog of Hibernation Promoting Factor (HPF) was also isolated from this hemolytic activity screen. Ribosomal hibernation is characterized by dimerization of two 70S ribosomes into a 100S complex. These 100S dimers are translationally inactive and important for survival during post-exponential growth in certain bacteria. HPF is conserved in long and short forms, which are present in different sets of bacteria and appear to be functionally distinct. Long HPF, which is present in *L. monocytogenes*, is also conserved in *S. aureus*, where it is necessary for 100S formation. In this work, we report the existence of a functional HPF homolog that is necessary for formation of 100S ribosomes in *L. monocytogenes*. HPF was observed to bind 100S ribosomes based on its co-migration through sucrose density gradients in the 100S fractions. We observed that the *hpf* transcript was upregulated by glucose

starvation in stationary phase media, and that several σ^B-inducing stresses also stimulated *hpf* expression. Bacteria lacking HPF showed dramatically reduced survival in stationary phase competitive co-culture with wild-type bacteria. Finally, HPF-deficient bacteria displayed a > 300-fold survival defect in the mesenteric lymph nodes of orally-infected mice. We conclude that the *L. monocytogenes* HPF is functional for formation of 100S ribosomes and is critical for optimal survival in competitive environments, both *in vitro* and *in vivo*.

If living things were vehicles, humans would be Greyhound buses.
Bacteria would be Ferraris.

-P. Lu

TABLE OF CONTENTS

LIST OF FIGURES

Chapter 1: Introduction

Chapter 2: Development of a *mariner*-based transposon for *Listeria monocytogenes*, and a blood plate screen for factors involved in regulation of the critical virulence factor, LLO

Chapter 3: Identification of a *Listeria* homolog of the ribosomal Hibernation Promoting Factor (HPF) and initial characterization of ribosomal hibernation in *Listeria monocytogenes*

LIST OF TABLES

ACKNOWLEDGEMENTS

This work would not have been possible without the generous contributions of many people around me. I am indebted to my fellow scientists, family, and friends for the important roles that they have all played during my time as a graduate student.

To my mentor, Dan Portnoy, thank you for your support and mentorship throughout my time in the lab. Your earnest scientific passion and curiosity are infectious, and the welcoming, playful environment that you have fostered in the lab has made it a joy to come in to work every day.

To my friend, bay-mate, and coworker, Jason Zemansky, your importance to this work cannot be overstated. Without your diligent work in developing a new transposon delivery vector for *L. monocytogenes*, the screen that laid the foundation for the last several years of work could not have been performed. Your company made the long hours screening plates and analyzing mutants downright enjoyable.

To Josh, JD, Nicole, Jason, Thomas, Susy, Matt, and all the other amazing people who have worked beside me in the Portnoy Lab, thank you for sharing your knowledge and friendship with me for all these years. Your personalities have made the lab the welcoming, fun-loving place that it has been for my entire time here. Let's make sure that Beer Ball in the Chiron room becomes an enduring tradition.

To all the members of the Portnoy lab who selflessly shared their expertise in mouse experiments: Nicole Meyer-Morse, JD Sauer, Chelsea Witte, Thomas Burke, and Aaron Whiteley, thank you. It's lonely down there in the NAF by yourself, especially when you don't know what you're doing.

To Andy Jackson and Sergio Covarrubias, thank you for teaching me my way around a sucrose gradient and an ISCO fractionator. My work on HPF would not have been possible without your help.

To Rich Calendar, thank you for your willing assistance with all things phage-related. Also, thank you for Santa Lucia and the many days of glögg that always followed.

To my undergraduate research assistant, Will Tang, thank you for all the help you've given me with my experiments over the past year and a half. I've enjoyed seeing you mature as a scientist and as a person during your time here.

To my Thesis Committee, Arash Komeili, Hiroshi Nikaido, and David Zusman, thank you for your advice and scientific insight over the past years. I took a winding path, but you helped to keep me on track.

To Mike (with the tattoos), Adam, and Brock, thank you for all the Thursday lunches, ballgames, and dinners at El Agavero. My only regret is that we didn't start hanging out sooner.

To Channing and its many progeny, Nick, Jaq, Kaspar, Leif, Megan, Phoebe, and all the rest, thank you for being such fantastic friends. The late night discussions ranging from physics to philosophy to powerful techniques have made my time in Berkeley an absolute joy.

To Terry, I can never thank you enough for your unwavering love, friendship, and support during the time we've spent together. You selflessly and single-handedly helped me to keep my sanity during long hours spent in the lab and even longer hours spent writing during the last and most difficult part of graduate school. I couldn't have done it without you.

To my grandparents, Dick and Lucille, thank you for always asking when I'm coming home next. I can never get back as much as I'd like, but it's wonderful to know you'll both be eagerly waiting to greet me when I get there.

To my sister, Holly, thank you for fearlessly blazing the trail and for being there each and every time I've needed you. You may have followed me to California, but I've been following your lead for the past 29 years.

Last but certainly not least, to my father and mother, Ken and Becky, thank you so much for raising me to think with an open mind and to live every day with curiosity. I wouldn't be where I am today if I hadn't had your love and support at every step along the way.

Chapter 1

Introduction

Listeria monocytogenes Background and Significance

Listeria monocytogenes is a Gram-positive, low G+C content, facultative intracellular pathogen capable of infecting a variety of vertebrate hosts ranging from humans to birds. It causes a localized or systemic infection referred to as listeriosis (Vazquez-Boland, Kuhn et al. 2001). *L. monocytogenes* is ubiquitous in the environment and leads a saprophytic lifestyle, subsisting primarily on decaying organic matter. It is abundant in soil, water, and silage. Passage to the pathogenic phase of its life cycle occurs when a host ingests *L. monocytogenes*-contaminated food. A variety of characteristics make *L. monocytogenes* a particularly efficient foodborne pathogen, including high tolerance to salt and low pH and the exceptional ability to grow at refrigeration temperatures (Lou Y 1999; Vazquez-Boland, Kuhn et al. 2001).

Although *L. monocytogenes* is well adapted to survive in the environment and contaminate food sources, it is primarily an opportunistic pathogen of humans (Vazquez-Boland, Kuhn et al. 2001). The majority of infections occur in individuals who are elderly, pregnant, or immunocompromised, manifesting most commonly as central nervous system infection and meningitis. As a result, the number of reported cases of listeriosis is relatively low compared to other prevalent foodborne illnesses. Once *L. monocytogenes* becomes established in a human host, however, it produces one of the deadliest bacterial infections, claiming the lives of between 20 and 30 percent of infected individuals even with antibiotic treatment (McLauchlin 1990; McLauchlin 1990; Vazquez-Boland, Kuhn et al. 2001). A recent multi-state outbreak of listeriosis in the United States during September and October of 2011, originating in contaminated cantaloupe, was responsible for at least 30 deaths (2011). Thus, despite causing relatively few cases of invasive disease, *L. monocytogenes* is an important human pathogen whose biology must be thoroughly understood.

In addition to its public health relevance as the causative agent of listeriosis, *L. monocytogenes* has also served as one of the most important model intracellular bacterial pathogens (Vazquez-Boland, Kuhn et al. 2001). It shares pathogenic mechanisms and modes of host immune interaction with other intracellular pathogens of serious concern, including *Mycobacterium tuberculosis*, *Salmonella* Typhimurium, and *Legionella pneumophila*. Study of *L. monocytogenes* has been responsible for several important advances in our understanding of the host-pathogen interaction, including the ineffectiveness of antibody in protection against intracellular pathogens and the importance of the T cell – macrophage interaction in the development of cell-mediated immunity (Mackaness 1962; Miki and Mackaness 1964; Mackaness 1969; North 1970; North 1978).

L. monocytogenes pathogenesis

L. monocytogenes infection normally begins when an animal ingests food contaminated with large numbers of bacteria (Farber and Peterkin 1991; Pinner, Schuchat et al. 1992). Passage through the harsh environment of the stomach eliminates a substantial number of bacteria (Wonderling and Bayles 2004), and invasion of the intestinal epithelium presents an even larger bottleneck (Melton-Witt, Rafelski et al. 2012). *L. monocytogenes* can either be taken up by professionally phagocytic M-cells that sample the contents of the intestines, or induce its own uptake by nonprofessional phagocytes. The bacterium can then escape from the phagosome into the cytosol, spread from cell to cell and pass to the mesenteric lymph nodes (MLNs), blood, and deep tissues (Reviewed in (Vazquez-Boland, Kuhn et al. 2001)). Below is a

brief summary of the infectious life cycle on a single-cell level, and a discussion of the virulence factors that are critically important to the success of *L. monocytogenes* as an intracellular pathogen.

Entry into a host cell can occur in one of two ways. *L. monocytogenes* can be taken up passively by professional phagocytes, or it can induce its own uptake using invasin proteins known as internalins (Vazquez-Boland, Kuhn et al. 2001). Internalin-mediated uptake is particularly important for invasion of nonprofessional phagocytes (Gaillard, Berche et al. 1991). Following uptake, *L. monocytogenes* finds itself enclosed in a phagosomal compartment (Fig. 1-1a) (Tilney and Portnoy 1989). It uses the cytolysin Listeriolysin O (LLO, encoded by *hly*) and two phospholipases C to escape from the phagosome (Camilli, Tilney et al. 1993; Schnupf and Portnoy 2007), avoiding the hostile environment of the maturing phagosome and phagolysosome. Escape has the added benefit of delivering *L. monocytogenes* to the nutrient-rich environment of the cytosol, in which it can grow rapidly with a doubling time of ≤ 60 minutes (Fig. 1-1b) (Portnoy, Jacks et al. 1988). Upon entry into the cytosol, *L. monocytogenes* produces and secretes ActA, a bacterial-membrane-tethered protein that recruits host actin nucleation machinery. Actin polymerization generates force that enables rapid motility of the bacterium throughout the cytosol, and produces the characteristic actin "comet tails" for which *L. monocytogenes* is known (Fig. 1-1c) (Domann, Wehland et al. 1992; Kocks, Gouin et al. 1992). When a motile *L. monocytogenes* cell encounters the host cytoplasmic membrane, the force of actin polymerization can push it into a filopodium-like membrane protrusion known as a listeriopod (Fig. 1-1d) (Gedde, Higgins et al. 2000). This protrusion can then be pinched off by the cytoplasmic membrane of an immediately neighboring cell, enclosing the bacterium in a double-membraned "spreading" vacuole within the neighboring cell (Fig. 1-1e). Escape from the spreading vacuole is again achieved by the activity of LLO and the phospholipases C, delivering the bacterium back to the host cytosol and beginning the cycle anew (Vazquez-Boland, Kocks et al. 1992).

The ability of *L. monocytogenes* to invade host cells and spread from one cell to the next without exposing itself to the extracellular milieu is critically important for two reasons. First, as mentioned above, the cytoplasm provides a nutrient-rich niche in which *L. monocytogenes* can replicate rapidly (Portnoy, Jacks et al. 1988). Second, taking up residence within host cells protects bacteria from recognition by immune sensing mechanisms including complement, antibodies, and neutrophils, which play central roles in the detection and elimination of extracellular pathogens (Harty, Tvinnereim et al. 2000; Glomski, Decatur et al. 2003). For these key reasons, preservation of the intracellular niche is one of the single most important factors in maintenance of *L. monocytogenes* virulence. However, the same virulence factors that allow *L. monocytogenes* to escape from the phagosome when properly regulated and expressed can endanger the intracellular niche if regulated or expressed inappropriately.

Listeriolysin O and the Cholesterol-Dependent Cytolysins

Of the seven currently recognized *Listeria* species, only *L. monocytogenes* and *L. ivanovii* are considered pathogenic (Vazquez-Boland, Kuhn et al. 2001). One of the defining characteristics of pathogenic versus nonpathogenic *Listeria* is the presence of a hemolysin critical for the pathogenic life cycle (Skalka, Smola et al. 1982). Members of this large, highly conserved (40-70% amino acid similarity) family of cholesterol-dependent cytolysins (CDCs) are

Figure 1-1

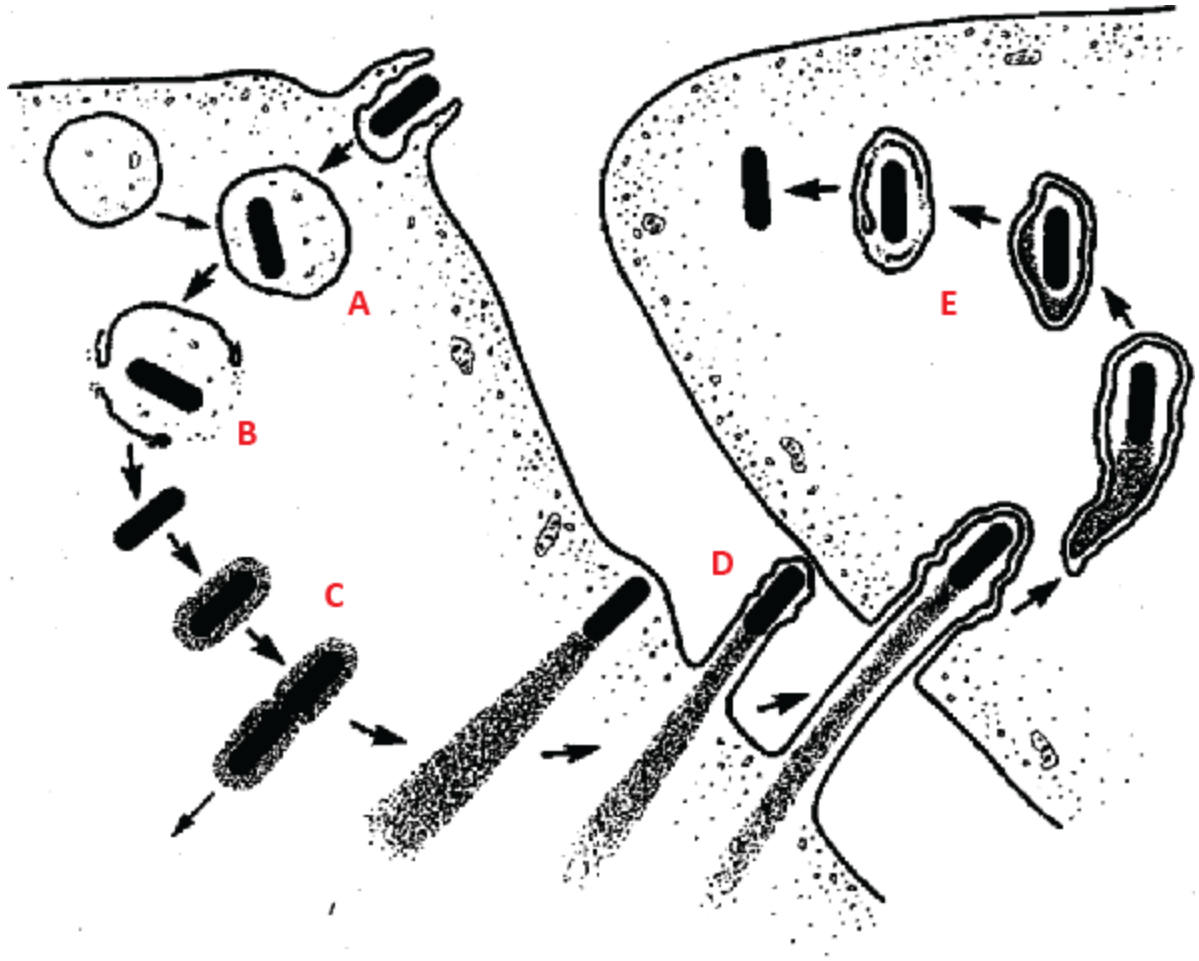

Figure 1-1. *L. monocytogenes* intracellular life cycle

(A) *L. monocytogenes* is trapped in a phagosome upon internalization; (B) LLO and phospholipases facilitate phagosomal escape into the cytosol; (C) Bacteria replicate and recruit host actin polymerization machinery for motility; (D) Actin-based motility forms listeriopods and facilitates cell-to-cell spread; (E) Escape from the double-membraned spreading vacuole is again facilitated by LLO and the phospholipases, and the cycle begins again. Adapted from (Tilney and Portnoy 1989).

present in all pathogenic *Listeria* species and absent in almost all nonpathogenic species (Vazquez-Boland, Kuhn et al. 2001). The *L. monocytogenes* CDC, LLO, is indispensable for escape from the phagosomal compartment into the host cytosol in most cell types (Portnoy, Jacks et al. 1988). This prevents bacterial access to the primary replicative niche within the host. Accordingly, *L. monocytogenes* mutants lacking LLO are avirulent, displaying a 10^5-fold defect in a murine model of listeriosis (Portnoy, Jacks et al. 1988).

Other members of the CDCs are produced by a variety of Gram-positive bacterial pathogens, including *Streptococcus pyogenes* (streptolysin O, SLO), and *Clostridium perfringens* (perfringolysin O, PFO) (Schnupf and Portnoy 2007). All CDCs act in essentially the same way. Binding of soluble monomers to cholesterol-containing membranes is followed by assembly of monomers into circular pre-pore complexes of roughly 35-50 subunits. A concerted insertion motion, which involves a dramatic structural rearrangement within each monomer, leads to formation of a pore 25 to 30 nm in diameter (Tweten 2005). Importantly, substitution of LLO with other CDCs can restore vacuolar escape but is ineffective in restoring virulence to Δ*hly L. monocytogenes* (Jones and Portnoy 1994). The non-interchangeability of LLO with other CDCs indicates that LLO production and activity are regulated differently from the other CDCs, allowing *L. monocytogenes* to compartmentalize pore forming activity and preserve its intracellular niche. A number of *in vitro* studies have revealed that LLO is highly regulated on the levels of transcription, translation, activity, and stability (Schnupf and Portnoy 2007).

Transcription of LLO is regulated primarily by the master virulence regulator PrfA and is sensitive to several factors, including temperature, pH, intracellular growth, and fermentable sugars (Datta and Kothary 1993; Bubert, Sokolovic et al. 1999). Translation is repressed in the host cytosol and during exponential growth in broth, but is activated during confinement in the phagosome (Folio, Chavant et al. 2004; Schnupf, Hofmann et al. 2006). The 5' region of the LLO transcript is particularly important for appropriate translational regulation; both the 5' UTR and the 5' end of the coding sequence contain elements that influence the timing and extent of translation (Shen and Higgins 2005). Strikingly, a silent point mutation (S44S) at the nucleotide level in the 5' coding sequence is capable of abolishing translational repression of LLO in broth and in the host cytosol. Cytosolic overproduction of LLO results in perforation of the host cytoplasmic membrane and host cell cytotoxicity. At the post-translational level, LLO is subject to phosphorylation, ubiquitination, and host proteasome-mediated degradation in the cytosol (Decatur and Portnoy 2000; Schnupf, Portnoy et al. 2006). Activity of LLO also is pH-dependent, and mutation of a single leucine residue (L461) to threonine removes this dependence and results in host cell cytotoxicity (Glomski, Gedde et al. 2002). All of these features are unique to LLO, and are absent from CDCs produced by other bacteria.

Disruption of any of the above mechanisms of LLO regulation has profoundly negative consequences on *L. monocytogenes* virulence. Complete loss of LLO decreases virulence by 10^5-fold, a level which is regarded as complete avirulence (Portnoy, Jacks et al. 1988). Deletion of the 5' UTR produces a 10-fold decrease in virulence (Shen and Higgins 2005). Translation-deregulating mutations in the S44 codon produce a > 10^4-fold virulence defect (Schnupf, Hofmann et al. 2006). The LLO L461T mutant, which has a disrupted pH optimum, confers a 100-fold virulence defect (Glomski, Gedde et al. 2002). LLO has been aptly described as a "double-edged sword" because of the dichotomy between its essentiality for virulence and its profound toxicity to the host cell when improperly regulated; *L. monocytogenes* must escape

from the phagosome in order to replicate and spread, but lysis of the host cytoplasmic membrane and exposure to the extracellular milieu is equally detrimental to bacterial virulence (Schnupf and Portnoy 2007).

The correlation between LLO production, activity, and virulence can be visualized as a bell-shaped curve. The peak of the curve corresponds to the wild-type virulence level associated with optimal LLO activity, while the tails represent the negative virulence consequences of either too little or too much LLO activity (Fig. 1-2). Given the variety of levels on which LLO is known to be regulated and the severe consequences of LLO misregulation, it is reasonable to hypothesize that even more systems of regulation exist that have yet to be appreciated. Even some of the known mechanisms of LLO regulation are not completely understood, so it is safe to say that the topic warrants further study. We have taken on this task using a transposon mutagenesis system newly adapted to *L. monocytogenes*. In the following chapters, we will describe in detail a transposon mutagenesis screen to explore LLO regulation further, and discuss several of the resulting mutants and their roles in *L. monocytogenes* homeostasis and virulence.

Blood plate assay for LLO activity

Production and secretion of LLO *in vitro* during growth in rich media is normally restricted to stationary phase (Schnupf and Portnoy 2007). To make LLO-based assays easier to perform *in vitro*, activated charcoal and glucose-1-phosphate (G1P) may be included in growth media. Activated charcoal has been shown to bind a diffusible autorepressor of PrfA activation (Ermolaeva 2004), while G1P provides a usable carbon source that does not repress PrfA activation like other fermentable carbon sources (Ripio, Brehm et al. 1997). In combination, these two additives are thought to make *in vitro* growth media induce more PrfA gene expression than it otherwise would. With these modifications, the presence and activity of LLO in a population of bacteria can be assayed quickly and easily by plating on LB-G1P-charcoal agar infused with sheep's blood. Secreted LLO perforates and lyses red blood cells within a small area around *L. monocytogenes* colonies (Portnoy, Jacks et al. 1988). The size and translucency of the zone of blood cell lysis around a colony can be used as a proxy for the relative quantity and activity of LLO produced.

PrsA2

The majority of proteins secreted by Gram-positive bacteria like *L. monocytogenes* are thought to traffic through the highly conserved Sec secretion system (Sarvas, Harwood et al. 2004). The heterotrimeric SecYEG channel is narrow enough that secretion substrates must be unfolded for translocation to proceed. As a result, membrane-proximal extracellular foldases are required for proper refolding of some secreted substrates. Several different structural features require these foldases to reform properly on the extracellular side of the plasma membrane. Proper disulfide bond formation is accomplished by the thiol-disulfide oxidoreductase family of proteins, and proper isomerization of prolines is accomplished by a family of peptidyl-prolyl isomerases of which PrsA2 is a member (Sarvas, Harwood et al. 2004).

Like any amino acid, proline can adopt the *cis* or the *trans* configuration due to the partial double-bond character of the peptide bond. The *trans* configuration is energetically favored for most amino acids, and dominates in prevalence in known protein structures by a

Figure 1-2

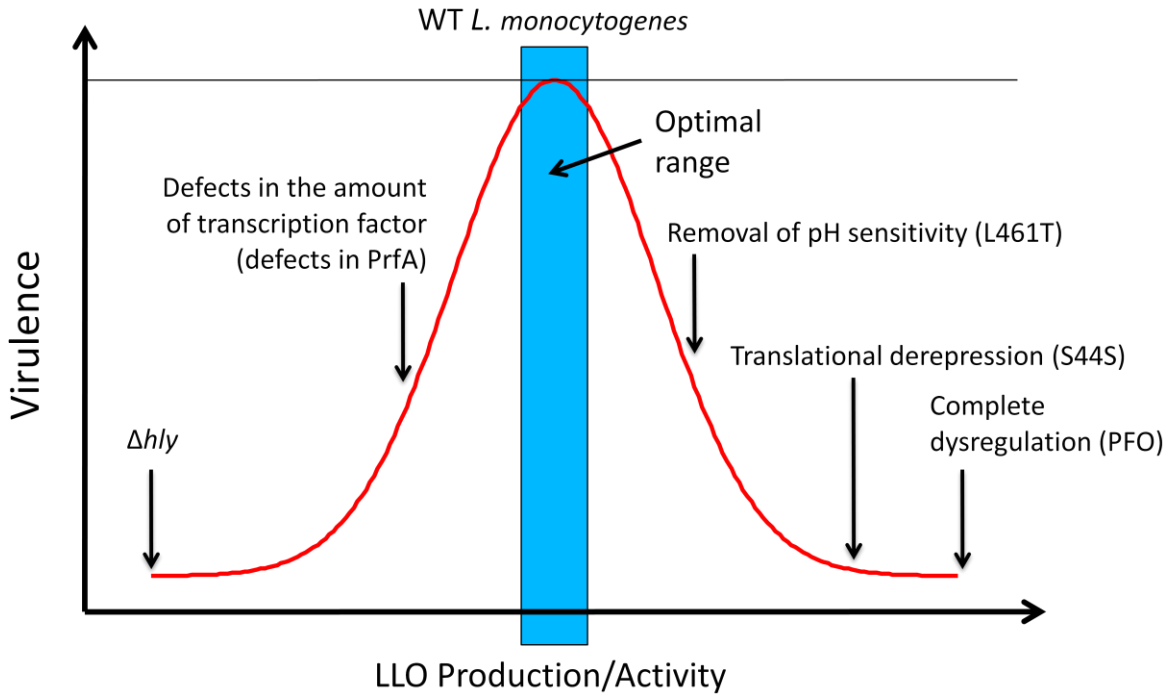

Figure 1-2. Listeria virulence as a function of LLO production and activity

In order to be optimally virulent, L. monocytogenes must properly control production and activity of LLO. WT levels of LLO production and activity can be visualized at the middle of a bell-shaped curve, where virulence is at a maximum. Decreases in LLO quantity or activity rapidly reduce virulence, while a Δ*hly* mutant represents complete avirulence (left side of curve). Increases in LLO quantity or activity for any of a variety of reasons, including loss of pH sensitivity or loss of translational regulation, can have equally detrimental influences on virulence (right side of curve). Complete loss of LLO-specific regulatory mechanisms (PFO, far right) allows for phagosomal escape but results in complete avirulence. Adapted and reproduced with permission from J. Zemansky; originally published in (Zemansky 2009).

ratio of ≥ 100 to 1 (Schmid 2001). Because of the unique cyclic structure of proline, however, its *cis* bonded form is almost energetically equivalent to the *trans* configuration, appearing in proteins at an estimated frequency of roughly seven percent (Schmid, Mayr et al. 1993). Isomerization from *cis* to *trans* is a slow process on the time scale of protein folding (Schmid, Mayr et al. 1993), and improperly isomerized residues may be disruptive to a protein's three-dimensional structure. It is therefore very important to the functional integrity of secreted proteins that proline *cis*/*trans* isomerization be allowed to occur properly (Schmid, Mayr et al. 1993). Because most virulence factors are secreted, extracellular chaperones like those discussed above have the potential to be particularly important for maintenance of virulence in pathogenic bacteria. In the following chapter, we will discuss the *L. monocytogenes* PrsA2 homolog, which we encountered in our screen for hemolytic activity mutants, and explore its influence on *L. monocytogenes* secretion and virulence.

PrpC/PrkC

Another interesting mutant that we encountered in our screen for *L. monocytogenes* hemolytic mutants harbored a transposon insertion in a gene encoding a eukaryotic-like serine/threonine phosphatase homologous to PrpC of *B. subtilis* (Madec, Laszkiewicz et al. 2002). This phosphatase and its predicted cognate kinase, PrkC, have demonstrated a broad range of functions in a variety of bacteria (Gaidenko, Kim et al. 2002; Rajagopal, Clancy et al. 2003; Kang, Abbott et al. 2005; Shah and Dworkin 2010). In some bacteria including *Streptococcus pneumonia*e, the pair appears to play a global regulatory role, influencing transcription of genes with such diverse functions as DNA repair, iron uptake, pyrimidine biosynthesis, and cell wall metabolism (Echenique, Kadioglu et al. 2004; Saskova, Novakova et al. 2007). However, the specific function that has been demonstrated for PrkC in *B. subtilis* is quite intriguing. PrkC, a membrane-bound kinase with extracellular sensory domains, has been shown to induce germination of *B. subtilis* spores upon sensing bacterial cell wall (peptidoglycan) fragments of the specific type that *B. subtilis* itself produces (Shah, Laaberki et al. 2008; Shah and Dworkin 2010). This appears to be an environmental monitoring mechanism that allows the bacterium to sense when conditions are favorable for germination based on the growth of other bacteria. Because *L. monocytogenes* is a non-spore-former, the roles that this kinase and its cognate phosphatase might play are unclear. We were attracted to the hypothesis that detection of peptidoglycan fragments might be a mechanism for *L. monocytogenes* to sense its arrival in the confined environment of the host cell. A set of preliminary experiments involving the phosphatase, PrpC, is described in the addendum to Chapter 2.

Bacterial Responses to Stress

A recent estimate indicates that far more prokaryotes exist on our planet than previously imagined – perhaps 4 to 6×10^{30} in all, or around 10^{20} bacteria or archaea for every human (Whitman, Coleman et al. 1998). One of the reasons that prokaryotes have enjoyed such phenomenal reproductive success is their ability to quickly sense and adapt to diverse environmental conditions. Although a given bacterial species may inhabit only a limited set of environmental niches, it must be able to tolerate sometimes-dramatic swings in temperature, nutrient availability, and a variety of other conditions within those niches. *L. monocytogenes*,

for instance, is a successful foodborne pathogen in part because of its ability to survive and even proliferate at low pH, high salt concentration, and low temperature (Vazquez-Boland, Kuhn et al. 2001).

Another stressful condition regularly encountered by bacteria, particularly in the environment, is the scarcity of essential nutrients. In the laboratory, the stationary phase that follows exponential growth in rich media is the most apparent example of bacterial adaptation to exhaustion of nutrients. Although experiments are often performed using bacteria from the actively growing logarithmic growth phase, nutrient availability in the average environmental niche is likely much lower (Martin and Macleod 1984). When bacteria encounter low-nutrient conditions, they must be able to modify their physiology and lifestyle to accommodate decreased amounts of raw material for construction of their basic macromolecular building blocks. Several systems are known to mediate this response. Most notably, the catabolite repression system is the primary regulator of carbon starvation (Poncet, Milohanic et al. 2009) and the stringent response is crucial for survival of amino acid scarcity (Jain, Kumar et al. 2006).

Ribosomal Hibernation and RMF

Although ribosomal complexes larger than the translationally active 70S form have been reported since at least the 1960s (Suzuki and Kilgore 1967), it was not until 1990 that the correlation between formation of a 100S ribosome population and adaptation to the nutrient-depleted post-exponential growth phase was noted. Wada *et al*. reported this correlation, and used 2-D gel electrophoresis to isolate a 100S-associated protein they called Ribosome Modulation Factor (RMF) (Wada, Yamazaki et al. 1990). The 100S ribosome was shown to be a homodimer of 70S ribosomes, with the two 30S subunits creating the dimer interface (Yoshida, Maki et al. 2002)(Fig. 1-3a). A subsequent report on an *rmf* deletion strain showed that RMF was required for 100S ribosome formation, and noted that the absence of RMF during prolonged post-exponential incubation resulted in a severe survival defect (Yamagishi, Matsushima et al. 1993). Several studies have since investigated the growth phase dependence of *rmf* expression, the translation-modifying activities of RMF, and more biological consequences of RMF deficiency (Wada, Igarashi et al. 1995; Apirakaramwong, Fukuchi et al. 1998; Apirakaramwong, Kashiwagi et al. 1999; Izutsu, Wada et al. 2001; Samuel Raj, Full et al. 2002; Niven 2004).

Formation of 100S ribosomes, termed “ribosomal hibernation” (Yoshida, Maki et al. 2002), is thought to be a shunt from the traditional ribosome cycle consisting of initiation, elongation, termination, and recycling of subunits (Fig. 1-3b) (Kato, Yoshida et al. 2010). As mentioned above, this process happens primarily in stationary phase in *E. coli*; accordingly, RMF is produced only during stationary phase, and its transcription follows the same pattern (Yamagishi, Matsushima et al. 1993). Expression of *rmf* is dependent on the amino acid starvation induced stringent response (Apirakaramwong, Kashiwagi et al. 1999; Izutsu, Wada et al. 2001). Purified and synthetic RMF have been shown to induce dimerization and block ribosome translational activity *in vitro* (Wada, Igarashi et al. 1995). However, despite its sufficiency for dimerization *in vitro* and its central importance to post-exponential survival, RMF is not the only factor involved in the process of ribosomal hibernation in Gram-negative bacteria.

Figure 1-3

A

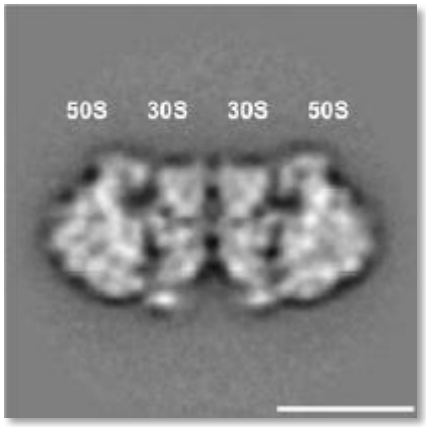

B

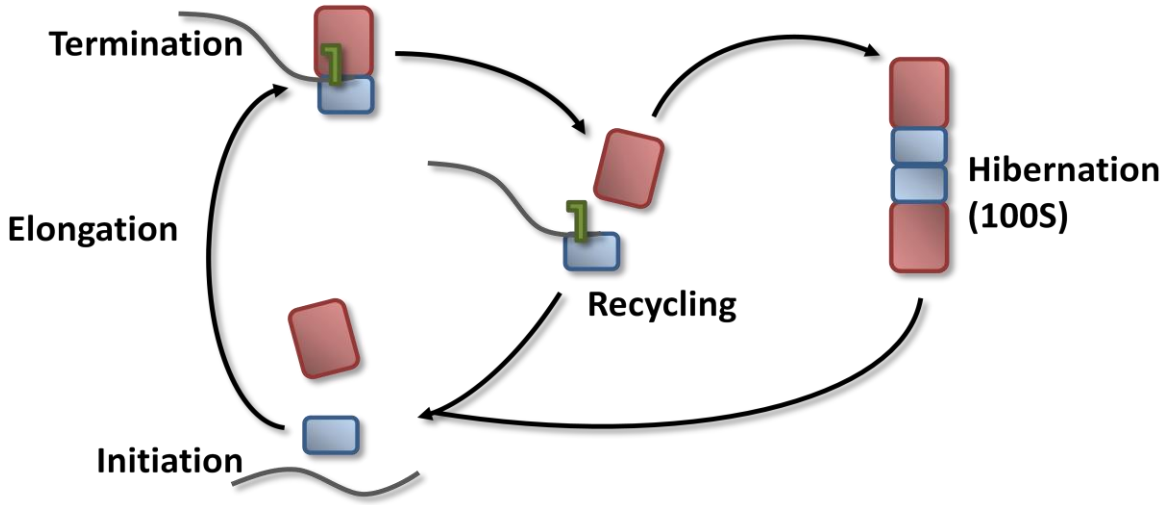

Figure 1-3. Appearance of 100S (hibernating) ribosomes and their proposed place in the ribosome cycle

(A) Cryo-electron microscopy has been used to show that 100S ribosomes consist of two 70S ribosomes dimerized along a 30S-30S contact surface; (B) Hibernation is proposed to act as a shunt from the traditional ribosome cycle, which consists of initiation, elongation, termination and recycling. 100S dimer formation is thought to occur immediately following the recycling step. (A) and (B) reproduced and adapted, respectively, from (Kato, Yoshida et al. 2010).

YfiA and YhbH (HPF)

Ten years after the first report of RMF's role in formation of 100S ribosomes, members of the same group reported the discovery of two additional factors associated with resting ribosomes. One, called YhbH, was associated exclusively with 100S ribosomes during stationary phase, while the other, YfiA, was associated with 70S ribosomes. The two proteins showed a high degree of sequence identity (≈40%), excluding an 18-amino-acid C-terminal extension on YfiA (Agafonov, Kolb et al. 1999; Maki, Yoshida et al. 2000). YhbH was later shown to stabilize and promote maturation of 100S ribosome formation, leading to its renaming as Hibernation Promoting Factor (HPF). On the other hand, YfiA was shown to antagonize 100S ribosome formation (Ueta, Yoshida et al. 2005). Both YfiA and HPF also decrease translational activity (Vila-Sanjurjo, Schuwirth et al. 2004; Ueta, Ohniwa et al. 2008). Unlike RMF, deletion of one or both of YfiA and HPF surprisingly produced no published growth or survival defects (Ueta, Yoshida et al. 2005; Bubunenko, Baker et al. 2007). Thus, although hibernation appears to be important under certain conditions, not all factors involved are important for survival under the sets of conditions normally observed in the laboratory.

The activities of RMF, HPF, and YfiA in producing and stabilizing 100S ribosomes are thought to be mediated by binding to the ribosome. Binding sites have been structurally established for both RMF and YfiA, and the HPF binding site is thought to be the same as the YfiA binding site based on sequence similarity and the observation that the total stoichiometry of YfiA + HPF is never greater than one per 70S ribosome (Yoshida, Maki et al. 2002; Vila-Sanjurjo, Schuwirth et al. 2004; Ueta, Yoshida et al. 2005). All bind to the 30S subunit of the ribosome; YfiA and HPF appear to bind near and almost completely occlude the P site, while RMF has been suggested to bind nearby, blocking the peptidyl transferase center and occluding the entrance to the peptide exit tunnel (Vila-Sanjurjo, Schuwirth et al. 2004; Yoshida, Yamamoto et al. 2004).

Long HPF and information from *S. aureus*

Bioinformatic analysis has revealed that the architecture of the ribosome hibernation machinery varies substantially among different groups of bacteria (Ueta, Ohniwa et al. 2008). Gamma Proteobacteria tend to produce RMF and one or both of YfiA and HPF. Members of other groups lack RMF, but generally produce one HPF homolog. These HPF homologs can be structurally similar to YfiA, HPF, or a third class of "long HPF" proteins found primarily in Gram-positive bacteria and exclusively in bacteria lacking RMF (Ueta, Ohniwa et al. 2008). Long HPF homologs are roughly twice the length of Gram-negative HPFs (≈180 to 190 amino acids), and consist of distinct N- and C-terminal domains. The N-terminal domain of a long HPF bears a high degree of sequence similarity to HPF, while the C-terminal domain bears very limited similarity to any known proteins. Some slight homology exists between the C-terminal domain and RMF, and it has been proposed that the C-terminal domain may perform the function that RMF performs in the Gamma Proteobacteria (Ueta, Wada et al. 2010).

In general, this class of long HPF proteins and the hibernation phenotypes of the bacteria that produce them remain almost completely unexplored. A single report from 2010 showed that *Staphylococcus aureus* produced a long HPF homolog (saHPF), that saHPF was sufficient to induce hibernation in purified ribosomes, and that saHPF was enriched in 100S ribosomes during exponential growth. The authors also observed that ribosome dimerization in

S. aureus was more prominent in less nutrient-rich media, consistent with the idea that hibernation is a response to the nutrient deprivation encountered in stationary phase (Ueta, Wada et al. 2010). However, no mutants of saHPF were presented and no functional phenotypes aside from 100S formation were attributed to saHPF. It remains unclear whether any functions or characteristics are unique to the RMF-independent hibernation induced solely by a long HPF.

Transcriptional regulation of the long HPF homolog *yvyD* has been studied in *B. subtilis*, and has been shown to be regulated by the stress-responsive sigma factors σ^B and σ^H. Similar regulation of the long HPF homolog (*lmo2511*, Chapter 3) has been shown by expression microarray profiling in *L. monocytogenes* (Chaturongakul, Raengpradub et al. 2011), but the *L. monocytogenes* homolog has never been examined individually or recognized for a role in the production of 100S ribosomes. Several proteomics-based approaches to identifying σ^B-regulated proteins have failed to identify HPF as a regulated factor (Abram, Starr et al. 2008; Abram, Su et al. 2008; Shin, Kim et al. 2010), leaving the regulation, production and function of the *L. monocytogenes* long HPF homolog an area ripe for further study. In Chapter 3, we will explore the presence, regulation, and functional consequences of ribosomal hibernation in *L. monocytogenes*.

Chapter 2

Development of a *mariner*-based transposon for *Listeria monocytogenes*, and a blood plate screen for factors involved in regulation of the critical virulence factor, LLO

Sections of this chapter were published in:

Zemansky J, Kline BC, Woodward JJ, Leber JH, Marquis H, Portnoy DA. Development of a *mariner* based transposon and identification of *Listeria monocytogenes* determinants, including the peptidyl-prolyl isomerase PrsA2, that contribute to its hemolytic phenotype. J Bacteriol. 2009 Jun;191(12):3950-64.

SUMMARY

Listeriolysin O (LLO) is a pore-forming toxin that mediates phagosomal escape and cell-to-cell spread of the intracellular pathogen *Listeria monocytogenes*. In order to identify factors that control the production, activity, or secretion of this essential virulence factor, we constructed a *Himar1 mariner* transposon delivery system and screened 50,000 mutants for a hypohemolytic phenotype on blood agar plates. Approximately 200 hypohemolytic mutants were identified, and the 51 most prominent mutants were screened *ex vivo* for intracellular growth defects. Eight mutants with a phenotype were identified, containing insertions in the genes: *lmo0964* (similar to *yjbH*); *lmo1268* (*clpX*); *lmo1401* (similar to *ymdB*); *lmo1575* (similar to *ytqI*); *lmo1695* (*mprF*); *lmo1821* (similar to *prpC*); *lmo2219* (*prsA2*); and *lmo2460* (similar to *cggR*). Some of these genes are involved in previously unexplored areas of research in *L. monocytogenes*: the genes *yjbH* and *clpX* regulate the disulphide stress response in *Bacillus subtilis*, and the *prpC* phosphatase has been implicated in virulence in other Gram-positive pathogens. Here we demonstrate that PrsA2, an extracytoplasmic peptidyl-prolyl cis/trans isomerase, is critical for virulence, and contributes to the folding of LLO and to the activity of another virulence factor, the broad-range phospholipase C (PC-PLC). Furthermore, although it has been shown that *prsA2* expression is linked to PrfA, the master virulence transcription factor in *L. monocytogenes*, we demonstrate that *prsA2* is not directly controlled by PrfA. Finally, we show that PrsA2 is involved in flagella-based motility, indicating that this factor likely serves a broad physiological role.

INTRODUCTION

Listeria monocytogenes is a Gram-positive, facultative intracellular pathogen capable of infecting a broad range of animal hosts, including humans (Vazquez-Boland, Kuhn et al. 2001). The cell biology of infection has been well characterized and is a model for pathogenesis. Upon internalization into host cells including macrophages and non-professional phagocytes, *L. monocytogenes* are initially enclosed in a single membrane vacuole. Bacteria rapidly lyse this primary vacuole and replicate in the cytosol, exploiting actin-based motility as a means to move within the cytoplasm and to spread from cell to cell. Actin-based propulsion of bacteria from the cytoplasm of one cell into the cytoplasm of a neighboring cell results in the formation of a double-membrane vacuole or secondary vacuole. Bacteria lyse the secondary vacuole and intracellular growth continues (Tilney and Portnoy 1989; Vazquez-Boland, Kuhn et al. 2001).

Central to the virulence of *L. monocytogenes* is the ability to lyse the primary and secondary vacuoles in order to gain entry into the host cytosol. Escape from both types of vacuoles is primarily mediated by the secretion of the cytolysin listeriolysin O (LLO) (Schnupf and Portnoy 2007). A member of a large family of pore-forming toxins called the cholesterol-dependent cytolysins (CDCs), LLO monomers bind cholesterol-containing host membranes. Upon binding, the monomers oligomerize and the resultant complex inserts into the membrane, producing pores up to 30 nm in diameter (Alouf 2001; Schnupf and Portnoy 2007). Bacteria deficient for LLO production or activity remain trapped within a phagosome (Gaillard, Berche et al. 1987; Schnupf and Portnoy 2007) and are unable to replicate in cells, resulting in a five log decrease in virulence in mice compared to wild-type (WT) bacteria (Kathariou, Metz et al. 1987; Portnoy, Jacks et al. 1988; Cossart, Vicente et al. 1989).

However, LLO activity must be compartmentalized to the acidic phagosome. Unrestricted activity can lead to premature host cell lysis, exposing the bacteria to the inhospitable extracellular environment (Jones and Portnoy 1994; Glomski, Decatur et al. 2003). Mutants incapable of restricting the activity of LLO to the vacuole have been isolated and are up to four orders of magnitude less virulent *in vivo* compared to wild-type bacteria (Decatur and Portnoy 2000; Lety, Frehel et al. 2001; Glomski, Gedde et al. 2002; Lety, Frehel et al. 2002; Glomski, Decatur et al. 2003). LLO is therefore regulated at multiple levels.

Expression of *hly*, the gene encoding LLO, is controlled by the *L. monocytogenes* master virulence transcriptional activator PrfA (Gray, Freitag et al. 2006; Scortti, Monzo et al. 2007). In addition to *hly*, PrfA coordinately regulates the expression of several other genes necessary for *L. monocytogenes* pathogenesis, such as the broad range phospholipase C (PC-PLC). Although a dramatic change in the expression profile of bacteria occurs during the transition into the infectious life cycle, only ten genes (including *hly*) have been demonstrated to be directly regulated by PrfA (Chakraborty, Leimeister-Wachter et al. 1992; Gray, Freitag et al. 2006; Scortti, Monzo et al. 2007). An unexplored possibility, therefore, remains that LLO production, activity, or secretion is regulated by other extragenic factors.

Transposon mutagenesis remains one of the most important tools in bacterial genetics, facilitating the discovery and exploration of gene function and protein interaction. Given that transposon mutagenesis has previously proved to be an effective tool in analyzing hemolysin mutants of *L. monocytogenes* (Gaillard, Berche et al. 1986; Kathariou, Metz et al. 1987; Portnoy, Jacks et al. 1988), we constructed a *Himar1 mariner* based transposon and performed a sheep's

blood agar screen for mutants with a hypohemolytic phenotype. We hypothesized that transposon insertion mutants deficient in the production of LLO would reveal either novel virulence factors or additional roles for known factors. To our knowledge, there has never been a published screen that sought to characterize mutants with hypohemolytic phenotypes.

Isolated from the hornfly *Haematobia irritans, Himar1* is a member of the *Tc1/mariner* superfamily of transposable elements (Robertson and Lampe 1995; Lampe, Churchill et al. 1996; Hartl, Lohe et al. 1997; Plasterk, Izsvak et al. 1999). *Himar1* based transposon systems provide an alternative to the most frequently used system in *L. monocytogenes*, a Tn*917* derivative (Camilli, Portnoy et al. 1990). Tn*917*-LTV3 is considerably larger in size (22 kb vs. 1.4 kb), has a relatively low transposition efficiency, a high rate of delivery vector retention, and a tendency for insertional "hot-spots" (Camilli, Portnoy et al. 1990; Garsin, Urbach et al. 2004; Cao, Bitar et al. 2007). In comparison, the *Himar1* based transposon system provides several distinct advantages. Transposition requires no additional factor other than the cognate transposase, and similar systems have been shown to be effective in multiple bacterial species, both Gram-negative and Gram-positive (Lampe, Churchill et al. 1996; Rubin, Akerley et al. 1999). Additionally, *mariner* elements have a low site specificity – the dinucleotide TA – an element common in *L. monocytogenes* (average of 39% GC content) (Lampe, Churchill et al. 1996; Glaser, Frangeul et al. 2001).

The increased genomic coverage of *Himar1* transposon based libraries (both within and between genes) has also facilitated the ease and resolution of negative selection screens (Sassetti, Boyd et al. 2001). These screens have proven to be a remarkably useful tool, not only in identifying new virulence factors, but also in characterizing which of these factors are necessary during different stages of an infection (Sassetti, Boyd et al. 2001; Sassetti, Boyd et al. 2003; Chan, Kim et al. 2005; Joshi, Pandey et al. 2006; Lawley, Chan et al. 2006; Weiss, Brotcke et al. 2007). Furthermore, these approaches have assisted in assigning function to previously uncharacterized virulence factors by mapping their genetic interactions (Joshi, Pandey et al. 2006).

Recently, a new *Himar1* based transposon system became available for use in *L. monocytogenes* (Cao, Bitar et al. 2007). This transposon does not contain features optimal for its use in a negative selection screen. Additionally, there is little control over the complexity of the library generated and instances of clones with multiple transposon insertions. Therefore, a new *Himar1* system for *L. monocytogenes* based on a different strategy of transposon delivery was constructed, one that minimizes the potential for multiple transposition events within a single chromosome and that allows control over the complexity of a library. The new transposon also includes elements that can take advantage of microarray technologies in order to perform negative selection screens.

Among the factors identified in the screen that lead to a hypohemolytic phenotype was *prsA2*. A peptidyl-prolyl extracytoplasmic cis/trans isomerase, PrsA2 has previously been shown to contribute to *L. monocytogenes* virulence, although the precise mechanism remains unknown (Milohanic, Glaser et al. 2003; Chatterjee, Hossain et al. 2006; Port and Freitag 2007). Furthermore, previous work found that *prsA2* is upregulated upon PrfA activation and is preceded by a putative PrfA-box, suggesting that *prsA2* is directly regulated by PrfA (Milohanic, Glaser et al. 2003; Chatterjee, Hossain et al. 2006; Port and Freitag 2007). Here we demonstrate that PrsA2 is critical for virulence, contributes to the secretion and activity of LLO

and the activity PC-PLC, but is not under direct PrfA control. Additionally, PrsA2 contributes to flagella-based motility, an aspect of the bacteria's life cycle separate from infection. These data suggest that PrsA2 plays a broader physiological role than previously appreciated.

RESULTS

Construction of a *Himar1 mariner* transposon delivery system.

A *Himar1* based transposon delivery system, pJZ037, was constructed for use in *L. monocytogenes* (Fig. 2-1a); the plasmids and primers used are listed in Table 2-1. To diminish the occurrence of multiple transposon hops within single clones and clonal populations, problems associated with a previously constructed *Himar1* system (Yeung, Zagorski et al. 2005; Cao, Bitar et al. 2007) (data not shown), as well as to add control over the complexity of the library, the C9 hyperactive variant of the *Himar1* transposase (Lampe, Akerley et al. 1999) was placed under the control of the constitutive, strong, exogenous promoter hyper-*Pspac*, *Pspac*(hy) (Quisel, Burkholder et al. 2001; Shen and Higgins 2005; Schnupf, Hofmann et al. 2006), and transposition events were allowed to occur on BHI plates. The transposon contains the Tn*917* ribosomal methyltransferase gene (erythromycin resistance, em) (Camilli, Portnoy et al. 1990) flanked by the TA insertion sites, the inverted repeats (IR), and T7 promoters oriented outwards from the vector phiMycoMarT7 in order to facilitate negative selection screens (Sassetti, Boyd et al. 2001). Both elements have been ligated into the Gram-positive suicide vector pKSV7 (Smith and Youngman 1992).

Evaluation of the new *Himar1* transposon delivery vector.

A library of approximately 30,000 distinct insertion mutants was generated using pJZ037. Based on the number of colonies that were chloramphenicol (cm) resistant (the drug marker carried by the delivery vector) compared to the number that were em resistant, approximately 99% of the clones in the library had transposon insertions and had lost the delivery plasmid. Twenty randomly selected clones were subjected to analysis via Southern Blot. All twenty clones examined contained a single transposon insertion and each insertion site was unique (data not shown).

As an additional measure of library coverage, transposon insertion mutants isolated from three screens in the lab (two unrelated to the one described in this report), focusing on different phenotypes, were mapped onto the assembled genome of *L. monocytogenes* EGD-e (Fig. 2-1b). Each site represents an insertion into a different feature (ORF, intragenic region, etc.). This map includes 197 insertions, and covers most of the genome with only minimal lengths of sequence lacking insertions. The largest of these regions covers a length of approximately 160,000 bp, a portion of the chromosome from *lmo401* to *lmo0539*, perhaps indicating the presence of many essential genes.

An *in vivo* negative selection screen was also performed similar to previously described screens (Sassetti, Boyd et al. 2003; Weiss, Brotcke et al. 2007). Preliminary analysis of the data revealed that genes within the PrfA regulon were negatively selected for growth *in vivo* in mice and guinea pigs (J. Leber, J.D. Sauer, J. Zemansky, and D. A. Portnoy, and C. Cooke, S. Wong, and A. Bakardjiev unpublished observations).

A transposon mutant screen for *L. monocytogenes* genes involved in the production or activity of LLO.

To identify determinants that govern LLO production, activity, or secretion, a screen for hypohemolytic transposon mutants on sheep's blood agar was performed. Approximately 50,000 transposon insertions were screened on 1% LB-G1P agar plates containing 5% defibrinated sheep's blood. The inclusion of the LB-G1P media increased the expression of

Figure 2-1

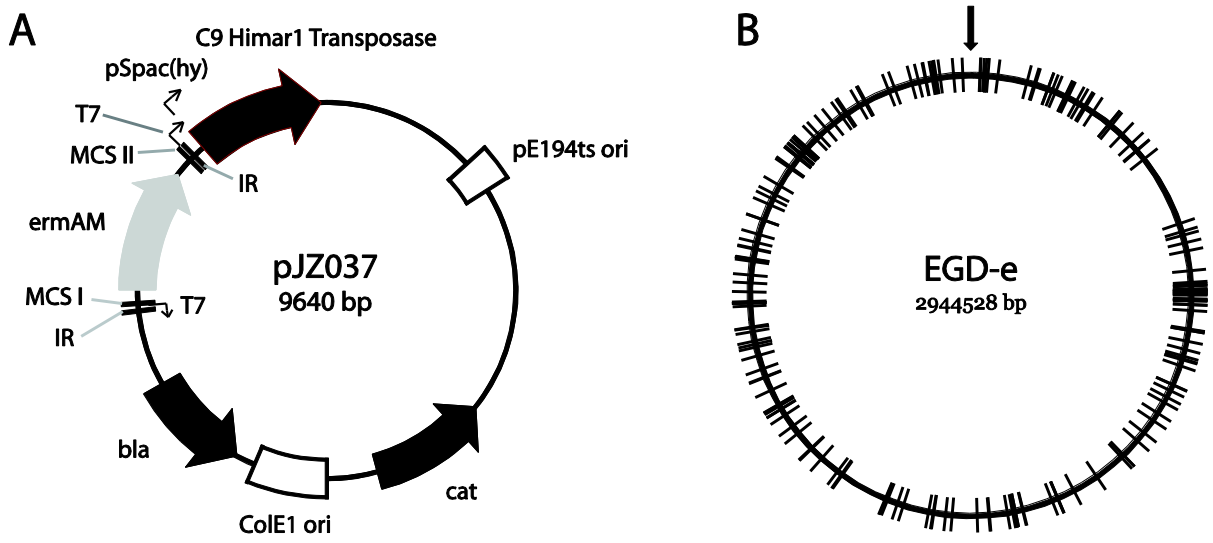

Figure 2-1. A *Himar1*-based transposon delivery system for *L. monocytogenes*

(A) The vector pJZ037 contains the following features: the ColE1 origin of replication and a β-lactamase resistance gene (*bla*) for propagation in *E. coli*, a Gram-positive temperature-sensitive origin of replication (pE194ts ori) and chloramphenicol resistance gene (*cat)* for plasmid curing in *L. monocytogenes* (Smith and Youngman 1992), the C9 hyperactive variant of the *Himar1* transposase (Lampe, Akerley et al. 1999) under the control of the pSpac(hy) promoter (Schuchat, Swaminathan et al. 1991; Quisel, Burkholder et al. 2001), and the transposon containing the erythromycin resistance gene (*ermAM)* (Camilli, Portnoy et al. 1990) for transposon insertion selection flanked on both sides by T7 promoters oriented outwards for negative selection screens and the inverted repeats (Sassetti, Boyd et al. 2001). Two multiple cloning sites (MCS I and MCS II) flank the em resistance gene. (B) The locations of 197 insertions mapped onto the *L. monocytogenes* EGD-e chromosome. Each line represents a different feature (ORF, intergenic region, rRNA, etc.). The insertions were obtained from multiple ongoing screens in the lab searching for different phenotypes. The downward arrow marks the origin of replication.

PrfA-regulated genes, including *hly*, and therefore enhanced visual resolution (Ripio, Brehm et al. 1997). Mutants were visually scored for a decrease in the size of and/or the opacity of the zone of hemolysis while avoiding small colonies. Two hundred fifty-one mutants were initially chosen, and 193 were confirmed and sequenced. The precise insertion site of the transposon was determined for 162 of these mutants, 111 of which were unique. These mutants mapped to a total of 57 unique features, including genes and intergenic regions (Table 2-2). Multiple *hly* mutants were isolated, representing 14 distinct transposon insertion sites. Of the remaining 31 mutants, the insertion site was determined approximately, to within ≈200 bp. Most of these sites overlapped with features already identified, however six were unique (Table 2-2). These data suggested that we were approaching saturation, and no additional screening was performed.

Analysis of transposon mutants displaying a hypohemolytic phenotype.

The intracellular lifecycle of *L. monocytogenes* can be evaluated *ex vivo* by the capacity of bacteria to form plaques on mouse L2 fibroblast monolayers. Defects in any component of this lifecycle – in particular LLO mediated escape from the primary vacuole, escape from the secondary vacuole during cell-to-cell spread, and failure to compartmentalize LLO activity to the phagosome – can influence plaque size and shape. In previous studies, small plaque mutants of *L. monocytogenes* invariably had *in vivo* defects (Sun, Camilli et al. 1990). To identify those mutants isolated from our initial screen likely to have *in vivo* relevance, the average plaque size of 51 transposon insertion mutants with the greatest observed hemolytic defects were evaluated (Table 2-2). Eight mutants consistently developed smaller plaques relative to wild-type: *lmo0964* (similar to *yjbH*), *lmo1268* (*clpX*), *lmo1401* (similar to *ymdB*), *lmo1575* (similar to *ytqI*), *lmo1695* (*mprF*), *lmo1821* (similar to *prpC*), *lmo2219* (*prsA2*) and *lmo2460* (similar to *cggR*) (Table 2-2). Of these genes, only two, *lmo1695* and *lmo2219*, have been characterized in *L. monocytogenes*.

The gene *lmo1695* encodes a protein with homology to multiple peptide resistance factor (MprF) of *Staphylococcus aureus*, a membrane protein that catalyzes the transfer of lysine residues to phosphatidylglycerol and is known to have a major role in conferring resistance to antimicrobial peptides (Thedieck, Hain et al. 2006). This gene was first identified in *L. monocytogenes* as a component of the VirR regulon, and bacteria lacking the response regulator VirR have a reduced ability to colonize and persist in the livers and spleens of infected mice (Mandin, Fsihi et al. 2005). *L. monocytogenes mprF* mutants are attenuated in virulence in mice and have an increased susceptibility to certain cationic antimicrobial peptides (Thedieck, Hain et al. 2006). Although no study has identified a relationship between LLO secretion and MprF, we eliminated this gene from further analysis as its role in virulence has already been explored (Thedieck, Hain et al. 2006), and we suspect that the role of *mprF* in LLO activity is indirect.

The gene *lmo2219* is one of two genes in *L. monocytogenes* that encode proteins with significant homology to the extracytoplasmic lipoprotein chaperone peptidyl-prolyl isomerase PrsA from *Bacillus subtilis*. An essential gene in *B. subtilis*, PrsA contributes to the folding of proteins following Sec-mediated translocation (Jacobs, Andersen et al. 1993; Kontinen and Sarvas 1993; Milohanic, Glaser et al. 2003; Chatterjee, Hossain et al. 2006; Port and Freitag 2007). Annotated as *prsA2* (as compared to *prsA1*, *lmo1444*) (Port and Freitag 2007), *lmo2219* was first identified as a putative virulence factor in a transcriptome analysis of genes

Table 2-1. Oligonucleotide primers, plasmids, and strains used in this study

#	Sequence (5'->3')	Restriction Enzyme	Reference
112	AAAgtcgacTAACAGGTTGGCTGATAAGTCCC	SalI	
24	aaaCTGCAGGTACCCGGGttccagtttgtaatacgactcac	SmaI, KpnI, PstI	
29	aaaCTGCAGaaaactagtctcgagTGGGGTACGCGTAATACGACTC	Pst I, SpeI, XhoI	
26	aaaAAGCTTGGATCCtaacaggttggctgataagtccc	BamHI, HindIII	
30	aaaCTGCAGctaaagttatggaaataagacttag	PstI	
31	aaaACTAGTattcaaatttatccttattgtacaaa	SpeI	
113	AAAggatccAATTTTGCAAAAAGTTGTTGACTTTATCTACAAGGTGTGGCATAATGTGTGTcggccgataaagcaagcatataatattgcgtttcatc	BamHI EagI	
114	aaaAAGCTTGTCGACttattcaacatagttcccttcaaga	SalI HindIII	
134	AAAcggccgATGgaaaaaaaggaatttcgtgttttg	EagI	
229	aaagtcgacTGGAACCGGAGAAGAAACGC	SalI	
230	GTGTTTTTTAGTGCTTATTTAGAtccaagaattaatttcttcttcatatgaagaagaaattaattcttggaTCTAAATAAGCACTAAAAAACAC		
231			
232	aaactgcagGAAACAGTAGACCTATTCTTGC	PstI	
241	AAcggccgTTTCACACCAATCGGACATTCC	EagI	
242	AAcggccgACCATAAGAATATCATTAAATTTCTTTC	EagI	
243	AAcggccgAtgAAGAAGAAATTAATTCTTGGAC	EagI	
249	AAAgtcgacTAAAGTACTAAAACATACAAAACCG	SalI	
MSPY5	ACTACGCACCGGACGAGACGTAGCGTC		(Tavazoie and Church 1998)
MSPY3	p-CGGACGCTACGTCCGTGTTGTCGGTCCTG		(Tavazoie and Church 1998)

Plasmids	Reference
pBADC9	(Lampe, Akerley et al. 1999)
phiMycoMarT7	(Sassetti, Boyd et al. 2001)
pUC19	Invitrogen
pLTV3	(Camilli, Portnoy et al. 1990)
pKSV7	(Smith and Youngman 1992)
pPL2	(Lauer, Chow et al. 2002)
pJZ025	This study
pJZ026	This study
pJZ029	This study
pJZ064	This study
pJZ065	This study
pJZ066	This study

Strains	Description	Reference
L. monocytogenes		
10403S	Wild-type	(Bishop and Hinrichs 1987)

DP-L5539	*Himar1* transposon generated library, 10403S	This study
DP-L5558	transposon insertion into lmo0964	This study
DP-L5566	transposon insertion into lmo1268	This study
DP-L5570	transposon insertion into lmo1401	This study
DP-L5575	transposon insertion into lmo1609	This study
DP-L5577	transposon insertion into lmo1695	This study
DP-L5580	transposon insertion into lmo1821	This study
DP-L5596	transposon insertion into lmo2219	This study
DP-L5600	transposon insertion into lmo2460	This study
DP-L5601	10403S Δ*prsA*$_{29\text{-}291}$	This study
DP-L5602	10403S Δ*prsA*$_{29\text{-}291}$, tRNA^{Arg}::pPL2 construct #1	This study
DP-L5603	10403S Δ*prsA*$_{29\text{-}291}$, tRNA^{Arg}::pPL2 construct #2	This study
DP-L5604	10403S Δ*prsA*$_{29\text{-}291}$, tRNA^{Arg}::pPL2 construct #3	This study
DP-L5605	10403S Δ*prsA*$_{29\text{-}291}$, tRNA^{Arg}::pPL2	This study
DP-L2161	10403S Δ*hly*	(Jones and Portnoy 1994)
DP-L5606	10403S Δ*hly, prsA2::Himar1*	This study
DP-L4057	10403S LLO$_{S44A}$	(Glomski, Decatur et al. 2003)
DP-L5607	10403S LLO$_{S44A}$, *prsA2::Himar1*	This study
DP-L4361	10403S LLO$_{FLAG}$	This study
DP-L5608	10403S LLO$_{FLAG}$, *prsA2::Himar1*	This study
DP-L861	SLCC-5764	(Leimeister-Wachter, Goebel et al. 1989)
DP-L5609	SLCC-5764, *prsA2::Himar1*	This study
DP-L1935	10403S *ΔplcB*	(Smith, Marquis et al. 1995)
DP-L4650	10403S *ΔflaA*	(Way, Thompson et al. 2004)
DP-L4317	10403S *ΔprfA*	H. Shen and J. F. Miller, (Cheng and Portnoy 2003)
DP-L3481	10403S LLO$_{(His)6}$	(Gedde, Higgins et al. 2000)
DP-L5633	10403S LLO$_{(His)6}$, *prsA2::Himar1*	This study

Table 2-2. Unique Transposon Insertions Producing a Hypohemolytic Phenotype					
Precise site of the transposon mapped					
Strain	Lmo#	Name[a]	Annotation[b]	Blood Plate Phenotype[c]	Relative Plaque Size[d]
DP-L5540	lmo0027	-	similar to PTS system, beta-glucosides specific enzyme IIABC	-	80-100%
DP-L5541	lmo0031	-	LacI family transcription regulator	-	nd
DP-L5542	lmo0134/0135	-	-	-	80-100%
DP-L5543	lmo0175/0176	-	-	-	80-100%
DP-L5544	lmo0201/0202	-	-	----	80-100%
DP-L5545	lmo0202	hly	listeriolysin O	----	nd
DP-L5547	lmo0223	cysK	similar to cysteine synthase	-	80-100%
DP-L5548	lmo0234	-	similar to *B. subtilis* YacL	-	80-100%
DP-L5550	lmo0279	-	similar to anaerobic ribonucleoside-triphosphate reductase	-	80-100%
DP-L5551	lmo0352	-	similar to regulatory proteins (DeoR family)	--	80-100%
DP-L5552	lmo0669	-	similar to oxidoreductase	-	80-100%
DP-L5553	lmo0734	-	similar to transcriptional regulator (LacI family)	-	nd
DP-L5554	lmo0785	-	similar to transcriptional regulator (NifA/NtrC family)	-	80-100%
DP-L5555	lmo0813	-	similar to fructokinases	-	80-100%
DP-L5556	lmo0821	-	-	---	80-100%
DP-L5557	lmo0833	-	similar to transcriptional regulator	-	80-100%
DP-L5558	lmo0964	-	similar to *B. subtilis* YjbH	---	Table 3
DP-L5559	lmo0964/0965	-	-	-	80-100%
DP-L5561	lmo1017	-	similar to phosphotransferase system glucose-specific enzyme IIA	-	80-100%
DP-L5562	lmo1079	-	similar to *B. subtilis* YfhO	-	80-100%
DP-L5563	lmo1254	-	similar to alpha,alpha-phosphotrehalase	--	80-100%

DP-L5564	lmo1255	-	similar to PTS system trehalose specific enzyme IIBC	-	80-100%
DP-L5566	lmo1268	clpX	ATP-dependent protease ATP-binding subunit	-	Table 3
DP-L5568	lmo1329	ribC	similar to riboflavin kinase and FAD synthase	-	80-100%
DP-L5569	lmo1354	-	similar to aminopeptidase P	-	nd
DP-L5570	lmo1401	-	-	--	Table 3
DP-L5571	lmo1475	hrcA	heat-inducible transcription repressor	-	80-100%
DP-L5572	lmo1514/1515	-	-	-	80-100%
DP-L5573	lmo1515	-	-	-	80-100%
DP-L5574	lmo1575	-	-	--	Table 3
DP-L5575	lmo1609	-	similar to thioredoxin	-	80-100%
DP-L5576	lmo1616	-	-	-	80-100%
DP-L5577	lmo1695	mprF	-	-	60-80%
DP-L5578	lmo1772	purC	phosphoribosylaminoimidazole-succinocarboxamide synthase	-	80-100%
DP-L5579	lmo1814	-	-	--	80-100%
DP-L5580	lmo1821	prpC	similar to putative phosphoprotein phosphatase	--	Table 3
DP-L5581	lmo1829	-	similar to fibronectin binding proteins	-	80-100%
DP-L5582	lmo1878	-	manganese transport transcriptional regulator	-	80-100%
DP-L5583	lmo1922	-	-	-	80-100%
DP-L5584	lmo1952/1953	-	-	--	80-100%
DP-L5586	lmo1954	drm	similar to phosphopentomutase	--	80-100%
DP-L5587	lmo1974	-	similar to transcription regulators, (GntR family)	-	80-100%
DP-L5590	lmo2055	-	-	-	nd
DP-L5591	lmo2072/2073	-	-	-	80-100%
DP-L5592	lmo2103/2104	-	-	--	80-100%
DP-L5593	lmo2110	-	similar to mannnose-6 phospate isomerase	-	80-100%
DP-L5594	lmo2203	-	similar to N-acetylmuramoyl-L-alanine amidase and to internalin B	-	80-100%
DP-L5595	lmo2217	-	-	-	nd

DP-L5596	lmo2219	prsA2	similar to post-translocation molecular chaperone	--	Table 3
DP-L5597	lmo2230	-	similar to arsenate reductase	--	80-100%
DP-L5598	lmo2361	-	-	-	80-100%
DP-L5599	lmo2376	-	similar to peptidyl-prolyl cis-trans isomerase	--	nd
DP-L5600	lmo2460	-	similar to *B. subtilis* CggR hypothetical transcriptional regulator	-	60-80%
DP-L5601	lmo2460/2461	-	-	-	80-100%
DP-L5602	lmo2461	sigL	RNA polymerase factor sigma-54	-	80-100%
DP-L5603	lmo2758	guaB	similar to inosine-monophosphate dehydrogenase	-	80-100%
DP-L5604	lmo2770	-	bifunctional glutamate--cysteine ligase/glutathione synthetase	-	nd
Approximate site of the transposon mapped					
DP-L5546	lmo0202/0203	-	-	-	nd
DP-L5565	lmo1255/1256	-	-	---	nd
DP-L5567	lmo1295/1296	-	-	-	nd
DP-L5585	lmo1953	pnp	similar to purine-nucleoside phosphorylase	--	nd
DP-L5588	lmo2016	cspB	similar to major cold-shock protein	---	80-100%
DP-L5589	lmo2020	divIVA	similar to cell-division initiation protein	-	nd

[a, b] As identified by NCBI annotation of *L. monocytogenes* EGD-e genome

[c] Qualitative hemolytic defect visually determined by comparison to an adjacent WT colony on a blood agar plate: approximately -, 75%; --, 50%; ---, 25%, ----, 0% of the activity of the WT colony.

[d] As compared to WT in L2 fibroblast plaque assay.

nd, not done.

differentially regulated by PrfA; the gene was upregulated under conditions in which PrfA was upregulated and a putative PrfA binding site was identified upstream of the gene (Milohanic, Glaser et al. 2003). PrsA2 transcript levels were also found to be upregulated during intracellular growth (Chatterjee, Hossain et al. 2006), and a proteomics approach found that PrsA2 secretion levels were increased upon PrfA activation (Port and Freitag 2007). These studies also found that *L. monocytogenes prsA2* mutants have a plaquing defect (Chatterjee, Hossain et al. 2006; Port and Freitag 2007), an intracellular growth defect in P388D1 murine macrophage-like cells (Chatterjee, Hossain et al. 2006), and a decreased ability to replicate in the livers and spleens of infected mice (Port and Freitag 2007). Speculation remains that PrsA2 contributes to the folding of extracellular virulence factors (Chatterjee, Hossain et al. 2006; Port and Freitag 2007). Given the possibility that one of these substrates could be LLO, we continued characterizing this mutant (see below).

Of the remaining mutants with plaque defects, none have been characterized in *L. monocytogenes*. Based on a BLAST search of the *B. subtilis* strain 168 genome (http://www.ncbi.nlm.nih.gov/), the gene *lmo0964* is similar to *yjbH* (37% identity, 57% similarity), a gene that confers resistance to nitrosative stress (Rogstam, Larsson et al. 2007). YjbH also plays a role in regulating the response to disulphide stress by acting as a negative effector of the transcriptional regulator Spx (Larsson, Rogstam et al. 2007). Upon disulphide stress, Spx induces the transcription of genes that maintain thiol-redox homeostasis (Nakano, Kuster-Schock et al. 2003). Interestingly, null *clpX* or *clpP* mutants, the genes encoding the ATP-powered AAA+ protease ClpXP, have the same phenotype as *yjbH* mutants. A model was proposed wherein YjbH facilitates the recognition and degradation of Spx by ClpXP (Larsson, Rogstam et al. 2007). Consistent with these findings, a transposon insertion in *lmo1268*, the *L. monocytogenes clpX*, was also identified. This mutant has a similar blood plate phenotype and plaque defect to the *lmo0964* mutant (Fig. 2-2, Table 2-3).

The gene *lmo1821* codes for a protein similar to the *B. subtilis* protein phosphatase *prpC* (49% identity, 67% similarity). In both *L. monocytogenes* and *B. subtilis*, *prpC* is directly upstream of the eukaryotic-like serine/threonine kinase *prkC;* the genes are co-transcribed and appear to have opposing physiological roles during stationary phase growth, and biofilm and spore formation (Gaidenko, Kim et al. 2002; Madec, Laszkiewicz et al. 2002). Consistent with its plaque defect, PrkC homologs have been shown to contribute to the virulence of *E. faecalis*, *S. pneumoniae*, *S. agalactiae*, and *S. pyogenes* (Rajagopal, Clancy et al. 2003; Echenique, Kadioglu et al. 2004; Jin and Pancholi 2006; Kristich, Wells et al. 2007).

Little is known about the remaining genes. The gene *lmo1401* encodes a protein similar to the *B. subtilis* YmdB (65% identity, 80% similarity) and contains a putative metallo-phosphoesterase domain. The gene *lmo1575* encodes a protein similar to the *B. subtilis* YtqI (55% identity, 72% similarity), a protein shown to have both oligoribonuclease and pAp-phosphatase activity (the conversion of 3'(2')phosphoadenosine 5' phosphate to AMP) (Mechold, Fang et al. 2007). The gene *lmo2460* encodes a protein similar to the *B. subtilis* CggR (54% identity, 75% similarity), a repressor of the *gapA* operon, which contains many of the genes necessary for glycolysis (Ludwig, Homuth et al. 2001; Doan and Aymerich 2003).

We continued to characterize six mutants: *lmo0964* (similar to *yjbH*), *clpX*, *lmo1401* (similar to *ymdB*), *lmo1575* (similar to *ytqI*), *lmo1821* (similar to *prpC*), and *prsA2* (Fig. 2-2; Table

Figure 2-2

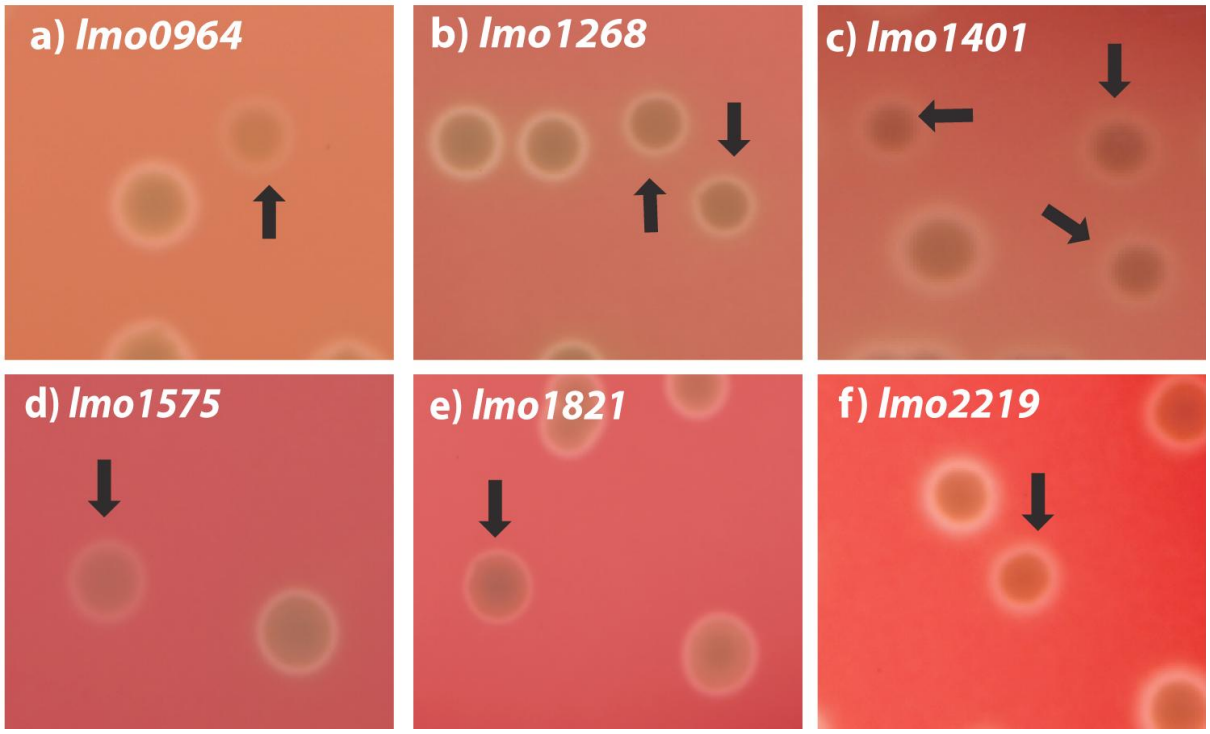

Figure 2-2. Blood plate phenotypes of hypohemolytic mutants of interest

Wild-type (10403S) bacteria were plated in a 1:1 ratio with the following transposon insertion mutants on LB-G1P agar containing 5% defibrinated sheep's blood: (a) *lmo0964* (similar to *yjbH*), (b) *lmo1268* (*clpX*), (c) *lmo1401* (similar to *ymdB*), (d) *lmo1575* (similar to *ytqI*), (e) *lmo1821* (similar to *prpC*), (f) *lmo2219* (*prsA2*). Arrows denote mutant colonies.

2-3). In addition to *mprF*, *lmo2460* (*cggR*) was not examined further as it had a small but reproducible growth defect in broth (G1P media), making it potentially difficult to separate a specific defect in LLO production or activity from a general metabolic defect. The remaining mutants grew the same as wild-type (data not shown). That each mutant's phenotype was due to the transposon insertion was confirmed by transduction (Hodgson 2000) into a wild-type background followed by comparison of the blood plate phenotypes and plaque defects (data not shown).

To assess defects in either the amount of LLO secreted or the activity of the secreted toxin, the hemolytic activity present in culture supernatants of each mutant was determined. As shown in Table 2-4, the majority of our mutants have decreased hemolytic activity. The insertion mutant *lmo1575* had the greatest defect, with an average of 29.6% the activity of WT, followed by the transposon insertions in *lmo0964* (40.3%), *lmo1268* (*clpX*) (55.9%), an in-frame deletion of *prsA2* (see below) (57.7%), and *lmo1401* (69.9%). Interestingly, the transposon insertion mutant *lmo1821* (*prpC*) had essentially the same level of hemolytic activity as WT, indicating that the conditions on the blood agar plate (incubation on solid media for 48 h) elicited a different phenotype than growth in broth culture over 5 h.

Western Blots were also performed to assess LLO secretion levels. Although there were small but reproducible qualitative differences in the amount of LLO secreted by the mutants as compared to WT, these differences were not significantly robust to draw any definitive conclusions (data not shown). It is therefore unclear whether the differences identified in the hemolytic-activity assay are due to subtle secretion defects or due to the activity of the LLO secreted (see discussion).

***In vivo* analysis of the plaque mutants**

To assess the potential virulence defect of each of our six transposon insertion mutants *in vivo*, a competitive index assay (Auerbuch, Lenz et al. 2001) was utilized to quantify the potential relative replication defect each mutant has in the liver and spleen of C57BL/6 mice co-infected with WT *L. monocytogenes*. For each transposon mutant, five mice were co-infected with 1.0×10^5 bacteria in a ≈1:1 ratio of mutant to WT via intravenous tail-vein injection. Livers and spleens were harvested 48 h postinfection, and the ratio of WT to mutant bacteria was assessed (Auerbuch, Lenz et al. 2001). The *prsA2* mutant displayed the greatest phenotype, as it was undetectable in our organ homogenates after patching several hundred colonies, consistent with the previously described virulence defect of this mutant of being greater than 2 log in the liver and spleen (Port and Freitag 2007). The insertion mutant *lmo1401* (*ymdB*) also displayed a significant decrease in bacterial numbers in both the liver and spleen, with a median log defect of 2.0 and 1.1. Consistent with previous studies of the role of *prpC*/*prkC* in virulence in other Gram-positive pathogens (Rajagopal, Clancy et al. 2003; Echenique, Kadioglu et al. 2004; Jin and Pancholi 2006; Kristich, Wells et al. 2007), the transposon insertion in *lmo1821* (*prpC*) had a 2.2 median log defect in the liver and a 1.1 median log defect in the spleen. Finally, consistent with our hypothesis that transposon insertions in *lmo0964* (*yjbH*) and *clpX* affect the same pathway, the relative decreases in bacterial loads between these two mutants (1.7 vs. 1.6 median log defect in the liver, 0.6 vs 0.7 median log defect in the spleen) were similar (Fig. 2-3).

Figure 2-3

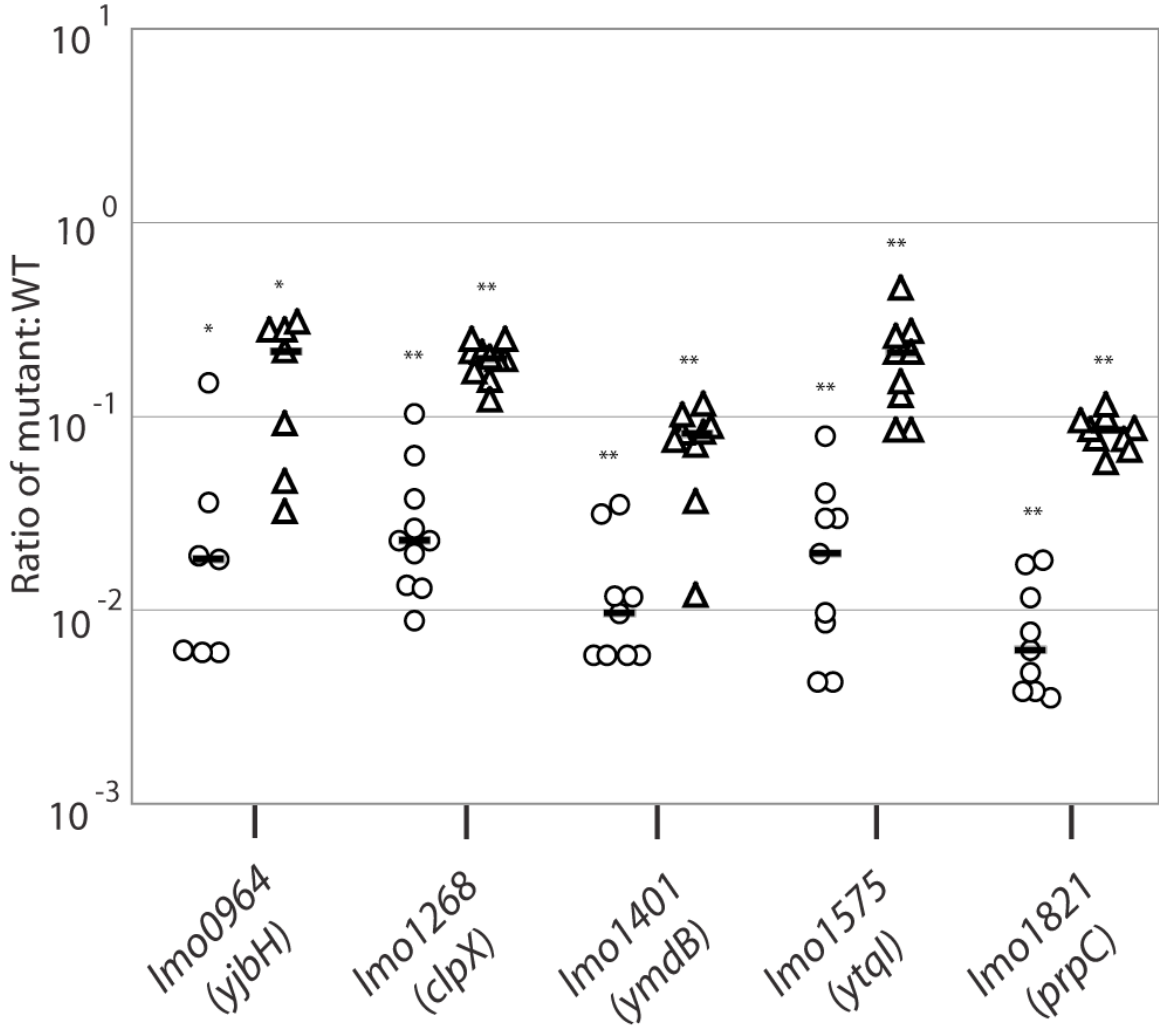

Figure 2-3. *In vivo* defects of transposon insertion mutants as measured by competitive index

Bacteria were harvested 48 h postinfection from five mice per mutant and the ratio of mutant:WT bacteria was determined for the liver (○) and spleen (△). All median values are represented by horizontal lines. We performed one-sample Wilcoxon tests on the ratios, using R (http://www.r-project.org/). Under the null hypothesis of no differences, the mean parameter is assumed to be one. A two-tailed p-value is reported for each mutant. *, $p < 0.05$; **, $p < 0.005$

TABLE 2-3. Plaque sizes of transposon insertion mutants		
Transposon Insertion	**Gene Name**	**Plaque Size[a]**
lmo0964	*yjbH*	51.6% ± 5.3%***
lmo1268	*clpX*	61.3% ± 2.7%***
lmo1401	*ymdB*	35.1% ± 4.5%*
lmo1575	*ytqI*	64.7% ± 5.3%**
lmo1821	*prpC*	72.4% ± 3.2%***
lmo2219	*prsA2*	16.2% ± 1.3%***

[a]Plaque sizes (± standard deviations) of L2 murine fibroblasts infected with transposon insertion mutants. The mean plaque size of the WT strain within each experiment was defined as 100%. The data shown here represent the mean mutant plaque size, relative to the WT strain. Each mutant strain was analyzed in at least three experiments. To test each hypothesis that the mean mutant plaque size differs from 100%, a one-sample two-sided *t*-test was performed using R (http://www.r-project.org/). * $p < 0.005$, ** $p < 0.001$, *** $p < 0.0005$.

In-frame Deletion and Complementation of PrsA2

Given that the insertion mutant in *prsA2* had the greatest defect *in vivo*, combined with data (Fig. 2-2, Table 2-4) suggesting a link between PrsA2 and LLO secretion and/or activity, we continued to characterize this gene. Two different transposon insertions into *prsA2* were isolated, one 317 bp from the start site, one 410 bp (Fig. 2-4a). Although one group of investigators was unable to delete PrsA2 (Milohanic, Glaser et al. 2003), this result – that *prsA2* is dispensable – is consistent with two additional groups that were able to inactivate this gene either by making an in-frame deletion (Chatterjee, Hossain et al. 2006) or by plasmid insertion (Port and Freitag 2007).

Both transposon insertions into *prsA2* had the same blood plate phenotype and plaque defect (data not shown). For the remainder of this study, the insertion 317 bp downstream from the start of the gene was used. However, to confirm that the observed phenotypes were the result of a disruption of *prsA2* and not due to an unlinked mutation, an in-frame deletion of *prsA2*, removing amino acids 9-291 (the protein is 293 amino acids long), was constructed (Camilli, Tilney et al. 1993). This strain, *ΔprsA2*, has the same plaque defect as either transposon insertion (Table 2-5).

To quantify the *in vivo* role of *prsA2*, mice were intravenously injected with WT or *ΔprsA2 L. monocytogenes* and livers and spleens were harvested 48 h postinfection to determine total bacterial loads. Consistent with the results of the competitive index assay for the transposon insertion into *prsA2*, the *ΔprsA2* strain was greater than 5 log less virulent in the liver and 2.8 less virulent in the spleen (Fig. 2-4b). To further confirm the *in vivo* role of *prsA2*, we complemented our in-frame deletion of *ΔprsA2* with a chromosomal copy. Previous studies had found an increase in *prsA2* transcript and protein levels upon *prfA* induction, and a putative PrfA-box had been identified 206 bp upstream of the start of the *prsA2* open reading frame (ORF) (Milohanic, Glaser et al. 2003; Chatterjee, Hossain et al. 2006; Port and Freitag 2007). However, this location places the start of the promoter 90 bp within the 3' end of the upstream gene, *lmo2218*. Of the ten genes confirmed to be directly regulated by PrfA, none have the promoter located within an upstream gene (Scortti, Monzo et al. 2007).

To test whether the putative PrfA-box was dispensable, three different constructs to complement the *ΔprsA2* mutant were designed, each differing at the 5' end. The first contains the putative PrfA-box (labeled #1); the second construct contains just the region directly downstream of the 3' end of the *lmo2218* ORF (labeled #2); and a third control construct that contains just the ORF of *prsA2* (labeled #3) (Fig. 2-4a). The 3' end of each construct includes the 131 bp region downstream of *prsA2*, including the terminator sequence (Fig. 2-4a). Each construct was placed into the integration vector pPL2 (Lauer, Chow et al. 2002) and integrated into the chromosome of the *ΔprsA2* strain. As an additional control, an empty pPL2 vector was also integrated into the parent *ΔprsA2* strain.

The ability of these constructs to complement the plaque defect of the *prsA2* transposon insertion mutant was analyzed. As expected, the *ΔprsA2* strains containing just the ORF or the empty pPL2 vector both produced plaques the same size as the transposon insertion mutant and the *ΔprsA2* strain (Table 2-5). Interestingly, both construct #1 and construct #2 complemented the transposon mutant equally well, suggesting that the PrfA-box was dispensable. The ability of the strain containing construct #2 to complement the in-frame deletion *in vivo* was tested. This construct restored full virulence, as well as complemented the

Figure 2-4

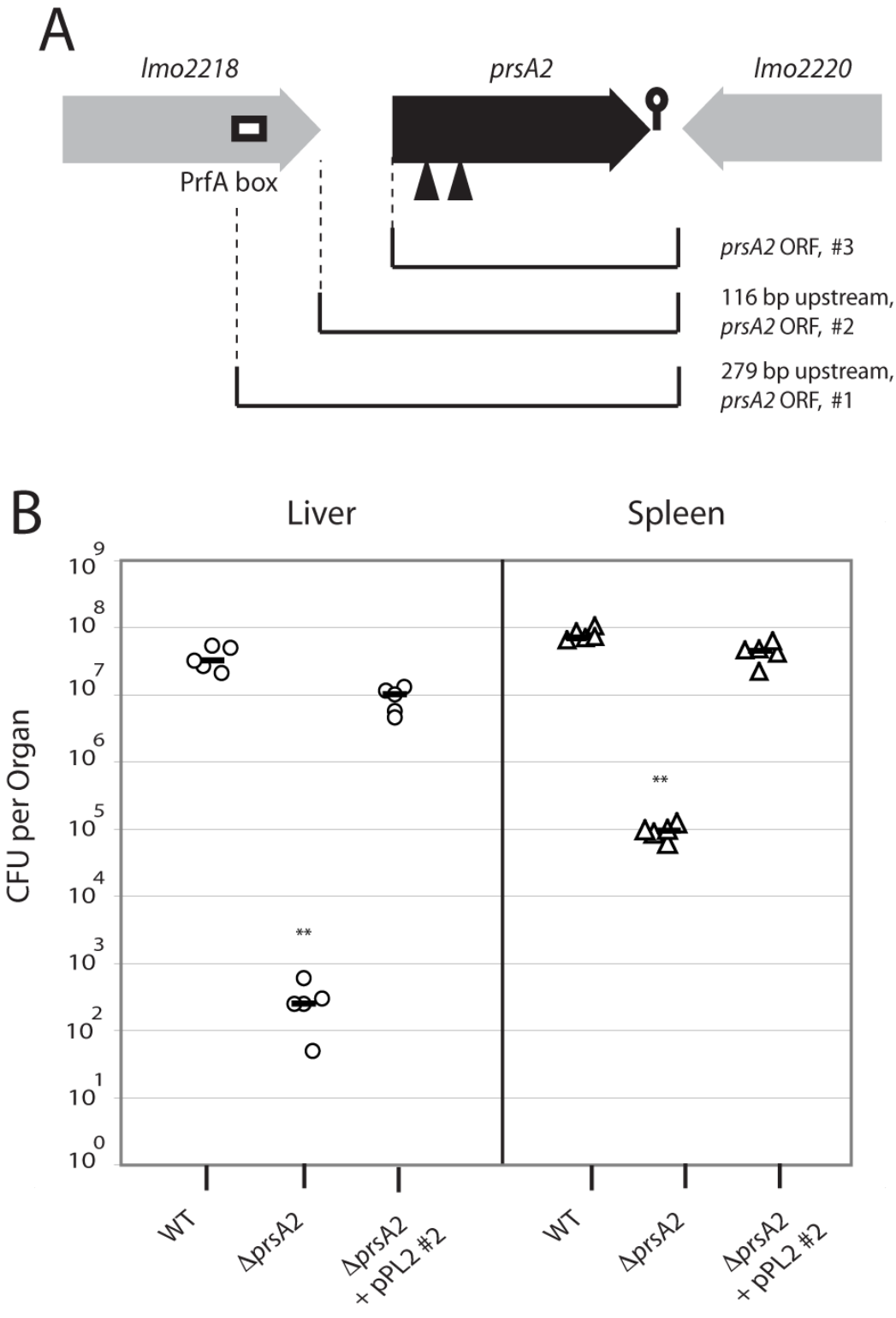
A
lmo2218
prsA2
lmo2220
PrfA box
prsA2 ORF, #3
116 bp upstream, prsA2 ORF, #2
279 bp upstream, prsA2 ORF, #1
B
Liver
Spleen
CFU per Organ
10^9
10^8
10^7
10^6
10^5
10^4
10^3
10^2
10^1
10^0
**
**
WT
ΔprsA2
ΔprsA2 + pPL2 #2
WT
ΔprsA2
ΔprsA2 + pPL2 #2

Continued from previous page

Figure 2-4. Virulence of *L. monocytogenes prsA2* mutants

(A) Schematic of the *prsA2* genomic loci and the three different constructs used to complement *ΔprsA2*. Each construct differed at the 5' end; construct #1 contained the identified PrfA-box; construct #2 contained the region immediately downstream of *lmo2218*; construct #3 contained just the ORF of *prsA2*. The two triangles below *prsA2* indicate the two transposon mutants isolated in this screen. Stem-loop structures denote transcription terminators. (B) WT, *ΔprsA2*, or *ΔprsA2* complemented with construct #2 were analyzed for total bacterial load in the livers (○) and spleens (△) of mice 48 h postinfection. All median values are represented by horizontal lines. Each experiment was repeated. We performed paired Student's t-tests on the total bacterial load data, using R. Under the null hypothesis of no differences, the mean parameter is assumed to be zero. A two-tailed p-value is reported for each mutant. **, $p < 0.005$

TABLE 2-4. Hemolytic Activity of Culture Supernatants and Purified Protein	
Strain	**Hemolytic Activity[a]**
lmo0964::Himar1	40.3% ± 10.6%**
lmo1268::Himar1	59.7% ± 17.1%*
lmo1401::Himar1	69.9 ± 3.9%**
lmo1575::Himar1	29.6 ± 2.6%***
lmo1821::Himar1	101.5% ± 14.3%
ΔprsA2	58.0% ± 13.3%*
ΔprsA2 + #2	88.7% ± 10.8%
Purified Protein	
prsA2::Himar1, $LLO_{(His6)}$	67.2% ± 6.1%**

[a] Hemolytic-activity (± standard deviations) of either culture supernatants or purified protein, relative to WT activity over at least four experiments. Statistical analysis was performed as described in Table 3. * $p < 0.05$, ** $p < 0.005$, *** $p < 0.0005$.

TABLE 2-5. Complementation Data	
Complement Strain	**Plaque Size[a]**
ΔprsA2	18.2% ± 4.6%*
prsA2::*Himar1* + #1	100.6% ± 5.1%
prsA2::*Himar1* + #2	99.1% ± 2.1%
prsA2::*Himar1* + #3	16.3% ± 3.2%
prsA2::*Himar1* + empty pPL2	17.0% ± 3.4%

[a] Plaque sizes (± standard deviations) of L2 murine fibroblasts infected with either the in-frame deletion of *prsA2* or the *prsA2* transposon insertion mutant complemented with different constructs. Statistical analysis was performed as described in Table 3. *, $p < 0.005$

hemolytic activity defect of the *ΔprsA2* culture supernatants (Table 2-4), again suggesting that the PrfA-box is dispensable for *prsA2* expression and activity (Fig. 2-4b).

A possible role for PrsA2 in folding exported LLO

Western Blot analysis of LLO secretion in the *ΔprsA2* mutants revealed an unusual banding pattern: in addition to a major band at approximately 58 kDa (LLO), there were two smaller, minor bands at approximately 43 and 41 kDa (Fig. 2-5a). This laddering pattern is absent in the *ΔprsA2* + #2 complemented strain.

To confirm that these additional bands were LLO, the transposon insertion mutant was transduced into two different backgrounds: a WT strain containing an in-frame deletion of *hly* (DP-L2161) and a WT strain containing a chromosomal copy of *hly* with the point mutation S44A (DP-L4057) that relieves translational inhibition of LLO. This strain produces and secretes LLO at a constant rate throughout the entire growth cycle of the bacteria (Jones and Portnoy 1994; Hodgson 2000; Schnupf, Portnoy et al. 2006). These additional strains were subjected to Western Blot analysis. In addition to the lack of the major LLO band in the Δ*hly*, *prsA2::Himar1* strain, both lower molecular weight bands were absent, consistent with the hypothesis that these bands were species of LLO. Additionally, in the LLO_{S44A}/*prsA2*::*Himar1* mutant there was an increase in the size and intensity of the major LLO band as well as in the smaller bands. Furthermore, a smaller set of two bands was visible at approximately 33.5 and 32 kDa; further comparison revealed the presence of these bands in the *ΔprsA2* mutant (Fig. 2-5a). These results strongly suggested that the additional bands in the *prsA2* mutant backgrounds were lower molecular mass species of LLO.

We hypothesized that these additional bands might be degradation products. Bacteria have several mechanisms to refold or degrade misfolded secreted proteins. *B. subtilis*, for example, has several known extracytoplasmic quality control systems including the serine protease family HtrA and CWBP52 (Tjalsma, Bolhuis et al. 2000). To investigate this possibility further, a C-terminal epitope tagged copy of LLO was first employed; LLO contains a cleavable signal sequence at its N-terminal end (Schnupf and Portnoy 2007).

The transposon insertion into *prsA2* was transduced into a WT strain containing a chromosomal copy of LLO with a C-terminal FLAG-tag (DP-L4361). The Western Blot was then repeated on the LLO_{FLAG} and the *prsA2*::*Himar1* LLO_{FLAG} strains, probing for both LLO and the FLAG epitope. Consistent with our previous results, when probed with the anti-LLO antibody, the discrete, smaller bands were of greater intensity in the LLO_{FLAG} *prsA2* transposon mutant. However, these bands did not appear when probed with the anti-FLAG antibody (Fig. 2-5b). These results are consistent with our hypothesis that LLO was undergoing C-terminal cleavage in the *prsA2*-disrupted backgrounds.

Purified LLO secreted by the *prsA2* mutant is less active

Both the WT and *ΔprsA2* mutant secreted approximately the same level of full-length LLO as indicated by Western Blot analysis of proteins isolated from culture supernatants (Fig. 2-5a). We wondered then if the decrease in LLO hemolytic activity of the *ΔprsA2* mutant (Table 2-4) was due to misfolded full-length LLO. Alternatively, it was possible that the smaller fragments of LLO were acting in a dominant negative fashion, perhaps by oligomerizing with the full-length toxin but preventing membrane insertion. To address this possibility, full-length LLO was purified from WT or *prsA2::Himar1* supernatants and tested for hemolytic activity.

Figure 2-5

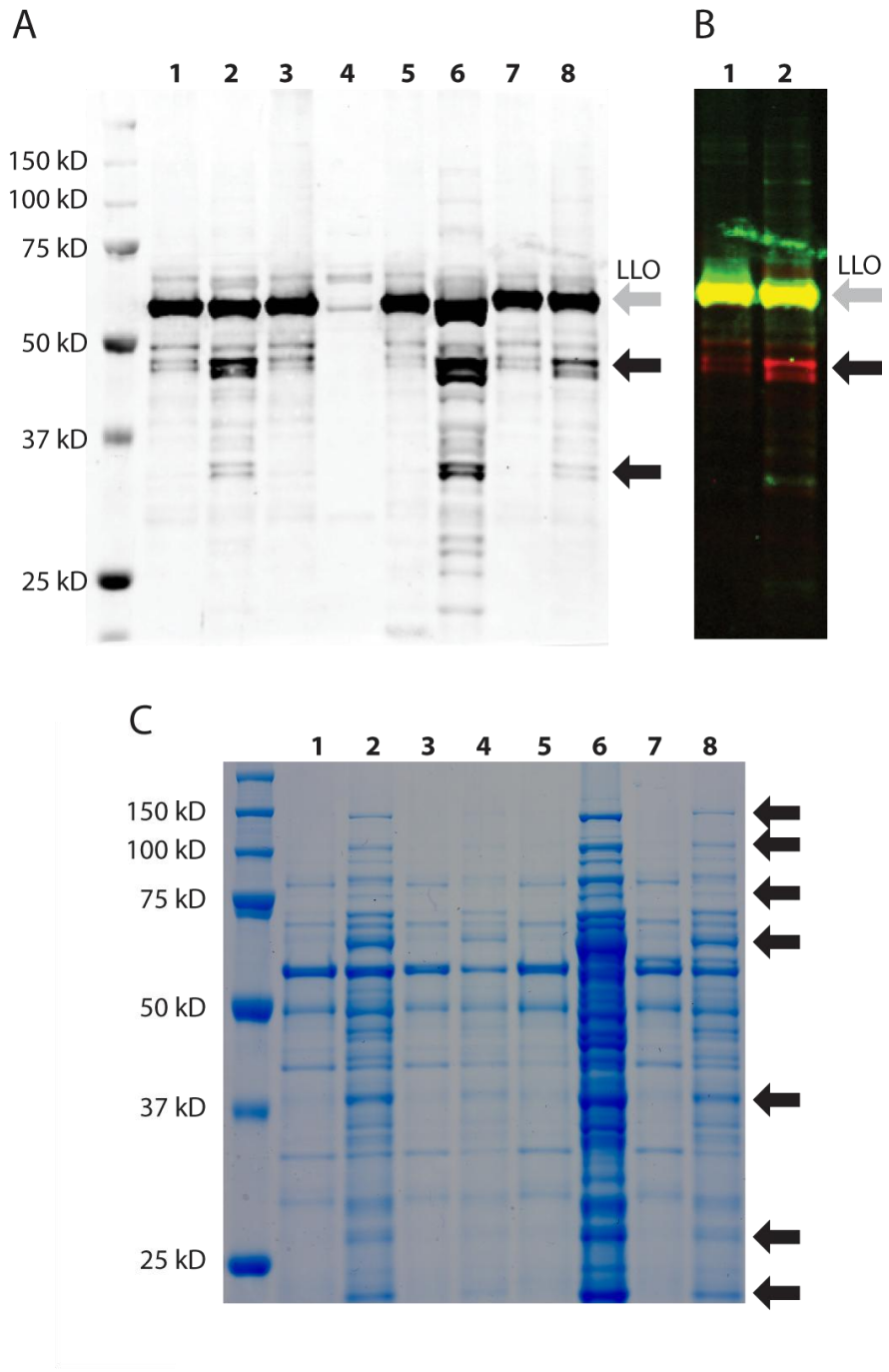
A
1 2 3 4 5 6 7 8
150 kD
100 kD
75 kD
50 kD
37 kD
25 kD
LLO
B
1 2
LLO
C
1 2 3 4 5 6 7 8
150 kD
100 kD
75 kD
50 kD
37 kD
25 kD

Continued from previous page

Figure 2-5. PrsA2 affects the secretion of LLO

(A) A Western Blot of secreted proteins probed with a polyclonal anti-LLO antibody from the following bacterial strains (from left-right): (1) WT; (2) *ΔprsA2*; (3) *ΔprsA2*, $tRNA^{Arg}$::pPL2 #2; (4) *⊿hly, prsA2*::*Himar1*; (5) LLO_{S44A}; (6) LLO_{S44A}, *prsA2*::*Himar1*; (7) LLO_{FLAG}; (8) LLO_{FLAG}, *prsA2*::*Himar1*. The black arrows indicate the increased presence of the two bands at ~42 kDa and at ~33 kDa in the *prsA2* mutant backgrounds relative to the non-mutated or complemented *prsA2* backgrounds. (B) Western Blot analysis of the strains (1) LLO_{FLAG} and (2) LLO_{FLAG}, *prsA2*::*Himar1* probed with anti-LLO (red) and anti-FLAG (green). The two probes overlap at the major band at 58 kDa, but do not at ~42 kDa. (C) Colloidal Coomassie stain of an SDS-PAGE gel of purified secreted proteins from the same strains as in (A). The black arrows indicate the presence of additional bands in the *⊿prsA2* mutant backgrounds (including *Δhly*), including molecular masses greater than that of LLO.

The *prsA2* transposon insertion was transduced into a WT strain of *L. monocytogenes* containing a C-terminally histidine-tagged allele of LLO (DP-L3481, LLO_{His6}) (Gedde, Higgins et al. 2000). LLO_{His6} was isolated from 8 h culture supernatants from both WT and the *prsA2::Himar1* strains by nickel affinity chromatography. Purity of the eluted toxin was confirmed by analysis of the preparation with SDS-PAGE. Additionally, Western Blot analysis was used to confirm that the smaller N-terminal fragments of LLO (Fig. 2-4a) were not present (data not shown). Toxin purified from both the WT and the *prsA2*::*Himar1* strains was then diluted appropriately and analyzed for hemolytic activity. The activity of the purified, full-length LLO_{His6} isolated from the *prsA2*::*Himar1* strain was 67.2% of WT activity, similar to the value obtained for the hemolytic activity obtained the from the *ΔprsA2* culture supernatants (Table 2-4). This data is consistent with our hypothesis that PrsA2 is specifically involved in the proper folding of secreted LLO.

Other potential substrates for PrsA2

Examination of a colloidal Coomassie stained SDS-PAGE gel of proteins precipitated from the supernatants of our strains revealed the addition of several bands – both higher in molecular weight than LLO and lower – in our *prsA2* mutant as compared to either the WT or *⊿prsA2* complemented strains (Fig. 2-5c).

L. monocytogenes secretes a broad range phospholipase C (PC-PLC), which contributes to the ability of the bacteria to escape from the primary and secondary vacuoles. The lecithinase activity of PC-PLC, encoded by *plcB*, can be assessed by measuring zones of opacity on an LB agar plate containing egg-yolk agar (Vazquez-Boland, Kocks et al. 1992; Marquis, Doshi et al. 1995; Smith, Marquis et al. 1995). To investigate whether PC-PLC was affected in the *prsA2* mutant, the *ΔprsA2* mutants were tested for lecithinase activity. The *ΔprsA2* strain showed a decrease zone of opacity on egg yolk agar compared to both WT and the #2 complemented *ΔprsA2* strains (Fig. 2-6a). To increase the resolution of this assay, the SLCC-5764 (DP-L861) strain of *L. monocytogenes* was utilized. SLCC-5764 contains a *prfA** allele, a dysregulated allele of *prfA* that increases the expression of the PrfA-regulated genes, including *plcB* (Leimeister-Wachter, Goebel et al. 1989; Grundling, Gonzalez et al. 2003). The *prsA2* transposon insertion was transduced into this strain, which was spotted onto an egg-yolk agar plate with the parent SLCC-5764 strain. Again, the disruption of *prsA2* caused a visible decrease in the amount of lecithinase activity (Fig. 2-6a).

Given that *prfA* appears to be dispensable for *prsA2* expression, we investigated whether the disruption of *prsA2* causes the disruption of other exported proteins not involved in virulence. *L. monocytogenes* is motile and flagellated at temperatures 30°C and below, while non-motile at 37°C (Grundling, Burrack et al. 2004; Gray, Freitag et al. 2006). Given that components of the flagellar machinery are recognized by elements of the immune system, it has been proposed that *L. monocytogenes* actively downregulates the expression of these components upon infection (Grundling, Burrack et al. 2004). Therefore, to assess the effect of PrsA2 on secretion in a context where PrfA activity is low, the flagella-based motility of the mutants was compared.

Cultures of WT, *ΔprsA2,* the #2 complemented *ΔprsA2* strain, *ΔflaA* (DP-L4650) and a strain containing in an in-frame deletion *prfA* (DP-L4317), were all spotted on low percentage motility agar LB plates for 24 and 48 h at 30°C. The *ΔprsA2* strain had a smaller swarm pattern than did the WT or #2 complemented strains, roughly half the size (Fig. 2-6b). This defect was, however, considerably smaller than the defect in the *ΔflaA* strain, indicating only a partial loss

of swarming ability. This phenotype is consistent with the previous results from the blood and egg-yolk agar plates: in all instances, there was only partial loss of activity rather than a complete abrogation. Finally, the *ΔprfA* strain's swarm size was equivalent to both WT and the *ΔprsA2 +* #2 complemented strain, consistent with the complementation results that PrfA appears dispensable for *prsA2* expression and activity.

Figure 2-6

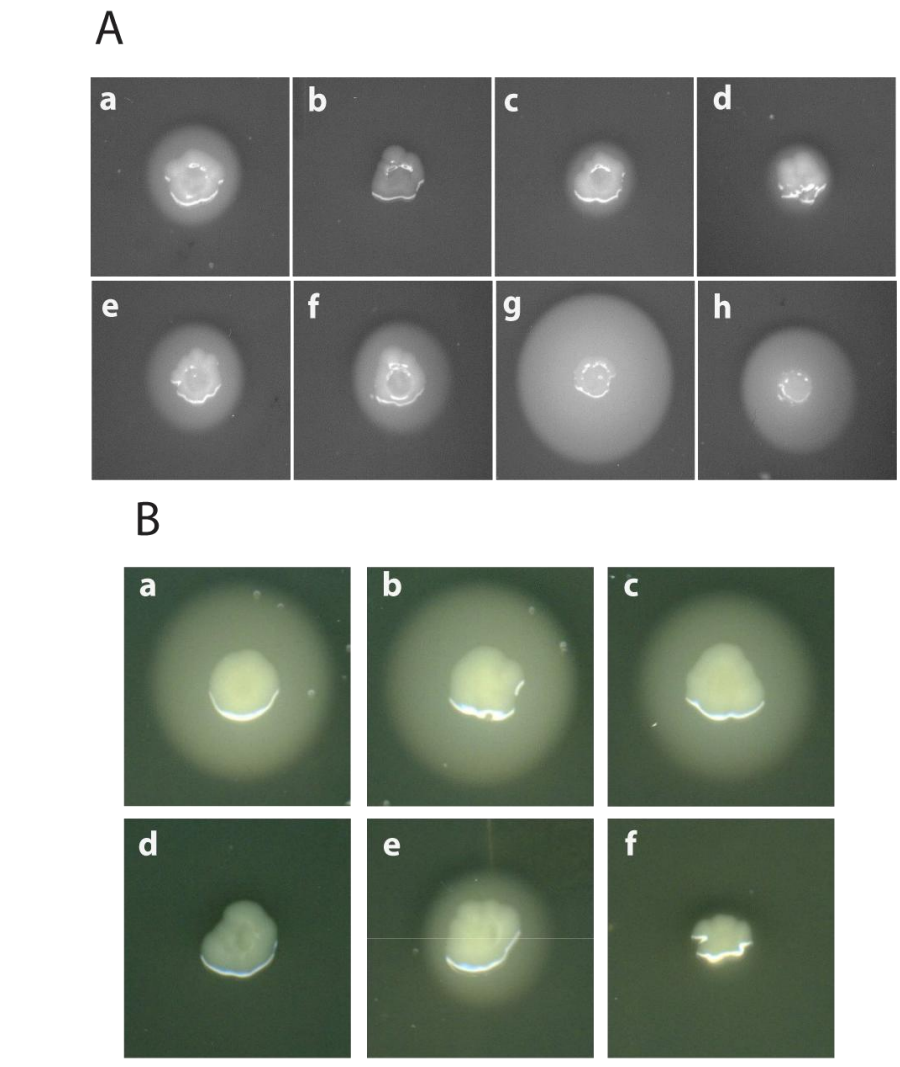
A
a
b
c
d
e
f
g
h
B
a
b
c
d
e
f
C
WT
ΔflaA
ΔprsA2
ΔprsA2 + #2
ΔprfA
24 h
48 h
a
b
c
d
e
f
g
h
i
j

Continued from previous page

Figure 2-6. PrsA2 affects the secretion of additional substrates

(A) PrsA2 mutants affect PC-PLC (lecithinase activity). Overnight cultures grown at 30°C were spotted on 5% w/v egg-yolk LB-G1P plates and grown for 24 h. (a) WT; (b) *⊿plcB* (DP-L1935); (c) *ΔprsA2*; (d) *prsA2*::*Himar1*; (e) *ΔprsA2*, $tRNA^{Arg}$::pPL2 #1; (f) *ΔprsA2,* $tRNA^{Arg}$::pPL2 #2; (g) SLCC-5764 strain of *L. monocytogenes*; (h) SLCC-5764, *prsA2*::*Himar1*. (B) PrsA2 mutants affect swarming ability. Overnight cultures grown at 30°C were spotted on 0.35% BHI plates and grown for 24 h (a-e) or 48 h (f-j) at 30°C. (a, f) WT; (b, g) *⊿flaA* (DP-L4650); (c, h) *ΔprsA2*; (d, i) *ΔprsA2*, $tRNA^{Arg}$::pPL2 #2; (e, j) *⊿prfA*.

DISCUSSION

In this study, we have described the construction of a *Himar1* based transposon system for use in *L. monocytogenes*. This construction decreases many of the issues observed using previous transposon systems in *L. monocytogenes*, specifically instances of multiple transposon hops within a single bacterium, clonal populations within a given library (Cao, Bitar et al. 2007), and insertion "hot spots" (Camilli, Portnoy et al. 1990). Furthermore, the inclusion of T7 promoters makes negative selection screens possible. This transposon delivery system is also effective in *B. anthracis* (J. Beaber, J. Zemansky, D. A. Portnoy, R. Calendar, unpublished results).

In order to identify extragenic factors involved in LLO production, activity, or secretion, 50,000 transposon insertions were screened on sheep's blood agar plates for hypohemolytic phenotypes. Critical for virulence, LLO is subject to multiple levels of regulation (Schnupf and Portnoy 2007). Given the increased complexity of *Himar1 mariner* transposon mutant libraries, the likelihood of identifying extragenic regulators of LLO, and therefore likely virulence determinants, was increased. Additionally, to our knowledge, this study represents the first published screen for mutants with a hypohemolytic phenotype rather than for those with an ahemolytic phenotype. As a result of the screen, 193 mutants were initially identified as having a hypohemolytic phenotype by visual inspection (Table 2-2). Plaque assays in murine cells were performed on 51 mutants with the most discernable visible defects (Table 2-2).

Given the importance of *hly* in virulence, we expected that a greater fraction of our mutants would exhibit defects escaping from the primary and secondary vacuole in the *ex vivo* plaque assay (Schnupf and Portnoy 2007). Curiously, of the mutants analyzed, only eight had repeatable, substantive plaque defects. One possibility for the discrepancy between blood plate phenotype and the lack of an *in vivo* defect may be that the phenotypes revealed on blood agar might be too subtle to be physiologically relevant. The blood plate assay is very sensitive, as zones of hemolysis are the result of discrete foci of toxin activity occurring over the course of 48 h.

The screen successfully identified both potential novel virulence factors and additional roles for previously described factors: of the eight mutants with both a blood plate phenotype and a plaque defect, six genes – *yjbH*, *clpX*, *ymdB*, *ytqI*, *prpC*, and *cggR* – have not previously been characterized in *L. monocytogenes*. Although the other two genes, *mprF* and *prsA2*, are known to contribute to virulence, a potential relationship between each of these factors and the secretion of LLO has not previously been established (Milohanic, Glaser et al. 2003; Chatterjee, Hossain et al. 2006; Thedieck, Hain et al. 2006; Port and Freitag 2007).

The six characterized mutants displayed a range of defects in the *ex vivo* plaque assay, the hemolytic-activity assay, and *in vivo* (Tables 3 and 4, Figures 3 and 4). The genes *ymdB* (the gene containing a putative metallo-phosphoesterase domain) and *ytqI* (the putative oligoribonuclease) have not been well characterized and speculating about a potential role in LLO regulation is difficult. Additional work is necessary in order to determine whether the phenotypes of these mutants are the result of a direct relationship with LLO, the PrfA regulon, or a more general pleiotropic effect. However, the identification of these genes does suggest that there are as yet unidentified factors or pathways that regulate LLO production, secretion, or activity.

More intriguing are the transposon insertions in *yjbH*, *clpX*, *prpC*, and *prsA2*. The association of a mutation in *prpC*, the phosphatase directly upstream of the eukaryotic-like serine/threonine kinase, with a virulence defect parallels a similar defect in *prpC*/*prkC* mutants of other Gram-positive pathogens (Rajagopal, Clancy et al. 2003; Echenique, Kadioglu et al. 2004; Jin and Pancholi 2006; Kristich, Wells et al. 2007). Based on BLAST alignments (http://blast.ncbi.nlm.nih.gov/), PrpC is approximately 40% identical and 60% similar to its likely homolog in each of *S. pyogenes* M1 GAS, *S. agalactiae* GBS, *E. faecalis*, and *S. pneumoniae*. Equally intriguing, a recent study has suggested a role for PrkC in *B. subtilis* in sensing the extracellular environment by binding fragments of peptidoglycan (Shah, Laaberki et al. 2008). It is therefore tempting to ascribe a direct role for *prpC* and *prkC* in *L. monocytogenes* virulence, possibly by allowing the bacterium to "sense" its environment. However, while mutations in these genes are known to cause changes in the expression of certain virulence factors, they have also been linked to effects on growth, morphology, cell division, and other pleiotropic effects (Rajagopal, Clancy et al. 2003; Jin and Pancholi 2006). Additional work is required to discern the precise relationship between this kinase/phosphatase and members of the PrfA regulon. The reason a difference exists between the phenotype on the blood agar plate (Fig. 2-2) and the results of the hemolytic-activity assay (Table 2-4) remains unclear.

Mutants in *yjbH* and *clpX* displayed similar blood plate phenotypes, similar hemolytic-activity, and similar virulence defects (Figures 2 and 3, Tables 3 and 4). In *B. subtilis*, their predicted homologs have recently been characterized as regulating the activity of the disulphide stress regulator Spx (Larsson, Rogstam et al. 2007). This transcription factor is responsible for maintaining thiol-redox homeostasis (Nakano, Kuster-Schock et al. 2003; Larsson, Rogstam et al. 2007), and it is tempting to speculate that the *L. monocytogenes spx* (*lmo2191*) gene product may explain one of the long-standing questions regarding the toxin. The CDCs, including LLO, are also known as the "thiol-activated" cytolysins due to the presence of a conserved cysteine residue (Smyth and Duncan 1978). Crude preparations of these toxins are readily oxidized and require the addition of a reducing agent to reverse the effects. However, this effect diminishes upon increasing the purity of the preparation, and mutating the cysteine to an alanine does not eliminate LLO hemolytic activity (Provoda and Lee 2000). One possible explanation for the conservation of this cysteine residue is that it serves a regulatory role, and may be the target site of some external molecule. Perhaps the *L. monocytogenes* Spx controls a factor that binds to this residue, sequestering activity. YjbH and/or ClpX would then work to limit the repression by Spx. Consistent with this hypothesis, a transposon insertion into a gene encoding thioredoxin-like protein (*lmo1609*) was identified (Table 2-2), although this mutant did not have a significant plaque defect.

Most interesting was our finding that a transposon insertion into *prsA2* affected LLO secretion and activity. There was a distinct blood plate phenotype and plaque defect for this mutant (Fig. 2-2, Table 2-3). Furthermore, *ΔprsA2* culture supernatant and purified, full-length LLO from a strain containing a transposon in *prsA2* had similar decreased levels of hemolytic activity relative to WT (Table 2-4). Finally, Western blot analysis revealed that while the total levels of LLO exported into the supernatant were similar to WT levels, there were additional lower molecular weight species of the toxin (Fig. 2-5a). The amounts of these species decreased in the complemented strains and drastically increased in a strain of *L. monocytogenes* that overproduced LLO (Fig. 2-5a). These additional bands did not stain with an

anti-FLAG antibody when purified from a *prsA2* mutant expressing a C-terminal FLAG-tagged copy of LLO, indicating C-terminal cleavage (Fig. 2-5b). These results strongly suggested that PrsA2 contributes to the proper folding of extracytoplasmic LLO.

Given the additional results that strains lacking PrsA2 have diminished lecithinase activity and ability to swarm, it is likely that PrsA2 contributes to the folding of several other exported proteins. We therefore hypothesize that the decrease in LLO activity, as well as both the plaque and *in vivo* defects, from *prsA2* mutants arises as a result of multiple misfolded virulence factors. Our lab is currently investigating this possibility.

Previous studies had identified a link between the expression of *prsA2* and the master virulence transcription factor *prfA*: *prsA2* transcript levels were upregulated during intracellular growth (Chatterjee, Hossain et al. 2006); upregulated in bacteria grown in cytosol mimicking media (Milohanic, Glaser et al. 2003); and PrsA2 protein was upregulated in a *prfA** background (Port and Freitag 2007). Given the computationally identified PrfA-box upstream of *prsA2*, it was hypothesized that this gene was directly regulated by PrfA (Milohanic, Glaser et al. 2003). However, our results suggest that PrfA does not directly regulate *prsA2* expression: a 116 bp region upstream of *prsA2* lacking the identified PrfA-box (Fig. 2-4a) was sufficient to complement the transposon insertion *ex vivo* (Table 2-5) and the in-frame deletion in the hemolytic-activity assay and *in vivo* (Fig. 2-4b). While PrfA may indirectly control *prsA2* expression, there appear to be environmental conditions unassociated with virulence, such as swarming, under which *prsA2* expression is independent of PrfA (Fig. 2-6b).

During infection, *L. monocytogenes* undergoes dynamic changes in gene and protein expression (Chatterjee, Hossain et al. 2006). This includes the translation of a variety of different PrfA-regulated genes within a short period of time: the internalins (InlA and InlB), to promote uptake into a cell; LLO, the phospholipases C (PI-PLC and PC-PLC), and Mpl to promote phagosome escape; and then ActA to hijack host-cell actin (Vazquez-Boland, Kuhn et al. 2001). The PrfA-regulated genes comprise the most abundant secreted proteins during this transition (data not shown) (Scortti, Monzo et al. 2007).

Interestingly, the effect of the *prsA2* mutants on secreted proteins became more pronounced the more LLO was secreted (Fig. 2-5c, lanes 2, 4, and 8); the presence of the additional bands noted in the figure legend is the most pronounced in the LLO_{S44A} background, followed by the WT background, and then the *Δhly* background. We therefore hypothesize that *L. monocytogenes* PrsA2 is necessary for the bacterium during times of increased export stress. This includes intracellular growth, when multiple virulence factors – especially LLO – are produced and secreted in large quantities. Export of these factors occurs through the Sec machinery. Entry and passage through the Sec translocation channel requires substrate proteins to be in a primarily unfolded state (Tjalsma, Bolhuis et al. 2000). Folding at the *trans* side of the membrane is then facilitated by a number of chaperones known as the foldases and including PPIases (of which PrsA2 is a member) (Tjalsma, Bolhuis et al. 2000). Accumulation of unfolded LLO in the space between the extracytoplasmic side of the membrane and the cell wall in the mutants lacking *prsA2* may lead to either protein degradation or the release of misfolded toxin, resulting in the decrease in hemolysis *in vitro* (Fig. 2-2, Table 2-4) and the virulence defect *in vivo* (Fig. 2-4). It is likely that other virulence factors, such as PC-PLC (Fig. 2-6a), are similarly affected, although whether these factors interact with PrsA2 directly remains unclear. Precedence for this model exists in *B. subtilis*, where the expression of chaperones has

been shown to increase in response to extracytoplasmic secretion stress (although these studies were performed in a mutant *prsA* background) (Hyyrylainen, Bolhuis et al. 2001; Westers, Westers et al. 2006).

Our hypothesis may explain results from other studies. Gram-positive bacteria have a quality control system for exported factors within the extracytoplasmic space between the cell membrane and peptidoglycan layer (Tjalsma, Bolhuis et al. 2000). These mechanisms include the proteolytic degradation of the misfolded protein, including the HtrA family of proteases (Tjalsma, Bolhuis et al. 2000; Clausen, Southan et al. 2002). A recent study found that *L. monocytogenes* HtrA levels increased in *prfA** strains (Port and Freitag 2007), and HtrA has been shown to contribute to virulence (Stack, Sleator et al. 2005; Wilson, Brown et al. 2006). Our hypothesis is consistent with a model in which under increased export stress, including that experienced upon infection, *L. monocytogenes* upregulates expression of several factors, including multiple external chaperones such as PrsA2 to manage this stress. These chaperones may prove to be potential targets for therapeutic interventions.

ADDENDUM

The genetic screen described above generated a large set of *L. monocytogenes* mutants presenting a variety of hemolytic phenotypes. Although PrsA2 was the only mutant that we initially pursued for publication, we explored the significance of other mutants in the context of virulence and general bacterial fitness as well. The mutants that drew the majority of our attention were in *lmo1821* (*prpC*), a hypohemolytic mutant in a eukaryotic-like serine/threonine phosphatase discussed above and below, and *lmo2511* (*hpf*), a hyperhemolytic mutant that will be described at length in Chapter 3. Each of these mutants exhibited a combination of phenotypes that indicated it might be important in bacterial virulence or physiology. In addition, a small follow-up secondary screen was done on the remainder of the hyperhemolytic mutants, which were not mentioned in the published work above but comprised roughly half of the mutants derived from the hemolytic screen. In the following pages we will present a small amount of background information on PrpC, explain why we selected it for further study, and describe the follow-up experiments that have been performed thus far. We will also list the remainder of the hyperhemolytic mutants and describe immediate follow-up experiments that were performed.

PrpC

As discussed above, previous research on eukaryotic-like serine/threonine kinase/phosphatase pairs homologous to those encoded by *lmo1820* and *lmo1821* in *L. monocytogenes* has been done in several bacteria, both pathogenic and non-pathogenic (Gaidenko, Kim et al. 2002; Rajagopal, Clancy et al. 2003; Kang, Abbott et al. 2005; Shah and Dworkin 2010). These proteins have been assigned a variety of names in the literature; we have chosen to adopt the *B. subtilis* nomenclature of PrpC and PrkC because of the close evolutionary relationship between *B. subtilis* and *L. monocytogenes*. PrkC and PrpC appear to be a matched pair in *L. monocytogenes* based on their genomic proximity and shared synteny with homologs from other species. One other predicted serine/threonine kinase of this type is encoded by *lmo0618*, but based on the lack of conservation of critical catalytic residues it is predicted to be inactive (M. L. Reniere, unpublished data). No other predicted serine/threonine phosphatases of this type are encoded in the *L. monocytogenes* genome.

Homologs of PrkC have been shown to regulate diverse panels of genes and affect a wide variety of bacterial activities, including biofilm formation, cell wall integrity, sporulation, virulence, and competence (Madec, Laszkiewicz et al. 2002; Echenique, Kadioglu et al. 2004; Kang, Abbott et al. 2005; Donat, Streker et al. 2009). While their regulatory roles are global in some organisms (Saskova, Novakova et al. 2007), very specific functional roles have been assigned in others. The *B. subtilis* homolog of PrkC has been shown to sense soluble peptidoglycan fragments at very low concentrations and induce germination of spores. This activity appears to be dependent on the presence of four extracytoplasmic PASTA (Penicillin binding protein and Ser/Thr kinase-associated) domains, which bind peptidoglycan fragments directly (Shah, Laaberki et al. 2008; Squeglia, Marchetti et al. 2011). There is no evidence for sporulation in *L. monocytogenes*, but we were intrigued by the concept of a kinase and phosphatase with opposing activities (Gaidenko, Kim et al. 2002) that sense bacterial cell wall fragments to regulate growth. It has been reported that the translation elongation factor EF-Tu

is a target of the *L. monocytogenes* homolog of PrpC, in keeping with a role in growth regulation. These phenotypes, along with the 10- to 100-fold virulence defect displayed by the *prpC*::*Himar1* transposon insertion mutant (Fig. 2-3), convinced us that further study might yield valuable insight into *L. monocytogenes* virulence or physiology.

Before proceeding further, we constructed an in-frame deletion in *prpC* to ensure that the phenotype we had observed was in fact the result of disruption of the *prpC* coding sequence rather than some unexpected side-effect of the transposon insertion. This mutant was constructed by allelic replacement as described above (Smith and Youngman 1992), although the low frequency at which the mutant was recovered indicated that the deletion carried a fitness cost. We also constructed an IPTG-inducible complementation vector that could be introduced into the *L. monocytogenes* chromosome in single copy at an ectopic site (Lauer, Chow et al. 2002). Using these strains, referred to as Δ*prpC* and Δ*prpC*-comp, we tested bacterial fitness and virulence potential using several well-established assays.

We first examined growth in rich media; the transposon insertion mutant in *prpC* showed a slight growth defect which we wanted to confirm was caused by disruption of *prpC*. WT, Δ*prpC*, and Δ*prpC*-comp with increasing concentrations of IPTG were observed over the course of nine hours' growth in BHI. The in-frame deletion displayed a virulence defect similar to that of the transposon insertion (not shown), and the inducible complemented strain showed a saturable, dose-responsive recovery of the wild-type growth rate (Fig. 2-7a). Bacterial doubling times calculated over the period between one and four hours post-inoculation reflected the same dose responsive complementation (Fig. 2-7b). The same complementation construct restored wild-type growth in the transposon insertion mutant (data not shown).

Next, we examined Δ*prpC* survival in two cell culture assays commonly used to assess *L. monocytogenes* fitness. We examined plaque formation in the mouse L2 fibroblast plaque assay described above (Sun, Camilli et al. 1990). Similar to growth in broth, a decrease in plaquing efficiency was evident in the Δ*prpC* mutant and plaquing efficiency was recovered in the Δ*prpC*-comp strain with IPTG induction (Fig. 2-8a). Although recovery was not as robust in this assay, we believe the rate or efficiency of IPTG penetration into host cells may have hindered induction of the complementation construct. Intracellular growth of the Δ*prpC* and *prpC*::*Himar1* strains was also examined in intracellular growth curve assays, but both grew almost identically to WT in the J774 macrophage cell line (Fig. 2-8b).

Whole-genome expression microarray analysis was then performed with the goal of better understanding the bacterial transcriptional response to the absence of PrpC. Two separate microarray analyses were performed, one comparing WT to Δ*prpC*, and the other comparing Δ*prpC*-comp in absence of IPTG to the same strain grown with 50 µM IPTG (a concentration that fully rescues growth rate in broth). Only transcripts that were regulated in the same direction by ≥ two-fold in both arrays are listed below (Table 2-6). Consistent with the reported cell-wall-specific functions of the PrkC/PrpC pair in other bacteria, we observed groups of cell division and shape determining factors (e.g. MreD, FtsW/RodA) and cell wall synthesis and remodeling genes (e.g. PBPs, autolysins and their regulators) in the set of transcripts upregulated in the absence of PrpC. Also present were some antibiotic- and cell-wall-stress response transcripts, suggesting the possibility that cell envelope integrity is compromised in the absence of PrpC.

Figure 2-7

A

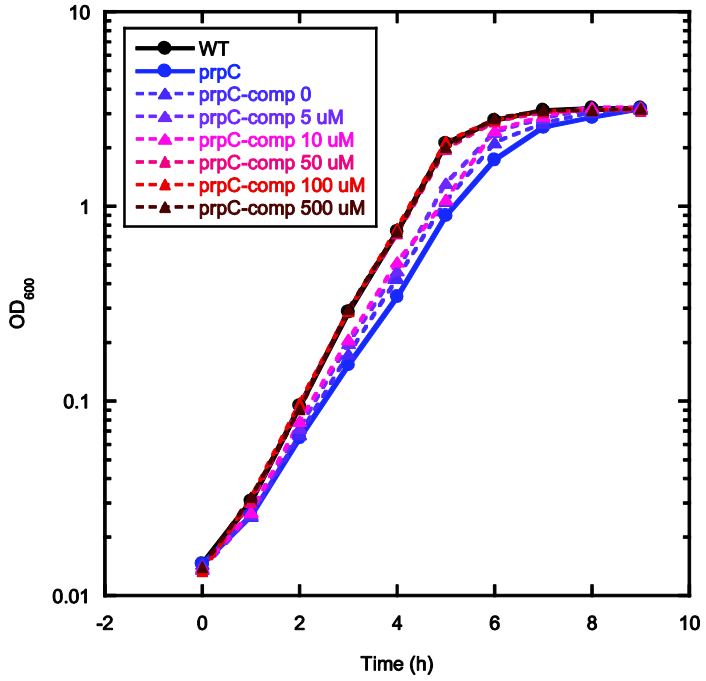

B

Strain	Doubling Time
ΔprpC	48.23
ΔprpC-comp 0mM	44.31
ΔprpC-comp .005mM	43.18
ΔprpC-comp .01mM	42.13
ΔprpC-comp .05mM	39.21
ΔprpC-comp .1mM	39.15
ΔprpC-comp .5mM	39.73
WT	39.07

Figure 2-7. Growth of Δ*prpC* and Δ*prpC*-comp in rich media

(A) Growth of WT (black symbols), Δ*prpC* (blue symbols), and Δ*prpC*-comp with varying concentrations of IPTG inducer (purple to red symbols with increasing IPTG concentration) were grown in BHI broth for a period of nine hours while OD_{600} was monitored hourly. (B) Average doubling times (minutes) of the above strains, calculated based on bacterial growth between one and four hours post-inoculation.

Figure 2-8

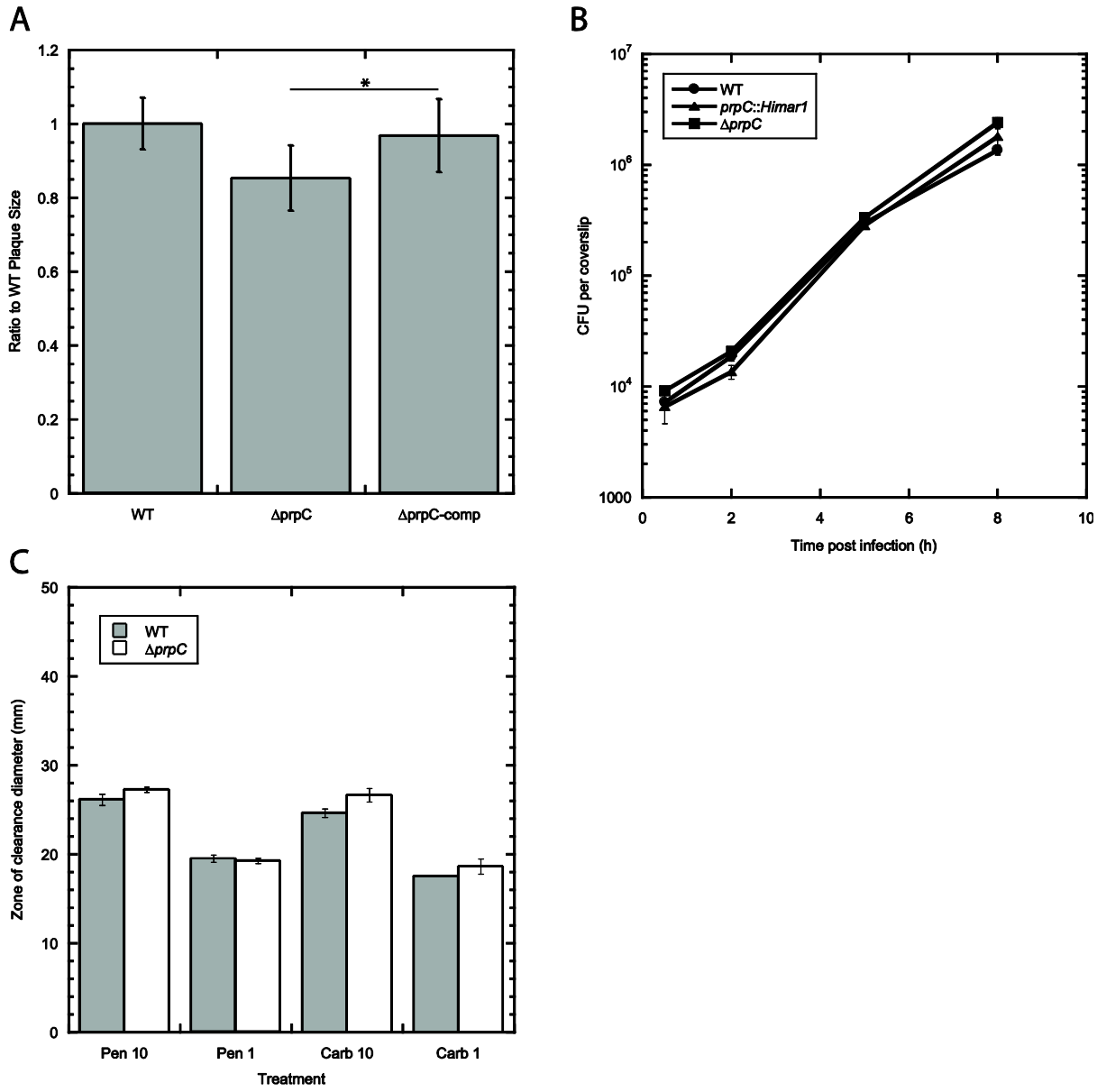

Figure 2-8. Growth and survival of PrpC mutants in host cells and in cell-wall-acting antibiotics

(A) Average sizes of plaques formed in a monolayer of L2 fibroblast cells after three days of growth at 37°C; (B) CFU counts from within J774 macrophage-like cells infected with WT (●) *prpC*::*Himar1* (▲) and Δ*prpC* (■) *L. monocytogenes* at the specified time points; (C) Diameters of growth inhibition zones observed when antibiotic-soaked filter disks were placed in the middle of a forming lawn of *L. monocytogenes*. Concentrations of antibiotic are listed in mg/mL. *$p < 0.05$.

Interestingly, the transcript of the c-di-AMP synthase gene *dacA* is among the most upregulated of all transcripts in the Δ*prpC* background. The function of c-di-AMP in the bacterial cell is not yet understood, but it is known to be essential for optimal growth and virulence (C.E. Witte *et al.*, submitted). A connection between peptidoglycan sensing by PrkC and c-di-AMP production is an intriguing possibility.

The set of downregulated transcripts includes an autolysin as well, suggesting that the particular remodeling responses controlled by PrkC/PrpC may involve certain peptidoglycan modifications but not others. Five PTS system components, a variety of catabolic enzymes, and flagellar components and regulators are also among the downregulated transcripts, suggesting that the response to *prpC* deletion may be one of slowed growth and stasis. Further investigation will be required to better understand the basis for and consequences of these transcriptional responses.

We hypothesized that the observed regulation of genes involved in cell wall remodeling and stress responses might indicate a weakened cell wall and increased susceptibility to cell-wall-acting antibiotics. A filter disk diffusion assay was used to test the sensitivity of WT and Δ*prpC* to the β-lactam antibiotics penicillin and carbenicillin. Surprisingly, Δ*prpC* showed no significant increase or decrease in sensitivity to either drug at the concentrations tested (Fig. 2-8c). However, the possibility remains that different concentrations or different antibiotics would reveal a cell wall weakness in Δ*prpC*.

The above results suggest potentially interesting roles for PrkC/PrpC in *L. monocytogenes* homeostasis and virulence. Others in the Portnoy Lab have continued to investigate these factors, and we remain hopeful that interesting links between this sensory apparatus and basic *L. monocytogenes* biology exist that have yet to be discovered.

Hyperhemolytics

The set of transposon mutants that produced hypohemolytic phenotypes has been published, described, and listed above. The set of transposon mutants that produced hyperhemolytic phenotypes has scarcely been investigated. To assess which of these mutants were worthy of future study, we performed additional secondary screening on the entire set of hyperhemolytic mutants. We elected to use the L2 fibroblast plaque assay as a secondary screen to identify mutants of particular interest because it has historically been an accurate predictor of virulence in *L. monocytogenes* (Sun, Camilli et al. 1990). One set of genes that appeared particularly interesting based on the results of plaque assays was the *opp* operon, *lmo2192* through *lmo2196*, encoding an oligopeptide permease complex. Due at least in part to a prominent blood plate phenotype, a total of 13 independent transposon insertion mutants were isolated in *lmo2194*, *lmo2195*, and *lmo2196*. These mutants ranged in plaque size from 9.5 to 19.2 percent of WT (Table 2-7), a defect large enough that we believed a virulence phenotype was all but certain. Perplexingly, no defect was observed, either in intracellular growth in tissue culture cells or in competitive index experiments in mice (data not shown). A single report on an *oppA* mutant in the LO28 strain of *L. monocytogenes* has shown defects in both of the above assays. Based these conflicting results, we believe this must be a strain- or cell-type-specific phenotype. The frustrating lack of agreement between our results and others' led us to abandon study of transposon mutants in the *opp* operon.

The balance of the hyperhemolytic transposon insertion mutants were also screened by L2 plaque assay. Many produced plaques near WT in size, but several showed promising defects (< 80% of WT size) that may indicate they are relevant during infection and warrant future study. The results of the secondary L2 plaque screening effort are presented in Table 2-7.

Table 2-6. Genes regulated >2-fold compared to WT in Δ*prpC* microarrays*		
Fold change	**Gene ID**	**Annotation**
-9.83	lmo1883	similar to chitinases
-6.58	lmo0428	similar to PTS fructose-specific enzyme IIC component
-6.57	lmo1821	similar to putative phosphoprotein phosphatase
-5.84	lmo1997	similar to PTS mannose-specific enzyme IIA component
-5.25	lmo1998	similar to opine catabolism protein
-4.29	lmo2159	similar to oxidoreductase
-3.84	lmo1538	similar to glycerol kinase
-3.76	lmo0027	similar to PTS system, beta-glucosides specific enzyme IIABC
-3.59	lmo0887	similar to B. subtilis YdcD protein
-3.00	lmo2691	similar to autolysin, N-acetylmuramidase
-2.77	lmo1525	similar to single-stranded-DNA-specific exonuclease (RecJ)
-2.77	lmo0482	similar to conserved hypothetical proteins, highly similar to B. subtilis YloN protein
-2.76	lmo1514	similar to unknown protein
-2.67	lmo0355	similar to Flavocytochrome C Fumarate Reductase chain A
-2.66	lmo0536	similar to 6-phospho-beta-glucosidase
-2.64	lmo0781	similar to mannose-specific phosphotransferase system (PTS) component IID
-2.62	lmo2042	similar to unknown proteins
-2.62	lmo2110	similar to mannnose-6 phospate isomerase
-2.59	lmo0680	similar to flagella-associated protein flhA
-2.52	lmo1298	glnR; similar to glutamine synthetase repressor
-2.48	lmo1840	pyrR; highly similar to pyrimidine operon regulatory protein
-2.40	lmo0096	similar to PTS system mannose-specific, factor IIAB
-2.39	lmo0218	polyribonucleotide nucleotidyltransferase domain present
-2.36	lmo1668	some similarity to hypothetical proteins
-2.36	lmo2040	ftsL; similar to cell-division protein FtsL
-2.34	lmo0683	similar to chemotactic methyltransferase CheR
-2.34	lmo1011	similar to tetrahydrodipicolinate succinylase
-2.33	lmo1558	similar to hypothetical GTP binding protein
-2.30	lmo0704	unknown
-2.27	lmo2449	similar to exoribonuclease RNase-R
-2.27	lmo0099	unknown
-2.26	lmo1486	unknown
-2.17	lmo1803	similar to FtsY of E. coli and SRP receptor alpha-subunit
-2.16	lmo0268	similar to phosphoglycerate mutase
-2.11	lmo2175	similar to dehydrogenase
-2.10	lmo0900	unknown
-2.01	lmo0505	similar to ribulose-5-phosphate 3-epimerase
2.08	lmo1215	similar to N-acetylmuramoyl-L-alanine amidase (autolysin)
2.10	lmo2515	similar to B. subtilis two-component response regulator DegU
2.10	lmo2208	similar to unknown protein
2.10	lmo1433	similar to glutathione reductase
2.14	lmo2578	unknown
2.19	lmo0602	weakly similar to transcription regulator
2.22	lmo0134	similar to E. coli YjdJ protein
2.24	lmo2250	arpJ; similar to amino acid ABC transporter, permease protein
2.29	lmo2438	unknown
2.30	lmo0133	similar to E. coli YjdI protein
2.31	lmo2688	similar to cell division protein FtsW
2.36	lmo1381	unknown
2.39	lmo2089	similar to lipases
2.43	lmo0043	similar to arginine deiminase
2.44	lmo2190	mecA; competence negative regulator mecA
2.44	lmo0920	similar to B. subtilis YcgR protein
2.56	lmo1432	unknown
2.60	lmo1864	similar to hemolysinIII proteins, putative integral membrane protein
2.60	lmo2371	similar to putative ABC-transporter transmembrane subunit
2.61	lmo1410	unknown
2.62	lmo2224	similar to unknown proteins

2.65	lmo1052	pdhA; highly similar to pyruvate dehydrogenase (E1 alpha subunit)
2.65	lmo1499	similar to unknown proteins
2.72	lmo0441	similar to penicillin-binding protein (D-alanyl-D-alanine carboxypeptidase)
2.72	lmo0626	similar to unknown protein
2.75	lmo1713	similar to cell-shape determining proteins
2.79	lmo1546	mreD; similar to cell-shape determining protein MreD
2.86	lmo0790	similar to transcription regulator (EbsC from Enterococcus faecalis)
2.89	lmo1229	similar to B. subtilis YshA protein
2.92	lmo0644	similar to conserved hypothetical proteins
2.97	lmo2428	similar to cell division proteins RodA, FtsW
2.98	lmo1412	modulates DNA topology
2.99	lmo2391	conserved hypothetical protein similar to B. subtilis YhfK protein
3.00	lmo1440	similar to unknown proteins
3.04	lmo2231	similar to unknown proteins
3.05	lmo1212	similar to unknown proteins
3.05	lmo0554	similar to NADH-dependent butanol dehydrogenase
3.06	lmo2571	similar to nicotinamidase
3.06	lmo2776	unknown
3.10	lmo1411	unknown
3.21	lmo0911	unknown
3.23	lmo0338	unknown
3.30	lmo0954	unknown
3.30	lmo2157	sepA; sepA
3.44	lmo2684	similar to cellobiose phosphotransferase enzyme IIC component
3.44	lmo1694	similar to CDP-abequose synthase
3.61	lmo0539	similar to tagatose-1,6-diphosphate aldolase
3.66	lmo2441	similar to transcription regulator; has winged HTH domain of GntR family
3.70	lmo0913	gabD?; similar to succinate semialdehyde dehydrogenase; may be gabD, has one low-complexity region
3.71	lmo0796	conserved hypothetical protein; annotated as YceI
3.72	lmo2572	similar to Chain A, Dihydrofolate Reductase
3.74	lmo0321	opuCB; similar to unknown proteins
3.82	lmo0999	unknown
3.83	lmo1919	similar to unknown proteins
3.95	lmo2573	similar to zinc-binding dehydrogenase; one domain listed as GroEL-like
4.09	lmo1428	opuCA; similar to glycine betaine/carnitine/choline ABC transporter (ATP-binding protein)
4.22	lmo2295	Protein gp8 [Bacteriophage A118]
4.26	lmo1375	similar to aminotripeptidase
4.39	lmo2119	similar to unknown proteins; 3 YbbR-like domains
4.51	lmo0953	unknown
4.57	lmo2748	similar to B. subtilis stress protein YdaG; region similar to pyridoxine 5'-phosphate (PNP) oxidase-like proteins
4.74	lmo2602	conserved hypothetical protein
4.82	lmo2570	unknown; 6 predicted TM domains
5.11	lmo1690	similar to hypothetical proteins
5.15	lmo1569	similar to unknown proteins
5.94	lmo2191	similar to unknown proteins
6.00	lmo0647	unknown
6.00	lmo0443	similar to B. subtilis transcription regulator LytR (putative autolysin regulator)
6.54	lmo2213	similar to unknown protein; antibiotic biosynthesis monooxygenase
6.58	lmo0445	similar to transcription regulator
6.77	lmo2829	similar to yeast protein Frm2p involved in fatty acid signaling
6.82	lmo0439	weakly similar to a module of peptide synthetase
7.58	lmo0880	similar to wall associated protein precursor (LPXTG motif); contains PG binding site and LysM domain
7.62	lmo2386	similar to B. subtilis YuiD protein
7.65	lmo2812	similar to D-alanyl-D-alanine carboxypeptidase; beta-lactamase region
7.96	lmo2120	similar to unknown proteins; diadenylate cyclase
8.28	lmo2230	similar to arsenate reductase; low MW protein phosphatase? (KEGG)
9.57	lmo0937	unknown; 53aa long, 2 predicted TM domains
12.99	lmo2420	unknown
14.74	lmo0994	unknown; 3 TM domains
16.55	lmo2210	unknown
50.10	lmo1416	unknown; contains motif from VanZ-like family, residues 17-199

Continued from previous page

*Total RNA from WT and Δ*prpC*, or Δ*prpC*-comp with and without IPTG, was reverse transcribed, amplified, labeled and hybridized to microarrays for two days. Only transcripts that were ≥ two-fold regulated in the same direction in both of the above microarray analyses are listed above. Fold changes represent the mean regulation between the two arrays. Note that while this filtering method improves our confidence that the above listed items are transcriptionally regulated in the absence of PrpC, it does not necessarily produce a statistically reliable dataset. These microarray data are presented purely for informational purposes, and have not been analyzed for statistical significance.

Table 2-7. Unique transposon insertions producing a hyperhemolytic phenotype

Strain	Lmo#	Common name[a]	Annotation[b]	Blood Plate Phenotype[b]	Plaque Phenotype
DP-L5640	lmo0013	*qoxA*	AA3-600 quinol oxidase subunit II	+	103.9%
DP-L5641	lmo0014	*qoxB*	AA3-600 quinol oxidase subunit I	+	98.7%
DP-L5642[e]	lmo0020	-	similar to transcriptional regulator (GntR family)	+++	nd
DP-L5643	lmo0110	-	similar to lipase	+	98.8%
DP-L5644[e]	lmo0201	*plcA*	phosphatidylinositol-specific phospholipase c	++++	45.3%
DP-L5645	lmo0203/0204	-	-	+	nd
DP-L5646	lmo0205	*plcB*	phosphatidylcholine phospholipase c	++	6.8%
DP-L5647	lmo0232	*clpC*	endopeptidase Clp ATP-binding chain C	+	94.8%
DP-L5648[e]	lmo0234	-	highly similar to *B. subtilis* YacL protein	++	nd
DP-L5649	lmo0290	-	similar to *B. subtilis* YycI	++	nd
DP-L5650	lmo0297	-	similar to transcriptional antiterminator (BglG family)	nd	96.6%
DP-L5651[e]	lmo0371	-	similar to transcription regulator (GntR family)	++	107.6%
DP-L5652	lmo0371/0372	-		+++	105.2%[g]
DP-L5653	lmo0401	-	highly similar to *E. coli* YbgG protein, a putative sugar hydrolase	+	76.4%[g]
DP-L5654[e]	lmo0558	-	-	++++	65.8%[g]
DP-L5655[e]	lmo0567	*hisD*	histidinol dehydrogenase	++	58.8%
DP-L5656	lmo0641	-	similar to heavy metal-transporting ATPase	++	nd
DP-L5657[e]	lmo0838	*uhpT*	sugar phosphate antiporter	++++	nd
DP-L5658	lmo0840	-	-	+	72.9%[g]
DP-L5659	lmo0840/0841	-	-	++	60.4%[g]
DP-L5660	lmo0850/0851	-	-	+	60.9%
DP-L5661	lmo0891	*rsbT*	highly similar to positive regulation of sigma-B activity	+	110.1%[g]
DP-L5662	lmo0895	*sigB*	RNA polymerase sigma factor SigB	+	107.3%[g]
DP-L5663	lmo1005	-	similar to 3-hydroxyisobutyrate dehydrogenase (*B. subtilis* YkwC protein)	++	104.1%[g]
DP-L5664	lmo1021	-	similar to two-component sensor histidine kinase in particular *B. subtilis* YvqE protein	+	104.3%
DP-L5665[e]	lmo1030	-	similar to transcriptional regulator, LacI family	++++	80.5%
DP-L5666	lmo1039/1040	-	similar to GTP-binding elongation factor	++	104.0%[g]
DP-L5667	lmo1067	-	-	+	92.1%
DP-L5668	lmo1348	*gcvT*	glycine cleavage system aminomethyltransferase T	++	110.7%[g]
DP-L5669	lmo1354/1355	-	-	++	103.6%
DP-L5670	lmo1402	-	similar to *B. subtilis* YmcA protein	+	92.3%
DP-L5671	lmo1434	-	-	+	87.7%
DP-L5672[e]	lmo1490	-	similar to shikimate 5-dehydrogenase (AroD)	++	51.4%
DP-L5673	lmo1585/1586	-	-		74.5%
DP-L5674	lmo1604/1605	-	-	+	107.8%
DP-L5675	lmo1608	-	-	+	103.6%
DP-L5676	lmo1710	-	similar to putative flavodoxin	++	nd
DP-L5677[e]	lmo1727	-	similar to transcription regulators (LacI family)	+++	98.3%[g]
DP-L5678	lmo1758	*ligA*	NAD-dependent DNA ligase LigA	+	102.8%
DP-L5679	lmo1774	*purK*	phosphoribosylaminoimidazole carboxylase ATPase subunit	+	100.3%
DP-L5680[e]	lmo1833	*pyrD*	highly similar to dihydroorotase dehydrogenase	+++	105.6%
DP-L5681	lmo1863	-	-	+	83.1%
DP-L5682	lmo1875/1877	-	within lmo01876, a described pseudogene	+	85.7%
DP-L5683[e]	lmo1877	-	-	++	98.8%
DP-L5684	lmo1886	-	similar to probable thermostable carboxypeptidases	++	101.0%
DP-L5685	lmo1888	-	-	++	81.3%[g]
DP-L5686	lmo1890	-	-	++	104.5%
DP-L5687	lmo2004	-	similar to transcription regulator GntR family	++	64.7%
DP-L5688	lmo2027	-	putative cell surface protein, internalin proteins	+	nd
DP-L5689	lmo2057	*ctaB*	protoheme IX farnesyltransferase	+	113.2%
DP-L5690	lmo2058	*ctaA*	similar to heme O oxygenase	+	116.4%
DP-L5691	lmo2190	*mecA*	enables recognition and targeting of proteins for proteolysis, involved in negative regulation of competence	nd	94.0%

DP-L5692	lmo2194	-	similar to oligopeptide ABC transporter (permease)	++	9.5%
DP-L5693	lmo2195	-	similar to oligopeptide ABC transporter (permease)	+++	12.9%
DP-L5694	lmo2195/2196	-	-	++	75.1%
DP-L5695[f]	lmo2196	-	similar to oligopeptide ABC transporter (permease)	++	19.6%
DP-L5696	lmo2196/2197	-	-	+	nd
DP-L5697[e]	lmo2248	-	-	++	76.4%
DP-L5698[e]	lmo2249	-	similar to low-affinity inorganic phosphate transporter	+++	nd
DP-L5699[e]	lmo2337	-	similar to regulatory protein DeoR family	++	97.6%[g]
DP-L5700	lmo2426	-	-	+	87.3%
DP-L5701[e]	lmo2511	-	similar to conserved hypothetical proteins like to *B. subtilis* YvyD protein	+++	100.8%
DP-L5702[e]	lmo2532	*atpH*	F0F1 ATP synthase subunit delta	++	47.4%
DP-L5703[e]	lmo2534/2534	-	-	++++	32.1%[g]
DP-L5704	lmo2586	-	similar to formate dehydrogenase alpha chain	+	99.4%
DP-L5705[e]	lmo2614	*rpmD*	50S ribosomal protein L30	+	58.2%
DP-L5706	lmo2708	-	similar to PTS system, cellobiose-specific enzyme IIC	+	95.7%
DP-L5707	lmo2744	-	weakly similar to transcription regulators CRP/FNR family	+	101.2%
DP-L5708	lmo2756	*topB*	similar to DNA topoisomerase III	+	99.3%
DP-L5709	lmo2768/2769	-	-	+	91.1%
DP-L5710	lmo2785/2786	-	-	++	96.3%
DP-L5711	lmo2795	-	similar to *E. coli* RpiR transcription regulator	+	98.6%
DP-L5712	lmo2823	-	similar to an hypothetical protein from Thermotoga maritima	++	111.4%
DP-L5713	lmo2842	-	-	+	nd
DP-L5714	lmor02	-	23S ribosomal RNA	+	84.1%
DP-L5715[d]	lmo0078	-	similar to phosphoglycerate dehydrogenase;	+	110.9%[g]
DP-L5716[d]	lmo0123	-	similar to protein gp18 from Bacteriophage A118;	+	90.2%[g]
DP-L5717[d]	lmo0184	-	similar to oligo-1,6-glucosidase;	++	96.7%
DP-L5718[de]	lmo1295/1296	-	-	+++	nd
DP-L5719[d]	lmo1585/1586	-	-	+	74.5%
DP-L5720[d]	lmo1832	*pyrF*	highly similar to orotidine 5'-phosphate decarboxylases	+	94.0%
DP-L5721[d]	lmo2092	*betL*	glycine betaine transporter BetL	+	99.4%

[a] As identified by NCBI annotation of the L. monocytogenes EGD-e genome. PTS, phosphotransferase system; NAD, nicotinamide adenine dinucleotide. -, no annotation assigned.

[b] Qualitative hemolytic defect visually determined by comparison to an adjacent WT colony on a blood agar plate as follows: +, 25% greater; ++, 50% greater; +++, 75% greater; ++++, 100% greater of the activity of the WT colony.

[c] Relative to the size of the WT in the L2 fibroblast plaque assay. nd, not determined.

[d] The approximate site of the transposon is mapped.

[e] Mutant colonies are substantially smaller than WT.

[f] Mutant colonies are substantially larger than WT.

[g] Small sample size; data represent the mean of fewer than ten plaques

MATERIALS AND METHODS

Bacterial strains, growth media, and reagents. The bacterial strains used in this study are listed in Table 2-1. All *E. coli* strains were grown in Luria-Bertani (LB) media. All strains of *L. monocytogenes* were grown in either brain heart infusion (BHI; Difco, Detroit, MI) media, LB, or LB supplemented with 25 mM glucose-1-phosphate, 0.2% activated charcoal, and pH adjusted to 7.3 with 50 mM MOPS (morpholinepropanesulfonic acid) (LB-G1P) as indicated. All bacterial stocks were stored at -80°C in BHI supplemented with 50% glycerol. L2 murine fibroblasts were passaged in Dulbecco modified Eagle medium (DMEM) with high glucose (Gibco/Invitrogen; Carlsbad, CA) supplemented with 1% sodium pyruvate, 1% L-glutamine, and 10% fetal bovine serum (GemCell; West Sacramento, CA) at 37°C with 5% CO_2. The following antibiotics were used as indicated at the following concentration: erythromycin (em), 2 μg/ml; lincomycin (lm), 25 μg/ml; streptomycin (sm), 200 μg/ml; chloramphenicol (cp), 7.5 – 20 μg/ml; gentamicin (gm), 10 μg/ml (Sigma-Aldrich; St. Louis, MO). All restriction enzymes, T4 DNA Ligase, Taq DNA Polymerase, VentR DNA Polymerase, and respective buffers were obtained from New England Biolabs (NEB; Beverly, MA).

pJZ037 construction. The plasmids and primers used to construct pJZ037 are listed in Table 2-1. The transposon was constructed in pUC19. Using vector phiMycoMarT7 (Sassetti, Boyd et al. 2001)as a PCR template, primer pair 112 and 24 and pair 29 and 26 were used to amplify the 5' and 3' ends, respectively, of this transposon, which included the TA insertion site, the inverted repeat, and the T7 promoter oriented outward (Sassetti, Boyd et al. 2001). Overhangs included in primers 24 and 29 contained a multiple cloning site consisting of SmaI, KpnI, PstI, the trinucleotide AAA, SpeI, and XhoI.

The transposon backbone was ligated into pUC19 in a three-way ligation to generate pJZ025 using the PstI sites in primers 24 and 29, a SalI site incorporated by primer 112, and a HindIII site incorporated by primer 26. Primers 30 and 31 amplified the Tn*917* ribosomal methyltransferase gene from pLTV3 (Camilli, Portnoy et al. 1990) and ligated it into the transposon backbone at the PstI and SpeI sites to generate pJZ029.

The transposase and its promoter were also assembled in pUC19. To increase the stability of the transposase transcript, the 5'UTR of *hly* (lmo0202) was first fused upstream of the C9 hyperactive transposase (Lampe, Akerley et al. 1999). Primers 113 and 114 were used to amplify the transposase; primer 113 contained a 64 bp overhang that included the 51 bp constitutive hyper-*Pspac* promoter, *Pspac*(hy) (Quisel, Burkholder et al. 2001; Shen and Higgins 2005; Schnupf, Hofmann et al. 2006) and a BamHI site; primer 114 included a SalI and a HindIII site. This product was ligated into pUC19 using the BamHI and HindIII sites, resulting in pJZ026.

The transposon was digested out of pJZ029 with BamHI and ligated into pJZ026 to generate pJZ032. The inclusion of the 5'UTR of *hly* upstream of the transposase, however, prevented plasmid curing. Therefore, this copy of the transposase was digested out of pJZ032 with EagI and HindIII and replaced with a copy of the transposase generated by primers 134 and primer 114 (which removed the 5'UTR), resulting in pJZ039. The transposon and transposase were digested out of pJZ039 with SalI and ligated into the Gram-positive suicide vector pKSV7 to generate pJZ037 (Fig. 2-1a) (Smith and Youngman 1992).

Generation of libraries. Electrocompetent *L. monocytogenes* were prepared as previously described (Park and Stewart 1990) with the exception that Vegetable Peptone Broth (Remel; Lenexa, KS) was used instead of BHI to increase electroporation efficiency.

Approximately 1 μg of pJZ037 was used to electroporate each 50 μL aliquot of electrocompetent cells. Bacteria were recovered in 1 ml of VB 0.5 M sucrose and plated over ≈10 BHI em/lm agar 100 mm plates. Plates were incubated 48 h at 30°C (the permissive temperature) and then replica plated onto BHI em/lm agar plates and incubated overnight at 41.5°C (the non-permissive temperature) to cure the plasmid. Colonies were then counted, scraped and resuspended in BHI 40% glycerol for storage at -80°C.

To test for plasmid retention, ten-fold serial dilutions were prepared from a small frozen aliquot of the library. Each dilution was plated on a BHI plate containing em (the resistance marker carried by the transposon) and on a plate containing cm (the resistance marker carried by the delivery vector).

Blood plate screen for hypohemolytic mutants. Swabs from frozen libraries were added to BHI and plated directly onto 1% LB-G1P agar supplemented with 5% defibrinated sheep's blood (HemoStat Laboratories; Dixon, CA) at a concentration of 150-200 colonies per 100 × 15 mm plate. Plates were incubated 48 h at 37°C and zones of hemolysin were evaluated by eye for both size and extent of translucency. Potential hits were restreaked on BHI agar containing em and lm to confirm the presence of the transposon and absence of plasmid. To confirm the phenotype, both mutant and WT bacteria were grown overnight at 37°C in BHI with aeration and plated on blood agar plates in a 1:1 ratio. Plates were scanned using Adobe Photoshop (Adobe Systems; San Jose, CA).

Identification of transposon insertion sites. Chromosomal DNA of two mL overnight cultures of each mutant were extracted using the MasterPure Gram-positive DNA Purification Kit (Epicentre; Madison, WI) with the exception that 10-15 units of mutanolysin (Sigma) was used for 1 h at 37°C instead of lysozyme. A mixture containing 8 pmol/μL of primers MSPY5 and MSPY3 in 1X T4 DNA Ligase buffer was boiled for 5 minutes and allowed to cool to room temperature (Tavazoie and Church 1998), creating a partially double-stranded "Y-linker." A reaction mixture containing the 2 μg of digested genomic DNA, 2 μL of the Y-linker, and 400 U of T4 DNA ligase was allowed to incubate at 16°C for 12 h before inactivation of the ligase. Approximately one third of this reaction mixture was used as template in an initial PCR to enrich for ssDNA fragments containing the transposon insertion. A 20 μL total reaction volume that included 0.02 mM dNTP (Fermentas; Glen Burnie, MD), 1.5 U Taq (NEB) and 1x ThermoPol Buffer, and 0.1 μM of primer 121 was first incubated at 95°C for 2 minutes, then incubated at 94°C for 1 minute, 61°C for 1 minute, and 72°C for 1 minute for 20 cycles, and then incubated at 72°C for 7 minutes. An additional 0.2 mM of dNTP, 7.5 U of Taq (and appropriate buffer), and 1.5 μM of primers 121 and 99 was added and the reaction volume increased to 100 μL total. This mixture was subjected to the conditions described above, except that the cycle number was increased from 20 to 25, and the final extension time was increased from 7 minutes to 10 minutes. The entire reaction volume was run out on a 1% agarose gel, visible bands were excised, and the DNA was purified using the QIAquick gel extraction kit (Qiagen; Valencia, CA). 100 ng of DNA was submitted to the UC Berkeley DNA Sequencing Facility with primer 184 and 185 for sequencing.

L2 Plaque Assays. Plaque assays on L2 murine fibroblasts were performed as previously described (Sun, Camilli et al. 1990). Briefly, overnight 30°C static cultures of *L. monocytogenes* were normalized by OD, washed 3x in PBS, and allowed to infect monolayers of L2 cells for 1 h.

Cells were washed and a 3 ml overlay containing 0.7% agar and gm. After 3 days at 37°C, an overlay containing 2 ml of 0.7% agar, gm was added, and ≈2.5X Neutral Red (Sigma-Aldrich) was added. Monolayers were stained overnight and plaque size was evaluated using ImageJ (http://rsbweb.nih.gov/ij/). At least three wells were used per mutant per experiment, and within each experiment the average size of each strain was measured as a percentage of the average size of the WT plaques.

Hemolytic-activity Assays. Hemolytic assays were performed as previously described (Portnoy, Jacks et al. 1988; Shen and Higgins 2005) with some modifications. Briefly, 1 mL of an overnight 30°C LB static culture of *L. monocytogenes* was diluted into 9 mL of LB and grown for 5 h at 37°C with aeration. The optical density at 600 nm (OD_{600}) was determined. Two-fold dilutions of culture supernatants were activated in assay buffer containing 1X PBS (Gibco/Invitrogen) and 8.5×10^{-5} M Cysteine-HCl (Sigma-Aldrich), final pH 5.5, at 37°C for 30 minutes before a 1/10 volume of 5% sheep's blood was added for another 30 minutes at 37°C. Purified LLO was first adjusted to an initial concentration of 2 μg/mL in assay buffer, before serial dilutions in assay buffer were made. The assay was completed as described above except that the 30 minute activation step was not performed. Hemolytic units were defined as the reciprocal of the dilution of culture supernatant that yielded 50% lysis of sheep red blood cells.

Purification of histidine-tagged LLO from *L. monocytogenes*. Ten mL of overnight cultures of DP-L3481 (Gedde, Higgins et al. 2000) and DP-L5633 grown at 37°C LB with aeration was diluted into 1 L of LB and grown for 8 h at 37°C with aeration. Culture supernatants were obtained by centrifugation at 6,000 × g rpm for 15 minutes and purified by Ni-NTA affinity chromatography (Qiagen) according to the manufacturer's recommendations. Samples were loaded onto the column using gravity. Columns were washed first with 30 mL of buffer B (Schuerch, Wilson-Kubalek et al. 2005) and then with 30 mL of buffer B with 150 mM imidazole. Bound LLO was eluted with 15 mL of buffer B with 500 mM imidazole. The eluted protein was dialyzed twice in 500 mL of storage buffer (Schuerch, Wilson-Kubalek et al. 2005) at 4°C, first overnight, and then again for 4 h. Toxin was then mixed with 10% (vol/vol) glycerol and stored at -80°C. Prior to analysis, thawed sampled were centrifuged at 13,200 × g for 10 minutes at 4°C to remove precipitated protein. Protein concentration was determined by diluting the toxin 1:10 in 6 M guanidine-HCl and 20 mM Na_2PO_4 (pH 6.5) and measuring the absorbance intensity at 280 nm, using the extinction coefficient obtained by primary sequence analysis using the ExPASy ProtParam tool (http://us.expasy.org/tools/protparam.html) (Woodward, Martin et al. 2007).

Competitive index and total CFU assays. Competitive indices (CIs) and total CFU assays were performed as previously described (Auerbuch, Lenz et al. 2001). A total of 1.0×10^5 CFU/mL of mutant or, in the case of the CI, a 1:1 ratio of mutant: WT was intravenously injected into the tail vein of 9-14 week old female C57/B6 mice (The Jackson Laboratory; Bar Harbor, ME). To confirm the bacterial load on the injection mixture, dilutions of the input pool were plated onto BHI sm plates. Livers and spleen were harvested 48 hpi and homogenized in 10 mL and 5 mL, respectively, of 0.2% NP-40. For the CIs, data was obtained for each mutant from at least seven livers and spleens as previously described (Auerbuch, Lenz et al. 2001). For the total CFU assay, five aged-matched mice were injected per strain, and the experiment repeated twice. All animal work was done in accordance with university regulations.

In-frame deletions and complementation. A WT strain carrying an internal deletion of *prsA2* was constructed as previously described (Camilli, Tilney et al. 1993). Briefly, primer pairs 229 and 230 and 231 and 232 were used to amplify the regions ≈900 bp upstream and downstream of *prsA2*, respectively. These fragments were fused together using splice overlap extension (SOE) polymerase chain reaction and were introduced into the *L. monocytogenes* via allelic exchange using pKSV7 (Ho, Hunt et al. 1989; Camilli, Tilney et al. 1993). Primers 241, 242, and 243 were each used as the 5' primer with 249 to generate the complementation fragments #1, #2, and #3 (Fig. 2-4b). These fragments were ligated into pPL2 to generate pJZ064, pJZ065, and pJZ066, respectively, and incorporated into the *L. monocytogenes* chromosome as previously described (Lauer, Chow et al. 2002).

Transductions. Transductions were performed as previously described using the phage U153 (Hodgson 2000). Briefly, 10^7 phage grown on the donor strain were incubated with 10^8 recipient bacteria, then transferred to em/lm BHI plates. Colonies were visible after 48 h incubation at 37°C.

Isolation of bacterial secreted proteins and subsequent analyses. Overnight 37°C shaking cultures of *L. monocytogenes* in LB-G1P were back diluted to an OD600 of 0.01 in LB-G1P. Cultures were grown for 8 h at 37°C with shaking, and OD's were taken every hour. Approximately 1.2 ml of culture was taken from each sample at 8 h and spun at 13,200 $\times$ g to pellet the bacteria. Supernatants were removed and stored at -80°C. In order to normalize for protein secretion during the entire growth curve, the area under the curve was derived using Kaleidagraph (Synergy Software; Reading, PA). Each sample was normalized to the lowest value in 1.2 mL total volume. Proteins were precipitated with a final concentration of 10% TCA, washed with ice-cold acetone, and resuspended in 2X sample buffer (Invitrogen) containing 5% beta-mercaptoethanol. The same fraction of each sample was run out on a NuPAGE 10% Bis-Tris 1.0 mm $\times$ 12 well gel (Invitrogen). Gels were either stained using the NOVEX Colloidal Blue Staining Kit (Invitrogen) or subjected to Western Blot analysis. Following Western transfer, blots were probed with a rabbit polyclonal LLO antibody and an Alexa-Fluor goat anti-rabbit IgG (Molecular Probes; Eugene, OR) or, additionally where noted, an anti-FLAG M2 monoclonal antibody (Stratagene; Cedar Creek, TX) and a Goat anti-mouse IRDye 800CW (LiCor Biosciences; Lincoln, NE) (Schnupf, Hofmann et al. 2006). Blots were visualized using the Odyssey Infrared Imaging System (LiCor).

Assay for egg yolk opacity. Preparation of egg yolk agar plates and assay conditions were performed as previously described (Yeung, Zagorski et al. 2005).

Assay for motility. Overnight 30°C BHI static cultures of *L. monocytogenes* were spotted on semi-solid (0.35% [wt/vol] agar) BHI plates and incubated for 24 h and 48 h at 30°C.

Intracellular growth curves. Growth curves in J774 macrophage-like cells were performed as previously described (Portnoy, Jacks et al. 1988). Following washing in PBS (Gibco, Grand Island, NY), bacteria were applied to J774 cells at a final dilution of 1:20000. Infections were continued for eight hours and samples were taken at 30 minutes, two hours, five hours, and eight hours.

Antibiotic Resistance Assays. 100 µL of an overnight culture was spread evenly on a 20 mL BHI agar plate. 0.7 cm autoclave-sterilized filter paper disks (Phenix, Candler, NC) were soaked with 10 µL of varying concentrations of antibiotics and placed onto the aforementioned plates. During overnight incubation at 37°C, an antibiotic gradient was established by diffusion

and a lawn was allowed to form with a zone of clearance in the area around the disk where antibiotic concentration was high enough to inhibit growth. Zones of clearance were measured manually.

Microarray analysis. Microarray experiments were performed as previously described (Crimmins, Schelle et al. 2009). Total RNA was isolated from mid-log (OD ≈0.5) WT and mutant *L. monocytogenes* strains were grown in BHI.

Chapter 3

Identification of a *Listeria* homolog of the ribosomal Hibernation Promoting Factor (HPF) and initial characterization of ribosomal hibernation in *L. monocytogenes*

SUMMARY

Ribosomal hibernation is characterized by the dimerization of two 70S ribosomes into a 100S complex. Although the role of ribosomal hibernation is not completely clear, it is thought to represent a conserved and adaptive response that contributes to optimal survival during stress and post-exponential growth. Hibernating ribosomes are formed by the activity of one or more highly conserved proteins; ribosome modulation factor (RMF) and hibernation promoting factor (HPF) play the most prominent roles in *E. coli*. Gram-positive bacteria generally lack RMF, but carry a long homolog of HPF with a C-terminal extension. Here we report the presence and initial characterization of the *L. monocytogenes* long HPF homolog (referred to as HPF), which is highly similar to that of *S. aureus*. 100S ribosomes were detected for the first time in *L. monocytogenes* extracts by sucrose density gradient centrifugation. They appeared during mid-logarithmic growth, peaked at the transition to stationary phase, and persisted at lower levels during post-exponential growth. Ribosomal hibernation was undetectable in bacteria harboring an *hpf*::*Himar1* transposon insertion, indicating that HPF is essential for 100S ribosome formation in *L. monocytogenes*. Additionally, epitope-tagged HPF co-migrated with 100S ribosomes. Transcription of *hpf* closely mirrored 100S ribosome abundance, with mRNA scarce early, increasing throughout logarithmic growth, and peaking at the transition between logarithmic and stationary phase. This transcriptional upregulation was largely ablated by supplementation of the growth medium with additional glucose, indicating that carbon starvation may be one of the signals that stimulate *hpf* expression during growth in broth. Bacteria lacking HPF displayed a severe competitive survival defect when co-cultured with wild-type bacteria during post-exponential growth. Finally, HPF-deficient bacteria showed a > 300-fold survival defect in the mesenteric lymph nodes of orally infected mice, the first virulence-associated phenotype attributed to ribosomal hibernation.

INTRODUCTION

Bacterial survival in a variety of environments is predicated on the ability to recognize and respond quickly and appropriately to a wide range of stresses (Marles-Wright and Lewis 2007). One common stress response is to temporarily halt growth or the affected cellular processes until the stress subsides. Stationary phase, defined by exhaustion of available nutrients and/or buildup of toxic byproducts, is one common circumstance in which downregulation of growth rate is an important adaptive response (Kolter, Siegele et al. 1993). Although rich media allows for rapid bacterial growth, this type of nutrient excess is the exception rather than the rule for bacteria growing in the environment (Martin and Macleod 1984). Facultative pathogens like *Listeria monocytogenes* that experience prolonged exposure to the environment must be particularly adept at surviving for long periods of time under sub-optimal nutrient conditions in order to persist and pass from one host to the next.

L. monocytogenes is a Gram-positive, foodborne, facultative intracellular pathogen that infects a broad range of vertebrate hosts (Vazquez-Boland, Kuhn et al. 2001). It leads a saprophytic lifestyle in the environment and is commonly found in soil, water, and decaying organic matter. *L. monocytogenes* most commonly causes disease in elderly, immunocompromised, or pregnant individuals, but can pose a general public health risk in cases of severe food contamination. Its ability to tolerate or thrive in a variety of unfavorable conditions, including high salt, low pH, and refrigeration temperatures, has made *L. monocytogenes* a formidable challenge to the food industry (Vazquez-Boland, Kuhn et al. 2001). For this reason, it is critically important to understand the set of factors that enable *L. monocytogenes* to survive so effectively in a wide variety of inhospitable environments. Some of these factors are parts of widespread bacterial stress responses, while others are more specific to *Listeria* spp. and their close relatives.

Protein synthesis, including the production of ribosomes, is the single most energy-intensive cellular process in bacteria, estimated to consume 40% of the total energy expended by *E. coli* during active growth (Wilson and Nierhaus 2007). As a result, energy-poor growth conditions dictate that bacteria must slow their rates of translation and ribosome production for optimal survival. In the ultramicrobacterium RB2256, ribosome content of starved cells drops by 10-fold compared to mid-log phase cells (Fegatella, Lim et al. 1998). Given the energetic cost of producing each >2 megadalton ribosomal complex, it follows that bacteria, frequently subject to nutrient stress in the environment, would have devised methods for storage rather than degradation of ribosomes. The process of ribosomal hibernation is thought to be one such storage method (Wada, Igarashi et al. 1995).

Each bacterial ribosome is composed of a small (30S) and large (50S) subunit, which heterodimerize to form the translationally active 70S complex. 70S complexes are assembled at the beginning and disassembled at the end of each round of protein synthesis (Kato, Yoshida et al. 2010). Dissociation of the two subunits and subsequent stripping of mRNA and tRNA from the 30S subunit is referred to as ribosome recycling, which readies the subunits for another round of translation. Ribosomal hibernation is thought to be an alternative to the classical recycling pathway, shunting ribosomes into mRNA- and tRNA-free 70S complex dimers that sediment at 100S (Kato, Yoshida et al. 2010). These complexes appear to be translationally

inactive *in vitro*, but can quickly dissociate and release translationally competent ribosomes within minutes (Yamagishi, Matsushima et al. 1993; Wada, Igarashi et al. 1995).

Ribosomal components are commonly isolated and separated by sucrose density gradient centrifugation (SDGC) of cell-free lysate. Hibernating ribosomes appear as an A_{260} peak that sediments at 100S (Wada, Yamazaki et al. 1990). The relative abundance of 100S ribosomes varies dramatically over the course of growth in broth, and this temporal hibernation profile varies from one bacterium to another. In *E. coli*, 100S ribosomes are quite scarce in mid-log lysates and increase dramatically at the entry to stationary phase, dwarfing 70S ribosome content in stationary phase lysates (Wada, Mikkola et al. 2000). In contrast, 100S ribosomes are fairly abundant in log-phase lysates of *S. aureus*, increasing to a peak at the entry to stationary phase and decreasing gradually in quantity over the next several hours of post-exponential growth (discussed further below) (Ueta, Wada et al. 2010).

In *E. coli* and other Gamma Proteobacteria, dimers of 70S ribosomes are formed by ribosome modulation factor (RMF, 55 amino acids, pI≈11), and are stabilized by hibernation-promoting factor (HPF, 95 amino acids) (Wada, Yamazaki et al. 1990; Ueta, Yoshida et al. 2005). Homologs of one or both of these genes are conserved in the majority of bacteria (Ueta, Ohniwa et al. 2008). HPF is one of two proteins in *E. coli* that carry a Ribosome-Associated Inhibitor (RaiA) domain. The other, known variously as RaiA, YfiA and PY, associates preferentially with 70S ribosomes, destabilizing 100S ribosome dimers and inhibiting translation (Maki, Yoshida et al. 2000; Ueta, Yoshida et al. 2005). Electron microscopy, X-ray crystallography, and NMR studies have provided insight into the structures and ribosome binding sites of RMF, YfiA, and HPF. RMF is predicted to bind to the 30S subunit near the ribosomal P site (Yoshida, Maki et al. 2002) while YfiA soaked into to crystallized 70S ribosomes occludes the P site completely, also indirectly inhibiting tRNA binding at the A site (Vila-Sanjurjo, Schuwirth et al. 2004). While the various activities of RMF, HPF, and YfiA complicate translational regulation in *E. coli*, Gram-positive bacteria generally produce a single, long HPF homolog and no YfiA or RMF homologs (Ueta, Ohniwa et al. 2008). This long HPF bears a C-terminal extension that makes it roughly twice as long as the Gram-negative HPF, and it has been suggested that this extension might perform the ribosome dimerization function for which RMF is responsible in Gram-negatives (Ueta, Wada et al. 2010).

The functions of ribosomal hibernation appear to be diverse, but have not yet been fully explored. RMF-deficient *E. coli* display a profound survival defect during prolonged post-exponential growth (Yamagishi, Matsushima et al. 1993). Accordingly, transcription and/or translation of both *rmf* and *hpf* are upregulated at the entry to stationary phase, when nutrient abundance is low and exponential growth ceases (Wada, Yamazaki et al. 1990; Maki, Yoshida et al. 2000). Hibernation-associated factors also appear to be important for optimal survival of various stresses in stationary phase, including acid, osmotic, and heat stresses, although the relevance of 100S formation to these processes is uncertain (Garay-Arroyo, Colmenero-Flores et al. 2000; Niven 2004; El-Sharoud and Niven 2007). A recent report examining gene regulation and stress tolerance in *Pseudomonas aeruginosa* biofilms showed that RMF is preferentially expressed by bacteria deep in biofilms and aids in survival of those bacteria (Williamson, Richards et al. 2012). Interestingly, while RMF is central to all of these phenotypes in the bacteria that produce it, HPF appears to be dispensable.

The only report of hibernation in Gram-positive bacteria, which produce the longer form of HPF discussed above, established *Staphylococcus aureus* HPF (saHPF)'s role in 100S ribosome formation (Ueta, Wada et al. 2010). The authors showed that hibernation in *S. aureus* was dependent on the nutrient content of the media, and that 100S ribosomes were present in *S. aureus* extracts at all phases of growth. Using 2D gel electrophoresis and mass spectrometry of ribosomal fractions isolated by SDGC, they demonstrated that saHPF was present almost exclusively in 100S ribosomes during logarithmic growth, but distributed relatively equally between 70S and 100S fractions during stationary phase. Finally, they showed that purified saHPF could reconstitute 100S ribosome formation in washed ribosomal monomers. However, the authors did not address the transcriptional regulation of saHPF or the phenotype(s) of saHPF deletion mutants (Ueta, Wada et al. 2010). Thus, the biological consequences of hibernation in bacteria expressing long HPF and lacking RMF are almost entirely unknown.

In addition to *S. aureus*, a long list of other important human pathogens including *M. tuberculosis*, *L. monocytogenes*, *B. anthracis* and the *Clostridia* maintain homologs of long HPF but none of RMF (Ueta, Ohniwa et al. 2008). Since RMF-dependent hibernation is important in the Gram-negative bacterial response to a variety of stresses and enhances survival under adverse conditions, it is important to determine whether long-HPF-dependent hibernation serves equally critical roles. If so, targeting of hibernation machinery with antimicrobials may be a valuable tool in combating a wide range of pathogens. In this work, we examine ribosomal hibernation in one of those pathogens, *Listeria monocytogenes*. We determined that *L. monocytogenes* forms 100S ribosomes in a pattern similar to *S. aureus*; 100S ribosomes were visible at nearly every point in broth growth, peaking at the entry to stationary phase then decreasing to a lower, steady level for several hours. HPF expression was regulated in patterns similar to those seen in RMF/short HPF-producing bacteria, with heavy regulation by growth phase, stress, and nutrient deprivation. We showed that HPF is indispensable for ribosomal hibernation in *L. monocytogenes*, and that it co-migrates through sucrose gradients predominantly with 100S ribosomes. Although no survival defect was apparent in post-exponential phase monoculture, HPF-deficient *L. monocytogenes* showed a substantial competitive disadvantage in post-exponential phase co-culture with WT *L. monocytogenes*. Mouse infection by the oral route also showed an organ-specific competitive defect. The particular nature of these *in vitro* and *in vivo* phenotypes suggests that hibernation plays an important role in Gram-positive bacterial survival under specific sets of circumstances that have yet to be fully defined.

RESULTS

Identification of *lmo2511* as an *L. monocytogenes* homolog of HPF

Several transposon insertions in *lmo2511* were isolated in a screen for *L. monocytogenes* mutants with altered hemolytic phenotypes on sheep's blood agar plates ((Zemansky, Kline et al. 2009); unpublished data). These mutants all produced larger zones of hemolysis than wild-type *L. monocytogenes*, suggesting that disruption of the gene causes overproduction or hyperactivity of LLO. *lmo2511* was also identified as one of the most highly downregulated genes in a microarray analysis of a *L. monocytogenes pdeA* mutant, which carries an in-frame deletion in the bacterium's only known cyclic-di-AMP phosphodiesterase (C.E. Witte *et al*., submitted). Because of its involvement in multiple pathways important for growth and virulence in *L. monocytogenes*, and due to its central role in the conserved process of ribosomal hibernation, we decided to examine the specific functions of Lmo2511 more closely.

Based on protein sequence homology, *lmo2511* encodes a long HPF homolog (referred to hereafter as HPF) highly similar to saHPF of *S. aureus* (Fig. 3-1a). In keeping with the organization other HPF genes of the same family, *L. monocytogenes* HPF consists of an N-terminal RaiA domain (residues 1-95, bearing 37 percent identity to the *E. coli* HPF) and a C-terminal extension (residues 96-187) bearing little homology to any known proteins. Homologs of the *L. monocytogenes* HPF are also present in each of the other six known species of *L. monocytogenes*, and all are very highly similar to the *L. monocytogenes* HPF (≥ 88 percent protein sequence identity), although functionality of these HPF homologs was not examined. A predicted transcriptional terminator is located just downstream of the *lmo2511* coding sequence (Fig. 3-1b), and tiling microarray analysis has previously shown that *lmo2511* is likely to be transcribed alone (Toledo-Arana, Dussurget et al. 2009). To study the production and function of 100S ribosomes in *L. monocytogenes*, we made use of two *Himar1* transposon insertions in opposite ends of the *hpf* coding sequence (*hpf*::*Himar1* and *hpf*::*Himar1-C*) (Fig. 3-1b). Although HPF function does not appear to be essential in other bacteria (Zhang, Ou et al. 2004; Williamson, Richards et al. 2012), attempts to generate an in-frame deletion of the *hpf* gene in *L. monocytogenes* have been unsuccessful thus far. The *hpf*::*Himar1* transposon mutant is predicted to encode a truncated, ≈30 amino acid form of the HPF protein, while *hpf*::*Himar1-C* is predicted to encode a still-disrupted but more complete form of the protein (Fig. 3-1b). The majority of the results presented below are based on the N-terminal transposon insertion, but the C-terminal insertion behaves in a similar manner.

L. monocytogenes produces 100S ribosomes in an HPF-dependent manner

We first set out to determine whether ribosomal dimers were present in *L. monocytogenes* extracts. Using previously described methods for isolation and separation of various ribosomal species in *S. aureus* (Ueta, Wada et al. 2010), we observed a 260 nm absorbance peak that migrated through sucrose density gradients at the rate expected for a 100S complex. To examine the abundance of the 100S ribosome species in *L. monocytogenes* cultures at different bacterial growth phases, and to compare this profile with those of other bacterial species, we analyzed ribosome samples isolated from *L. monocytogenes* at several points along the course of growth in rich media. Based on these samples, 100S ribosomes

Figure 3-1

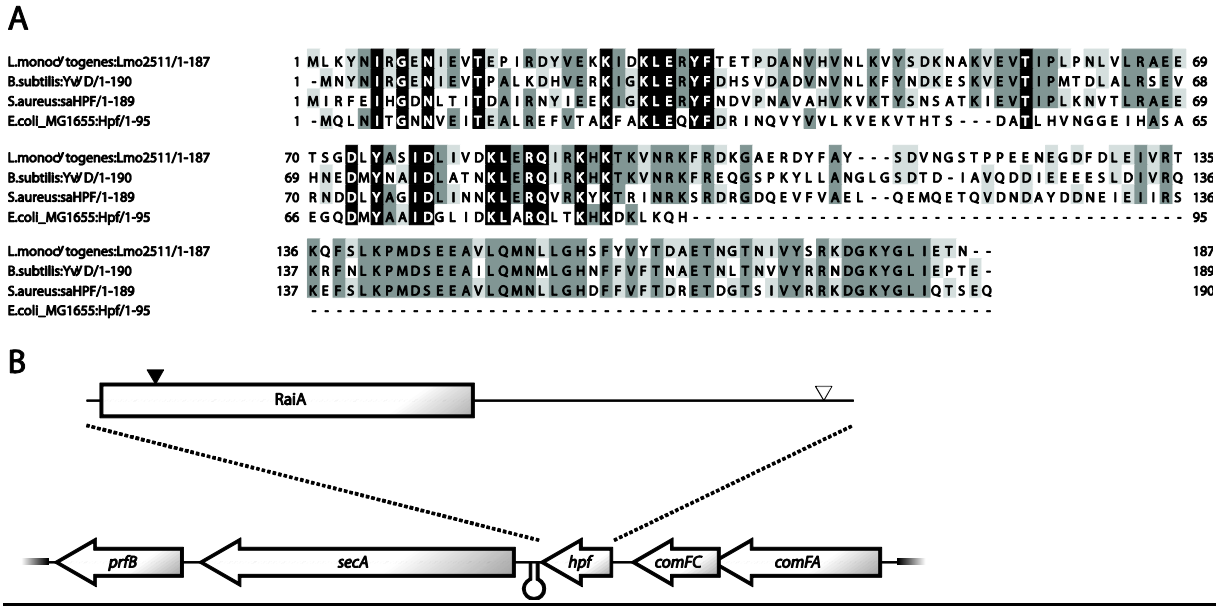

Figure 3-1. *L. monocytogenes* produces a homolog of long HPF

(A) Alignment of *L. monocytogenes* HPF with long homologs from *S. aureus* and *B. subtilis,* and short homolog from *E. coli*. Five of the six residues predicted to be important for ribosome binding in YfiA (Vila-Sanjurjo, Schuwirth et al. 2004; Ueta, Yoshida et al. 2005) are conserved in *L. monocytogenes* HPF. (B) Genomic context of *L. monocytogenes hpf*. A transcriptional terminator is located 3' of the *hpf* CDS. *Himar1* transposon insertions are noted by arrowheads: black (*hpf*::*Himar1*) and white (*hpf*::*Himar1-C*).

appeared to be quite scarce in early exponential growth and increased in relative quantity during mid- to late-exponential phase. The abundance of 100S relative to 70S ribosomes peaked at the transition from logarithmic to stationary phase growth (OD_{600} ≈ 2.5 to 3.0). Upon entry into stationary phase, relative abundance of 100S dimers fell back to roughly mid-log levels and was maintained at this ratio for several hours (Fig. 3-2). Bacteria exposed to prolonged post-exponential growth (72 to 96 hours) appeared to enter another, ribosomally distinct phase in which the vast majority of ribosomal RNA migrated in the vicinity of 30S subunits (Fig. 3-2). This likely represents a population in which the majority of bacteria have died and their ribosomes have been degraded to form the observed lower molecular weight species.

We examined *hpf*::*Himar1* extracts by SDGC to determine whether disruption of *hpf* influenced formation of 100S ribosomes in *L. monocytogenes*. 100S complexes were completely absent from ribosome samples isolated from *hpf*::*Himar1 L. monocytogenes* even at the transition from exponential to stationary phase growth, in stark contrast to WT *L. monocytogenes* ribosomes isolated at the same growth phase (Fig. 3-3a,b). To confirm that loss of 100S ribosome content was due to disruption of *hpf* rather than the presence of the *Himar1* transposon, we examined ribosomes of randomly selected *Himar1* transposon insertion mutants, which produced ribosome profiles identical to WT (data not shown). Although several small peaks were sometimes observed at 100S and larger in both WT and *hpf*::*Himar1*, these peaks always appeared in a pattern typical of actively translating polysomes rather than 100S ribosome complexes (Fenwick 1968).

A C-terminally 6xHis-tagged complementation construct was generated in a site-specific integration vector (Lauer, Chow et al. 2002) and introduced in single copy onto the chromosome of the *hpf*::*Himar1* strain to confirm that the ablation of 100S dimer formation was caused by disruption of *hpf*. Ribosome profiles from this complemented strain recovered a substantial amount of 100S dimer production, although they did not quite reach WT levels of 100S content (Fig. 3-3c). An untagged copy of *hpf* restored an equivalent amount of 100S production, confirming that the presence of the epitope tag did not interfere with complementation (data not shown). We hypothesized that the lack of full complementation might be a dominant-negative effect exerted by the transposon-disrupted copy of *hpf* that remains on the chromosome. We tested this by introducing the transposon-disrupted *hpf* gene into WT *L. monocytogenes* using the above complementation vector, but found that ectopic addition of the transposon-disrupted gene had no effect on ribosome dimerization. We are forced to hypothesize that some aspect of the endogenous *hpf* locus influences its regulation in a way that is difficult to replicate by complementation at an ectopic site.

The *S. aureus* HPF homolog saHPF was previously isolated from bacterial extracts bound specifically to 100S ribosome complexes during growth (Ueta, Wada et al. 2010). Using the tagged HPF_{6xHis} described above, we observed that this binding preference held true in *L. monocytogenes* whole-cell ribosome extracts as well. Quantitative Western blot analysis of ribosome fractions collected from *L. monocytogenes* carrying the epitope-tagged *hpf* gene showed that HPF_{6xHis} co-migrated through sucrose gradients predominantly with 100S dimers. Over 80 percent of total HPF_{6xHis} was localized to fractions in which 100S complexes were the dominant species (Fig. 3-3d). The small amount of HPF associated with other fractions is not surprising, as some saHPF was previously shown to associate with 70S ribosomes, particularly at

Figure 3-2

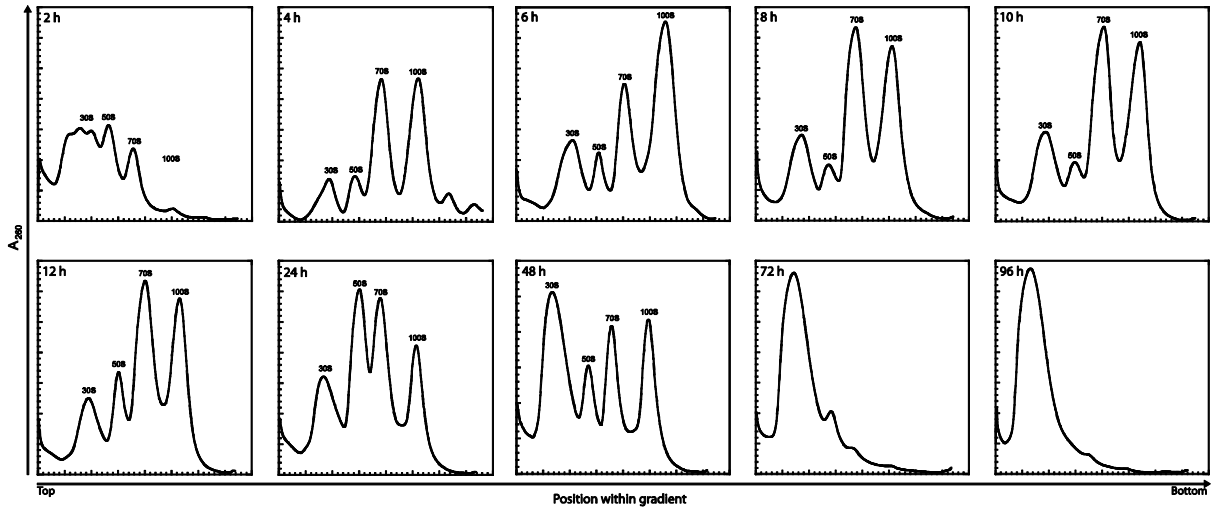

Figure 3-2. Time course of ribosome hibernation in *L. monocytogenes*

Presence or absence of 100S ribosome dimers in *L. monocytogenes* extracts was visualized over 96 h of growth in broth by SDGC. Each gradient was loaded with ≈150 µg of total nucleic acid, as measured by A_{260} (y-axes). Each graph depicts the top of the gradient on the left and the bottom of the gradient on the right (x-axes).

stationary phase (Ueta, Wada et al. 2010). To confirm that the 6xHis tag itself was not aberrantly localizing HPF to 100S ribosomes, a FLAG epitope tag was substituted. The resulting HPF protein showed the same pattern of localization (data not shown).

Nutrient- and stress-dependent control of HPF transcription

Both RMF and HPF have exhibited growth-phase-specific regulation in *E. coli* (Wada, Yamazaki et al. 1990; Maki, Yoshida et al. 2000), but little is known about the growth-phase-dependent expression of long HPF genes. Carbon and amino acid starvation are involved in this process in Gram-negatives, but it is not known whether the same signals govern hibernation in Gram-positive bacteria, which produce substantially different hibernation machinery and handle nutrient starvation responses differently (Okada, Makino et al. 2002; Ueta, Ohniwa et al. 2008). In addition, other signals independent of nutrient depletion may influence *hpf* expression and modulate ribosome hibernation. To approach these questions, we observed the transcriptional response of mid-log bacteria to various bacterially conditioned media. Conditioned media were generated by culturing WT *L. monocytogenes* in broth to a given growth phase, then removing the bacteria by centrifugation and filtration. In keeping with the observation that 100S ribosomes appeared throughout logarithmic growth and peaked upon entry to stationary phase, *hpf* transcript was most highly upregulated (approximately 100-fold) in response to early stationary phase conditioned BHI. Transcription of *hpf* was substantially lower, but still present, in conditioned BHI from earlier in growth and intermediate in BHI from later in growth (Fig. 3-4a). This transcriptional profile roughly mirrors the profile of 100S ribosome formation seen by SDGC (Fig. 3-2).

To test whether the observed increase in *hpf* expression in early stationary phase was caused by depletion of usable carbon sources from the growth medium, we exposed mid-log bacteria to stationary phase conditioned media supplemented with glucose and measured transcript levels. This treatment reduced *hpf* expression to levels very similar to those seen in fresh BHI (Fig. 3-4b). Based on this observation, it appears that a large proportion of *hpf* upregulation during the transition to stationary phase in BHI is mediated by carbon starvation. However, preliminary experiments showed that addition of concentrated late-log phase supernatants to mid-log cultures may also stimulate *hpf* production to a small extent, suggesting that secreted bacterial factors may accumulate in the growth medium and contribute to the induction of hibernation (data not shown). Overall, these results led us to conclude that *hpf* expression in *L. monocytogenes* is stimulated primarily by depletion of carbon pools in the growth media, but we cannot rule out a role for accumulated bacterial products.

Because nutrient limitation is capable of stimulating *hpf* expression, we decided to examine the *hpf* transcriptional response to other common stresses. Transcriptional control of *hpf* by stress-responsive sigma factors, σ^B and σ^H, has been reported in *L. monocytogenes* and *B. subtilis* (Drzewiecki, Eymann et al. 1998; Eymann and Hecker 2001; Chaturongakul, Raengpradub et al. 2011). We confirmed the stress responsiveness of *hpf* transcription in *L. monocytogenes* by growing bacteria to mid-log phase, then transferring them to one of several stress conditions for a period of five minutes. Bacteria were then collected rapidly by filtration and flash frozen, preserving the stress-induced transcriptional profile until RNA could be isolated. Using this method, we found that 4% v/v ethanol, 4% w/v sodium chloride, and 46°C heat shock were all efficient inducers of *hpf* expression. Deletion of *sigB* completely ablated the

Figure 3-3

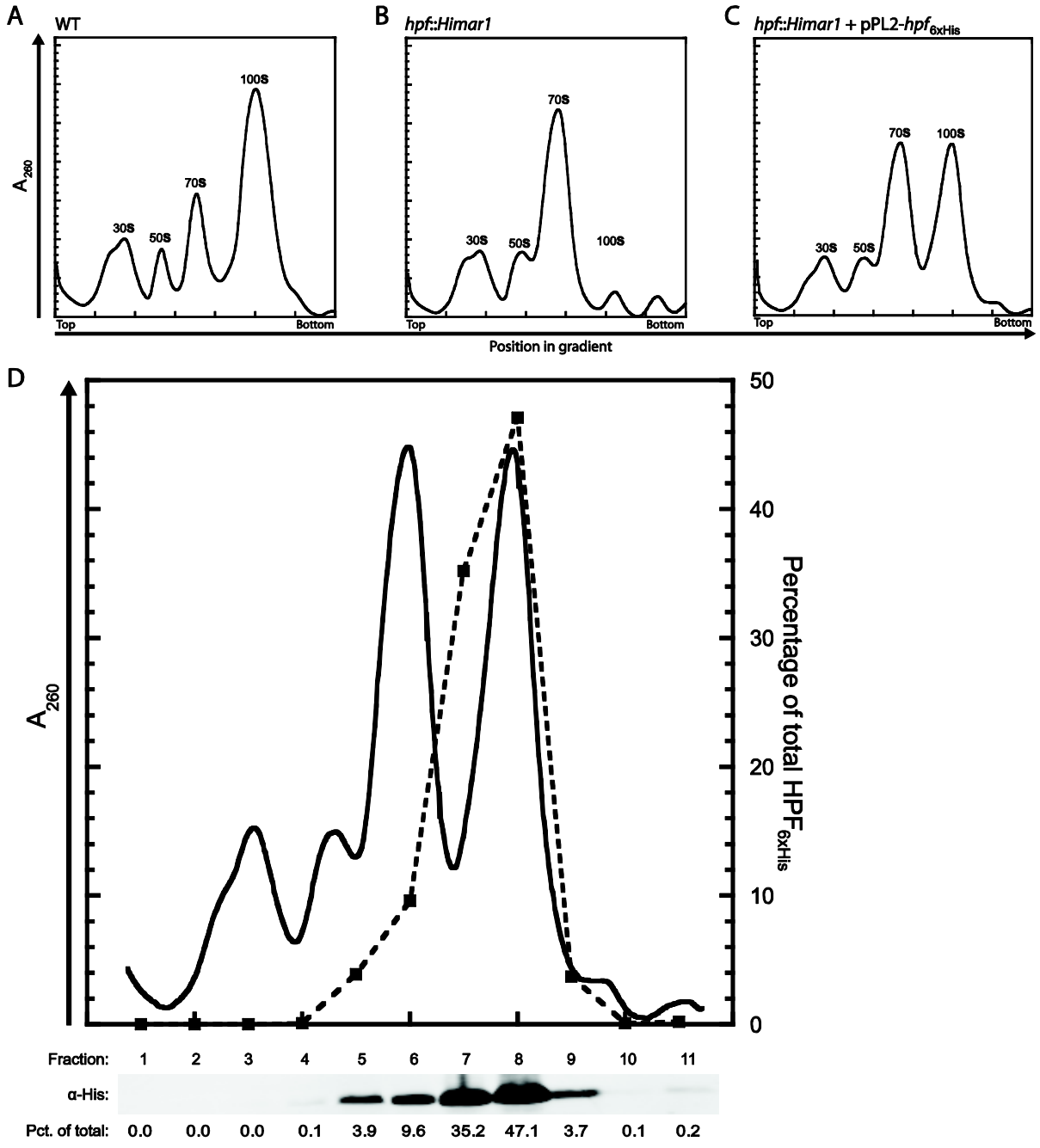
A
WT
B
hpf::Himar1
C
hpf::Himar1 + pPL2-hpf6xHis
A260
30S
50S
70S
100S
Top
Bottom
Position in gradient
D
A260
Percentage of total HPF6xHis
0
10
20
30
40
50
Fraction: 1 2 3 4 5 6 7 8 9 10 11
α-His:
Pct. of total: 0.0 0.0 0.0 0.1 3.9 9.6 35.2 47.1 3.7 0.1 0.2

Continued from previous page

Figure 3-3. HPF is required for 100S ribosome formation, and migrates through sucrose gradients with 100S ribosomes

SDGC profiles of ribosomes collected from WT *L. monocytogenes* (A), *hpf*::*Himar1* (B), and *hpf*::*Himar1* + pPL2-hpf_{6xHis} (C) at the transition between logarithmic and stationary phase (OD_{600} ≈ 2.5 to 3.0). (D) Western blot analysis of fractions collected from sucrose density gradients of *hpf*::*Himar1* + pPL2-hpf_{6xHis}. Plot shows A_{260} across sucrose gradient (solid line) and percentage of total HPF_{6xHis} in each fraction (dashed line). Western blot and numerical percentages of total signal are shown below.

upregulation of *hpf* observed in WT bacteria in response to all of these stresses (Fig. 3-4c), in agreement with the previously reported transcriptional phenotypes.

We next examined the SDGC ribosome profiles of bacteria subjected to both conditioned media (+/- glucose supplementation) and environmental stresses. Supplementation of conditioned media with glucose produced a notable upward shift in the ratio of 70S to 100S ribosome complexes (Fig. 3-4d), indicating that nutrient supplementation stimulated bacteria to decrease the extent of ribosome dimerization. Treatment with each of the σ^B-inducing stresses discussed above produced a small but consistent downward shift in the ratio of 70S to 100S ribosome complexes, indicating that stress induces bacteria to increase ribosome dimerization (Fig. 3-4e). Optimization of the timing of these treatments would likely yield more dramatic results.

Competitive disadvantage of HPF mutant bacteria in rich media

Given the substantial transcriptional regulation of HPF and the importance of hibernation for survival of other species in various *in vitro* conditions, we subjected *hpf*::*Himar1* to a variety of *in vitro* assays commonly used to assess fitness and virulence of *L. monocytogenes*. Bacterial growth curves in rich media showed that *hpf*::*Himar1* has a very slightly increased doubling time compared to WT. Little to no defect was observed in intracellular growth in resting bone-marrow-derived macrophages; based on infection and growth kinetics, *hpf*::*Himar1* appeared to infect, escape, and replicate equivalently to WT. Very slight defects were occasionally observed in L2 fibroblast plaque assays, but were not consistent enough to reach statistical significance (all data not shown). Each of these assays is typically performed in favorable, nutrient-rich conditions, so the absence of a defect in the HPF-deficient background is not entirely surprising.

Since *hpf* expression is so highly induced by nutrient-depleted media and stressful conditions, and since the inability to hibernate reduces the fitness of *E. coli rmf* mutants in prolonged post-exponential growth (Yamagishi, Matsushima et al. 1993), we reasoned that a *L. monocytogenes hpf* mutant was most likely to display growth or survival defects when exposed to stationary phase conditions. Surprisingly, transposon insertion mutants in *hpf* survived equivalently to WT when each was grown in pure culture in rich media over a period of several days. However, when transposon insertion mutants were grown in competitive co-culture with WT bacteria, they displayed a striking defect in post-exponential survival. After four days in competition with WT, *hpf*::*Himar1* comprised an average of only $1/100^{th}$ of the total bacterial population by CFU, while *Himar1* insertion mutants picked at random from a transposon insertion library maintained populations roughly equivalent to WT over the same period (Fig. 3-5a). Although its magnitude varied, this survival defect appeared consistently. Complementation of *hpf*::*Himar1* with pPL2-hpf_{6xHis} largely rescued the competitive defect (Fig. 3-5b).

One characteristic change in stationary phase growth media is a decrease in pH, from neutral to ≈5.5 (Wada, Mikkola et al. 2000). To determine whether pH change might contribute to the HPF competitive disadvantage, we grew WT and *hpf*::*Himar1* in co-culture in MOPS-buffered BHI. Although the appearance of the full competitive defect was slightly delayed, buffering was eventually overcome and the competitive defect reached that of the unbuffered media (Fig. 3-5c). This may indicate that a general increase in stress susceptibility is responsible

Figure 3-4

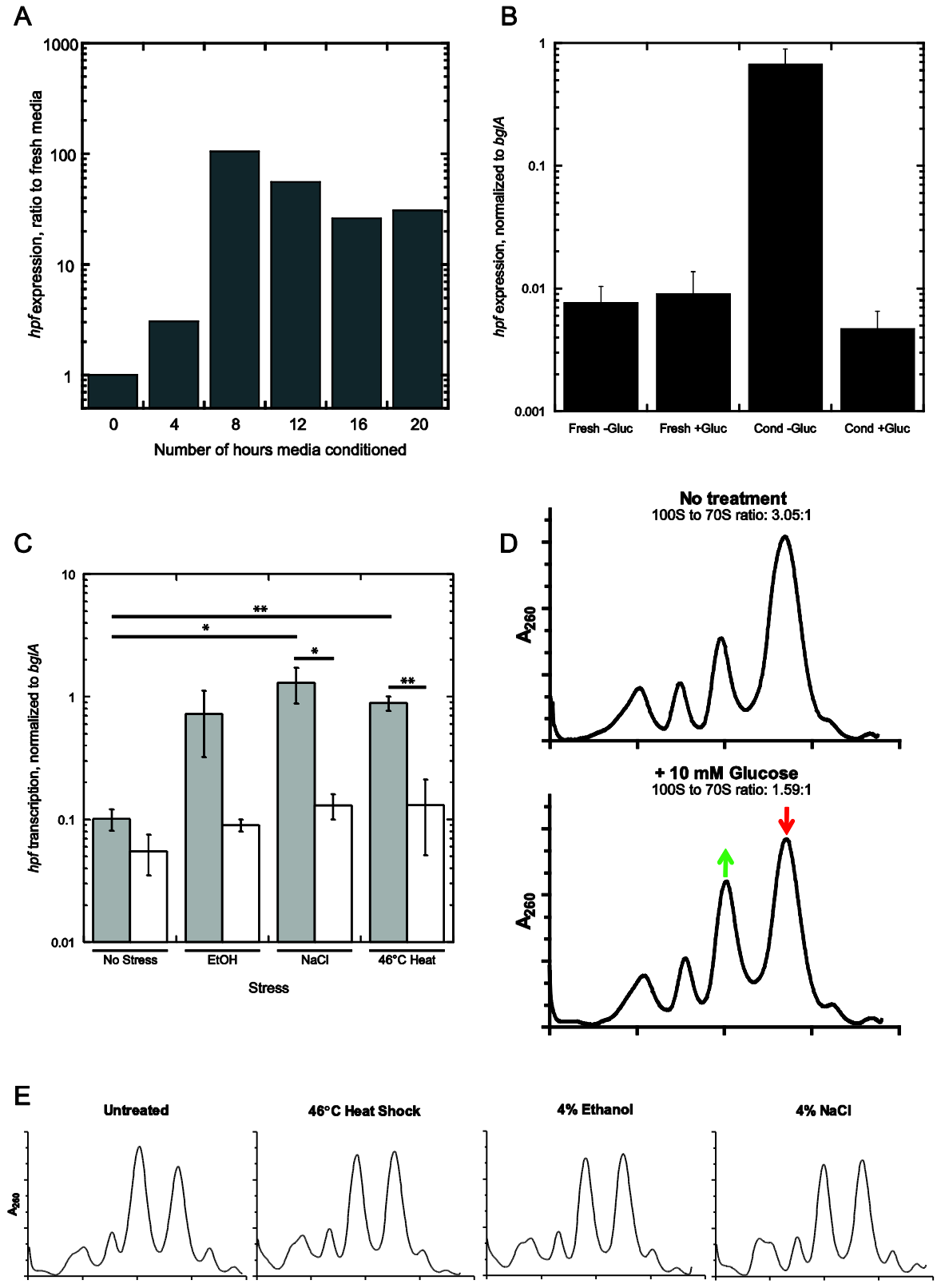
A
1000
100
10
1
hpf expression, ratio to fresh media
0
4
8
12
16
20
Number of hours media conditioned
B
1
0.1
0.01
0.001
hpf expression, normalized to bglA
Fresh -Gluc
Fresh +Gluc
Cond -Gluc
Cond +Gluc
C
10
1
0.1
0.01
hpf transcription, normalized to bglA
**
*
*
**
No Stress
EtOH
NaCl
46°C Heat
Stress
D
No treatment
100S to 70S ratio: 3.05:1
A260
+ 10 mM Glucose
100S to 70S ratio: 1.59:1
A260
E
Untreated
46°C Heat Shock
4% Ethanol
4% NaCl
A260

Continued from previous page

Figure 3-4. Transcriptional regulation of *hpf*

(A)-(C) Quantitative RT-PCR of *hpf* transcripts under various conditions. (A) WT *L. monocytogenes* grown to mid-log phase were treated with BHI conditioned by WT bacteria. Media conditioned by WT bacteria for the specified lengths of time were applied for 30 min, then bacteria were flash frozen and RNA was collected for qRT-PCR analysis. (B) WT *L. monocytogenes* grown to mid-log phase were treated with BHI conditioned for 8 hours by WT bacteria, with and without added glucose as noted. (C) Mid-log WT (gray bars) and Δ*sigB* (white bars) bacteria were treated for five minutes with unaltered BHI, BHI + 4% Ethanol, BHI + 4% w/v NaCl, or BHI at 46°C, followed immediately by flash freezing and later RNA extraction for qRT-PCR analysis. (D) and (E) Sucrose density gradient profiles of bacteria treated with the listed conditions for five minutes (stress treatments) or 30 minutes (glucose supplementation) prior to lysis and preparation of ribosomes. Ribosomal peak ratios were determined by integration of the area under each peak. *p<0.05, **p<0.01.

for the competitive defect of HPF-deficient bacteria during long-term post-exponential growth, but if so, media acidification is only one contributing factor. A role for HPF in stress tolerance would be consistent with the hibernation literature in other bacteria and with the stress-induced regulation of HPF transcription presented above. One clue about the specific stress that puts *hpf*::*Himar1* at a disadvantage in stationary phase may come from the growth medium itself. When competition experiments were performed in media sterilized by autoclaving, the expected competitive defect was observed. However, when the experiments were performed in media sterilized by filtration, the defect was completely ablated (Fig. 3-5d). The specific differences between these two treatments may give valuable insight into the biology of the *hpf*::*Himar1* strain, but these differences have yet to be explored.

Impact of HPF on virulence in a mouse model of infection

Although HPF is highly conserved across a diverse array of bacteria (Ueta, Ohniwa et al. 2008), the effects of *hpf* deletion on virulence of a human pathogen remain completely unknown. We used an intravenous mouse model of *L. monocytogenes* infection to determine whether *hpf*::*Himar1* bacteria are less fit for growth and survival in association with a mammalian host. We performed the previously described competitive index assay, which allows for a direct fitness comparison between two bacterial strains in the same animal (Auerbuch, Lenz et al. 2001). In this assay, the ratio of mutant to WT CFU recovered from the animal is used as a measure of the relative virulence of the mutant strain; a 1:1 ratio indicates that a mutant is equally virulent to WT. Six- to eight-week-old mice were infected with 10^5 *L. monocytogenes* (a 1:1 mixture of WT and *hpf*::*Himar1*) via tail vein injection and CFU/organ were counted at 48 hours postinfection. *hpf*::*Himar1* bacteria grown to mid-log (Fig. 3-6a), stationary phase (18 hour overnight culture) and extended stationary phase (3 day culture) (data not shown) prior to infection were all recovered at roughly a 1:1 ratio to WT bacteria, indicating that HPF has little impact on virulence of intravenously introduced *L. monocytogenes* at 48 hours in the organs examined.

Because it has been shown that RMF is important for acute acid stress tolerance in *E. coli* (El-Sharoud and Niven 2007), we reasoned that the *L. monocytogenes* HPF might be important for optimal passage through the acidic environment of the stomach or subsequent survival during oral infection. Such a defect would not have appeared in the above intravenous infections since those bacteria were injected directly into the bloodstream. Survival of passage through the stomach was assayed by homogenizing and plating feces at 24 hours postinfection, while subsequent dissemination of bacteria was examined by plating organ homogenates at 72 hours postinfection. WT and *hpf*::*Himar1* emerged at a roughly 1:1 ratio in feces, indicating that HPF does not play an important role in immediate survival of stomach acid (data not shown). By 72 hours, however, *hpf*::*Himar1* showed a median defect of roughly 10-fold in the liver, spleen, and intestine, and a median defect of >300-fold in the mesenteric lymph nodes of infected mice (Fig. 3-6b). The relatively small defects in the liver, spleen and intestine over 72 hours of infection may be explained by the small growth defect displayed by *hpf*::*Himar1*, but the large defect in the MLN is likely indicative of some susceptibility of HPF-deficient bacteria to the particular conditions encountered in the lymph node.

Figure 3-5

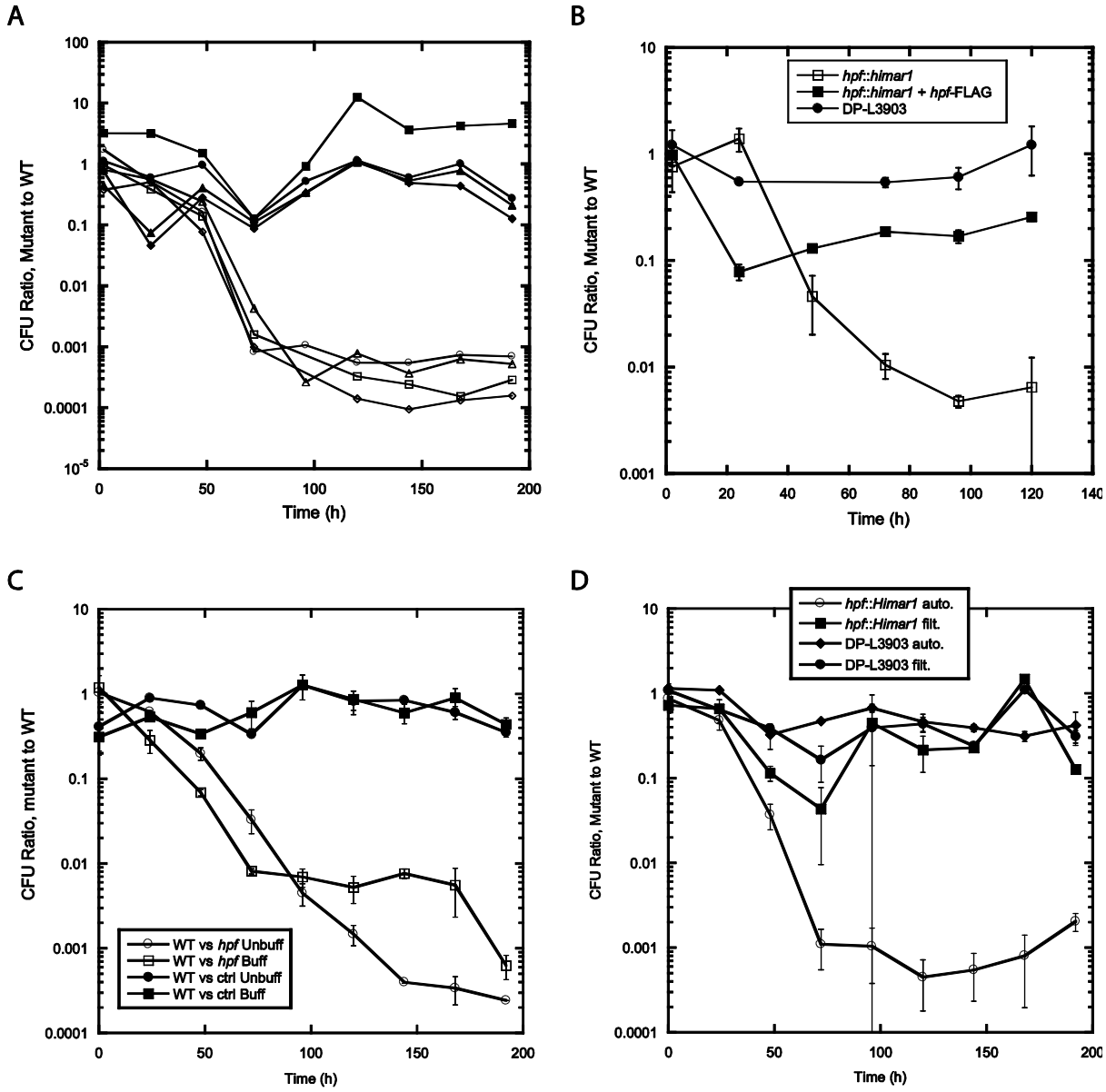
A
CFU Ratio, Mutant to WT
Time (h)
B
hpf::himar1
hpf::himar1 + hpf-FLAG
DP-L3903
CFU Ratio, Mutant to WT
Time (h)
C
CFU Ratio, mutant to WT
WT vs hpf Unbuff
WT vs hpf Buff
WT vs ctrl Unbuff
WT vs ctrl Buff
Time (h)
D
hpf::Himar1 auto.
hpf::Himar1 filt.
DP-L3903 auto.
DP-L3903 filt.
CFU Ratio, Mutant to WT
Time (h)

Continued from previous page

Figure 3-5. Competition experiments in BHI broth

Strains indicated in legends were co-inoculated at a 1:1 ratio into autoclave-sterilized BHI, unless indicated otherwise. Cultures were incubated at 37°C and samples diluted and plated for CFU every 24 hours. (A) Randomly selected *Himar1* transposon insertion mutants (filled symbols) or *hpf*::*Himar1* (open symbols) were each competed with WT in BHI. (B) *hpf*::*Himar1*, *hpf*::*Himar1* + pPL2-hpf_{FLAG}, or DP-L3903 (control strain carrying an Erm^R transposon insertion at a separate site) were each competed with WT in BHI. (C) *hpf*::*Himar1* and DP-L3903 were each competed with WT in both unbuffered and pH 7.0 MOPS-buffered BHI. (D) *hpf*::*Himar1* and DP-L3903 were each competed with WT in both autoclave- and filter-sterilized BHI. Error bars show standard deviations of two concurrently grown cultures (where applicable).

Figure 3-6

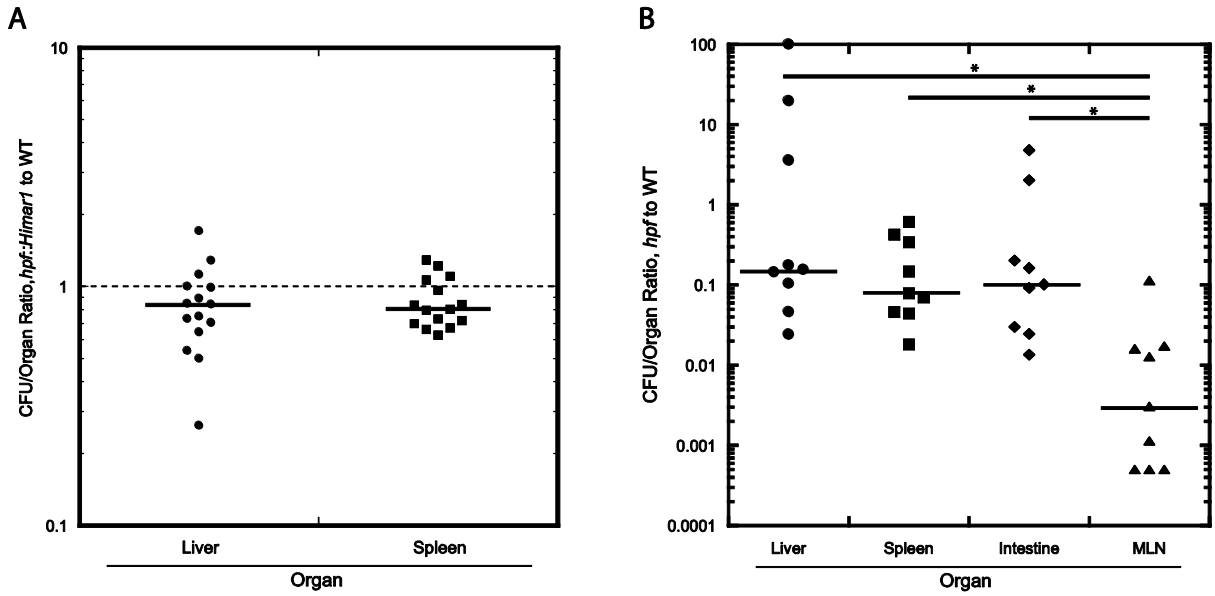

Figure 3-6. Competition in intravenous and oral models of murine infection

Competitive index infections of C57BL/6 mice were performed with 1:1 mixtures of WT and *hpf*::*Himar1 L. monocytogenes*. (A) Intravenous infection with 10^5 total bacteria. Livers and spleens were harvested at 48 hours postinfection, homogenized, and plated on appropriate selective media to determine CFU for each strain. Data shown are compiled from three independent experiments. (B) Infection with 10^8 bacteria by oral gavage. Mice were starved for 16 hours prior to infection. Organs were harvested at 72 hours postinfection, homogenized, and plated on appropriate selective media to determine CFU for each strain. Limit of detection for MLN: 5×10^{-4} *hpf*::*Himar1* CFU per WT CFU. *p<0.005.

Potential connections to other mechanisms of growth regulation in *L. monocytogenes*

SDGC analysis of several other strains of interest was also performed to determine whether ribosomal hibernation is modulated by systems already implicated in *L. monocytogenes* virulence or growth regulation. Because deletion of the gene encoding the c-di-AMP phosphodiesterase, *pdeA*, dramatically decreased expression of *hpf* (C.E. Witte, unpublished results), we examined the ribosome profiles of the Δ*pdeA* strain at both the mid-logarithmic and stationary phases. Surprisingly, deletion of the *pdeA* gene did not produce any significant decrease in ribosomal hibernation during either growth phase. Similarly, a conditional deletion mutant in the *L. monocytogenes* diadenylate cyclase, *dacA*, failed to show the predicted increase in ribosomal hibernation, although ribosomal integrity did seem to be generally compromised in the absence of DacA. Another protein of interest, PrpC (discussed in greater detail in Chapter 2), which is thought to be involved in homeostasis and growth regulation, was also tested for a shift in ribosomal hibernation and showed minimal difference from WT (all data not shown).

Microarray analysis of *hpf*::*Himar1*

We performed whole-genome expression microarray analysis to explore the transcriptional changes that disruption of *hpf* produces in *L. monocytogenes* at early stationary phase (8.5 hours post-inoculation). We observed a strong bias towards transcriptional downregulation of ribosomal proteins and elongation factors in the *hpf*::*Himar1* background. Twenty-four ribosomal proteins from both the small and large ribosomal subunits and four elongation factors were downregulated >2-fold, while only two ribosomal proteins and no elongation factors were upregulated. We also noted that σ^B and three of its associated regulators were downregulated. Conversely, σ^L and nine predicted phosphotransferase system (PTS) genes were upregulated > 2-fold. These transcriptional changes imply that *hpf*::*Himar1* is biased towards a biological state distinct from WT, but more work will be required to understand the basis for and consequences of the changes in gene regulation. The complete set of genes regulated > 2-fold is listed in Table 3-1.

Table 3-1. Genes regulated >2-fold compared to WT in *hpf*::*Himar1* microarrays		
Fold change	**Gene ID**	**Annotation**
-6.16	lmo2157	sepA
-5.75	lmo2655	ribosomal protein S7
-4.72	lmo0641	similar to heavy metal-transporting ATPa
-4.71	lmo1375	similar to aminotripeptidase
-4.66	lmo2157	sepA
-4.66	lmo2654	fus; highly similar to translation elongation factor G
-4.56	lmo2654	highly similar to translation elongation
-4.55	lmo0641	similar to heavy metal-transporting ATPase
-4.46	lmo1375	similar to aminotripeptidase
-4.34	lmo1606	similar to DNA translocase
-4.31	lmo2626	ribosomal protein S3, rpsC
-4.00	lmo2656	ribosomal protein S12
-3.95	lmo1422	similar to glycine betaine/carnitine/cho
-3.92	lmo1360	highly similar to methylenetetrahydrofol
-3.90	lmo2654	fus; highly similar to translation elongation factor G
-3.81	lmo1606	similar to DNA translocase
-3.78	lmo2620	ribosomal protein L5
-3.73	lmo0790	similar to transcription regulator (EbsC
-3.69	lmo1421	similar to glycine betaine/carnitine/cho
-3.59	lmo0445	similar to transcription regulator
-3.59	lmo1375/lmo1376	intergenic
-3.56	lmo0894	sigma-B activity negative regulator RsbW
-3.49	lmo0893	anti-anti-sigma factor (antagonist of Rs
-3.47	lmo1065	similar to B. subtilis YktB protein
-3.46	lmo2456	highly similar to phosphoglycerate mutas
-3.43	lmo1300	similar to arsenic efflux pump protein
-3.41	lmo2621	ribosomal protein L24
-3.41	lmo0851	unknown
-3.39	lmo1356	similar to acetyl-CoA carboxylase subunit (biotin carboxyl carrier subunit)
-3.38	lmo0896	Indirect negative regulation of sigma B
-3.37	lmo1360	highly similar to methylenetetrahydrofolate dehydrogenase and methenyltetrahydrofolate cyclohydrolase
-3.36	lmo2457	highly similar to triose phosphate isome
-3.29	lmo0434	Internalin B
-3.28	lmo1359	similar to transcription termination pro
-3.28	lmo1357	acetyl-CoA carboxylase subunit (biotin c
-3.28	lmo2031	similar to unknown proteins
-3.27	lmo1878	similar to transcriptional regulators, GntR family of repressors
-3.23	lmo2460	similar to B. subtilis CggR hypothetical transcriptional regulator
-3.19	lmo2624	ribosomal protein L29
-3.18	lmo1088	similar to teichoic acid biosynthesis pr
-3.17	lmo0968	similar to conserved hypothetical protei
-3.17	lmo1849	similar to metal cations ABC transporter
-3.09	lmo2458	highly similar to phosphoglycerate kinas
-3.06	lmo2222	similar to unknown proteins
-3.06	lmo2623	ribosomal protein S17
-3.04	lmo1713	similar to cell-shape determining proteins
-3.02	lmo1376	similar to 6-phosphogluconate dehydrogenase
-3.01	lmo2631	ribosomal protein L4
-3.01	lmo1456	similar to unknown proteins
-3.00	lmo2626	ribosomal protein S3
-3.00	lmo1357	acetyl-CoA carboxylase subunit (biotin carboxylase subunit)
-3.00	lmo2031	similar to unknown proteins
-3.00	lmo2622	ribosomal protein L14
-2.99	lmo1077	similar to teichoic acid biosynthesis pr
-2.98	lmo2627	ribosomal protein L22
-2.96	lmo1720	similar to phosphotransferase system (PT
-2.96	lmo1711	highly similar to aminopeptidases

-2.94	lmo0968	similar to conserved hypothetical protei
-2.91	lmo0554	similar to NADH-dependent butanol dehydr
-2.90	lmo0025	similar to phosphoheptose isomerase
-2.90	lmo1421	similar to glycine betaine/carnitine/choline ABC transporter (ATP-binding protein)
-2.89	lmo0880	similar to wall associated protein precursor (LPXTG motif)
-2.88	lmo1078	similar to putative UDP-glucose pyrophos
-2.88	lmo0969	similar to ribosomal large subunit pseud
-2.88	lmo2625	ribosomal protein L16
-2.88	lmo2460	similar to B. subtilis CggR hypothetical
-2.88	lmo2130	similar to unknown protein
-2.88	lmo2116	unknown
-2.87	lmo1719	similar to phosphotransferase system (PT
-2.85	lmo0928	similar to 3-methyladenine DNA glycosyla
-2.84	lmo1848	similar metal cations ABC transporter (p
-2.84	lmo2618	ribosomal protein S8
-2.82	lmo1358	similar to B. subtilis YqhY protein
-2.82	lmo0722	similar to pyruvate oxidase
-2.82	lmo2632	ribosomal protein L3
-2.81	lmo1848	similar metal cations ABC transporter (permease protein)
-2.81	lmo1713	similar to cell-shape determining protei
-2.81	lmo1947	similar to two-component sensor histidin
-2.81	lmo0896	Indirect negative regulation of sigma B dependant gene expression (serine phosphatase)
-2.76	lmo0692	two-component sensor histidine kinase Ch
-2.76	lmo1392	similar to putative proteases
-2.75	lmo0880	similar to wall associated protein precu
-2.75	lmo1392	similar to putative proteases
-2.75	lmo2222	similar to unknown proteins
-2.75	lmo2254	similar to unknown proteins
-2.74	lmo1074	highly similar to teichoic acid transloc
-2.73	lmo0820	some similarity to acatyltransferases
-2.72	lmo1315	similar to undecaprenyl diphosphate synt
-2.72	lmo1440	similar to unknown proteins
-2.72	lmo2619	ribosomal protein S14
-2.71	lmo0696	similar to flagellar hook assembly prote
-2.71	lmo0956	similar to N-acetylglucosamine-6P-phosph
-2.70	lmo0937	unknown
-2.69	lmo2629	ribosomal protein L2
-2.69	lmo0644	similar to conserved hypothetical protei
-2.69	lmo2639	unknown
-2.69	lmo2222	similar to unknown proteins
-2.68	lmo1650	similar to hypothetical proteins
-2.67	lmo0850	hypothetical protein
-2.66	lmo0593	similar to transport proteins (formate?)
-2.66	lmo0958	similar to transcription regulator (GntR
-2.65	lmo0895	RNA polymerase sigma-37 factor (sigma-B)
-2.65	lmo0967	similar to B. subtilis YjbM protein
-2.64	lmo2633	ribosomal protein S10
-2.64	lmo0694	unknown
-2.64	lmo2630	ribosomal protein L23
-2.64	lmo2030	similar to unknown proteins
-2.64	lmo2494	similar to negative regulator of phospha
-2.63	lmo2166	unknown
-2.62	lmo2222	similar to unknown proteins
-2.62	lmo2509	PrfB; highly similar to peptide chain release factor 2
-2.62	lmo1392	similar to putative proteases
-2.61	lmo2201	similar to 3-oxoacyl-acyl-carrier protei
-2.61	lmo0820	some similarity to acatyltransferases
-2.60	lmo1455	DnaG; DNA primase
-2.60	lmo0799	unknown
-2.59	lmo2038	MurE; similar to UDP-N-acetylmuramoylalanyl-D-glutamate-2,6-diaminopimelate ligase
-2.59	lmo0524	similar to putative sulfate transporter

-2.58	lmo2614	ribosomal protein L30
-2.58	lmo0236	similar to B. subtilis YacN protein
-2.58	lmo1650	similar to hypothetical proteins
-2.57	lmo1870	similar to alkaline phosphatase
-2.57	lmo2061	similar to unknown protein
-2.56	lmo2616	ribosomal protein L18
-2.56	lmo0246	transcription antitermination factor
-2.55	lmo0820	some similarity to acatyltransferases
-2.55	lmo1657	translation elongation factor
-2.54	lmo0236	similar to B. subtilis YacN protein
-2.54	lmo2038	similar to UDP-N-acetylmuramoylalanyl-D-
-2.54	lmo1878	similar o transcriptional regulators
-2.54	lmo2628	ribosomal protein S19
-2.53	lmo1420	weakly similar to UDP-N-acetylglucosamin
-2.52	lmo1455	DnaG; DNA primase
-2.52	lmo1954	Drm; similar to phosphopentomutase
-2.52	lmo0956	similar to N-acetylglucosamine-6P-phosphate deacetylase (EC 3.5.1.25)
-2.51	lmo2037	similar to phospho-N-acetylmuramoyl-pent
-2.51	lmo0234	highly similar to B. subtilis YacL prote
-2.51	lmo1018	similar to E. coli copper homeostasis pr
-2.51	lmo2037	MraY; similar to phospho-N-acetylmuramoyl-pentapeptide transferase
-2.51	lmo2626	RpsC; ribosomal protein S3
-2.51	lmo1080	similar to B. subtilis minor teichoic ac
-2.50	lmo0606	similar to transcription regulator MarR
-2.49	lmo2616	ribosomal protein L18
-2.49	lmo1878	similar o transcriptional regulators
-2.47	lmo1316	similar to phosphatidate cytidylyltransf
-2.47	lmo2165	similar to transcription regulator CRP/F
-2.46	lmo0699	similar to flagellar switch protein FliM
-2.46	lmo1675	similar to 2-succinyl-6-hydroxy-2,4-cycl
-2.46	lmo1865	similar to conserved hypothetical protei
-2.46	lmo1316	similar to phosphatidate cytidylyltransferase (CDP-diglyceride synthase)
-2.46	lmo1569	similar to unknown proteins
-2.45	lmo0821	unknown
-2.45	lmo2450	similar to carboxylesterase
-2.45	lmo2640	unknown
-2.44	lmo1086	similar to CDP-ribitol pyrophosphorylase
-2.43	lmo2099	similar to transcription antiterminator
-2.42	lmo2034	similar to cell-division initiation prot
-2.42	lmo0787	similar to amino acid transporter
-2.42	lmo1453	conserved hypothetical protein
-2.42	lmo1396	similar to phosphatidylglycerophosphate
-2.41	lmo2857	hypothetical protein
-2.41	lmo0957	similar to glucosamine-6-Phoasphate isom
-2.40	lmo0784	similar to mannose-specific phosphotransferase system (PTS) component IIA
-2.40	lmo1568	similar to unknown proteins
-2.40	lmo1676	similar to menaquinone-specific isochori
-2.39	lmo0995	similar to B. subtilis YkrP protein
-2.39	lmo1724	similar to ABC transporter, ATP-binding
-2.39	lmo1568	similar to unknown proteins
-2.39	lmo1431	similar to ABC transporter (ATP-binding
-2.38	lmo2230	similar to arsenate reductase
-2.38	lmo1392	similar to putative proteases
-2.38	lmo0970	similar to enoyl- acyl-carrier protein r
-2.38	lmo1494	similar to 5-methylthioadenosine/S-adeno
-2.38	lmo0693	similar to flagellar motor switch protei
-2.37	lmo2015	similar to alpha-mannosidase
-2.37	lmo1455	DnaG; DNA primase
-2.36	lmo0783	similar to mannose-specific phosphotrans
-2.36	lmo2615	ribosomal protein S5
-2.36	lmo2455	Eno; enolase

-2.36	lmo1594	similar to B. subtilis negative regulato
-2.35	lmo1933	similar to GTP cyclohydrolase I
-2.35	lmo1567	highly similar to citrate synthase subun
-2.35	lmo0956	similar to N-acetylglucosamine-6P-phosphate deacetylase (EC 3.5.1.25)
-2.34	lmo0001	Chromosomal replication initiation protein DnaA
-2.34	lmo0539	similar to tagatose-1,6-diphosphate aldo
-2.34	lmo1237	RacE
-2.34	lmo1711	highly similar to aminopeptidases
-2.33	lmo1004	conserved hypothetical protein
-2.33	lmo1675	MenD; similar to 2-succinyl-6-hydroxy-2,4-cyclohexadiene-1-carboxylate synthase / 2-oxoglutarate decarboxylase
-2.33	lmo1354	similar to aminopeptidase P
-2.33	lmo1315	similar to undecaprenyl diphosphate synthase
-2.32	lmo2036	similar to UDP-N-acetylmuramoylalanine D-glutamate ligase
-2.32	lmo2093	unknown
-2.32	lmo0880	similar to wall associated protein precursor (LPXTG motif)
-2.31	lmo0559	putative membrane protein
-2.31	lmo1785	translation initiation factor IF-3
-2.31	lmo2201	similar to 3-oxoacyl-acyl-carrier protein synthase
-2.31	lmo0274	unknown
-2.31	lmo0237	highly similar to glutamyl-tRNA syntheta
-2.31	lmo0439	weakly similar to a module of peptide synthetase
-2.31	lmo1331	PupA; polynucleotide phosphorylase (PNPase)
-2.30	lmo1566	highly similar to isocitrate dehyrogenas
-2.30	lmo1331	polynucleotide phosphorylase (PNPase)
-2.30	lmo2389	similar to NADH dehydrogenase
-2.30	lmo2490	similar to B. subtilis CsbA protein
-2.30	lmo1064	similar to membrane and transport protei
-2.30	lmo0440	hypothetical protein
-2.30	lmo0235	similar to nucleotidylyl transferase, pyrophosphorylase
-2.29	lmo2605	ribosomal protein L17
-2.28	lmo2034	smbA
-2.28	lmo1673	similar to dihydroxynapthoic acid synthe
-2.28	lmo2724	similar to unknown proteins
-2.28	lmo1013	similar to conserved hypothetical protei
-2.28	lmo2436	similar to transcription antiterminator
-2.27	lmo2094	similar to L-fuculose-phosphate aldolase
-2.27	lmo0784	similar to mannose-specific phosphotrans
-2.27	lmo2459	highly similar to glyceraldehyde 3-phosp
-2.27	lmo0235	similar to nucleotidylyl transferase, py
-2.26	lmo1241	conserved hypothetical protein
-2.26	lmo2507	highly similar to the cell-division ATP-
-2.26	lmo1955	similar to integrase/recombinase
-2.26	lmo0781	similar to mannose-specific phosphotrans
-2.25	lmo0992	conserved hypothetical protein
-2.25	lmo1711	highly similar to aminopeptidases
-2.25	lmo0019	unknown
-2.25	lmo0325	similar to transcriptional regulators
-2.24	lmo0819	unknown
-2.24	lmo1595	similar to unknown protein
-2.23	lmo1946	similar to similar to acyl-CoA hydrolase
-2.23	lmo2491	unknown
-2.22	lmo2760	similar to ABC transporter (ATP-binding protein)
-2.22	lmo0001	Chromosomal replication initiation prote
-2.22	lmo2033	FtsA
-2.22	lmo2040	similar to cell-division protein FtsL
-2.21	lmo2058	similar to heme O oxygenase
-2.21	lmo0098	similar to PTS system mannose-specific,
-2.20	lmo1317	similar to deoxyxylulose 5-phosphate reductoisomerase
-2.19	lmo0169	similar to a glucose uptake protein
-2.19	lmo0993	similar to Na -transporting ATP synthase subunit J

-2.18	lmo0957	similar to glucosamine-6-Phoasphate isomerase (EC 5.3.1.10)
-2.18	lmo1849	similar to metal cations ABC transporter, ATP-binding proteins
-2.18	lmo0722	similar to pyruvate oxidase
-2.18	lmo1237	RacE
-2.18	lmo0596	similar to unknown proteins
-2.18	lmo1089	highly similar to glycerol-3-phosphate c
-2.18	lmo0539	similar to tagatose-1,6-diphosphate aldolase
-2.17	lmo0959	similar to undacaprenyl-phosphate N-acetylglucosaminyltransferase
-2.17	lmo1569	similar to unknown proteins
-2.17	lmo0691	Chemotaxis response regulator CheY
-2.17	lmo1883	similar to chitinases
-2.17	lmo0648	similar to membrane proteins
-2.17	lmo1237	similar to glutamate racemase
-2.16	lmo2612	highly similar to preprotein translocase
-2.16	lmo1355	Efp, similar to elongation factor P
-2.16	lmo2590	similar to ATP binding proteins
-2.16	lmo1396	similar to phosphatidylglycerophosphate synthase
-2.16	lmo1933	similar to GTP cyclohydrolase I
-2.16	lmo0781	similar to mannose-specific phosphotransferase system (PTS) component IID
-2.15	lmo1528	similar to unknown proteins
-2.15	lmo2573	similar to zinc-binding dehydrogenase
-2.15	lmo1241	unknown
-2.15	lmo2506	highly similar to cell-division protein
-2.14	lmo2167	similar to unknown proteins
-2.14	lmo2096	similar to PTS system galactitol-specifi
-2.14	lmo1271	similar to signal peptidase I
-2.14	lmo1545	similar to cell-division inhibition (sep
-2.14	lmo1067	similar to GTP-binding elongation factor
-2.14	lmo2232	similar to unknown proteins
-2.14	lmo1599	catabolite control protein A
-2.14	lmo1567	CitZ
-2.13	lmo1899	similar to ATP-dependent helicases
-2.13	lmo2641	similar to heptaprenyl diphosphate synth
-2.13	lmo2039	similar to penicillin-binding protein 2B
-2.13	lmo0958	similar to transcription regulator (GntR family)
-2.13	lmo2167	similar to unknown proteins
-2.13	lmo1266	unknown
-2.13	lmo0096	similar to PTS system mannose-specific,
-2.12	lmo0789	similar to conserved hypothetical proteins
-2.12	lmo1595	similar to unknown protein
-2.12	lmo2779	similar to probable GTP-binding protein
-2.12	lmo1883	similar to chitinases
-2.12	lmo1782	similar to 3-exo-deoxyribonuclease exoA
-2.12	lmo1365	similar to D-1-deoxyxylulose 5-phosphate
-2.11	lmo1847	similar to adhesion binding proteins and
-2.11	lmo0272	conserved hypothetical protein similar to B. subtilis YxeH protein
-2.11	lmo0439	weakly similar to a module of peptide sy
-2.10	lmo0210	similar to L-lactate dehydrogenase
-2.10	lmo0782	similar to mannose-specific phosphotrans
-2.10	lmo0579	similar to unknown protein
-2.10	lmo2505	Spl, peptidoglycan lytic protein P45
-2.10	lmo2827	similar to transcriptional regulator (Ma
-2.10	lmo1705	similar to deoxyguanosine kinase/deoxyadenosine kinase(I) subunit
-2.10	lmo0237	GltX, highly similar to glutamyl-tRNA synthetase
-2.10	lmo2042	similar to unknown proteins
-2.10	lmo1912	similar to unknown proteins (hypothetica
-2.09	lmo0581	conserved hypothetical protein
-2.09	lmo1675	MenD; similar to 2-succinyl-6-hydroxy-2,4-cyclohexadiene-1-carboxylate synthase / 2-oxoglutarate decarboxylase
-2.09	lmo1866	similar to conserved hypothetical proteins
-2.09	lmo0044	ribosomal protein S6

-2.09	lmo2770	similar to gamma-glutamylcysteine synthe
-2.09	lmo1979	similar to unknown proteins
-2.08	lmo1782	similar to 3-exo-deoxyribonuclease exoA
-2.08	lmo1376	similar to 6-phosphogluconate dehydrogen
-2.08	lmo1019	similar to B. subtilis YitL protein
-2.08	lmo2130	similar to unknown protein
-2.08	lmo1085	similar to teichoic acid biosynthesis protein B
-2.08	lmo1076	similar to autolysin (EC 3.5.1.28) (N-acetylmuramoyl-L-alanine amidase)
-2.08	lmo2778	unknown
-2.08	lmo0993	similar to Na+-transporting ATP synthase
-2.07	lmo1953	similar to purine-nucleoside phosphoryla
-2.06	lmo1091	similar to glysosyltransferases
-2.06	lmo1337	similar to B. subtilis yqgP
-2.06	lmo2103	Pta; similar to phosphotransacetylase
-2.06	lmo1542	ribosomal protein L21
-2.06	lmo2102	glutamine amidotransferase, SNO family
-2.05	lmo0292	similar to heat-shock protein htrA serin
-2.05	lmo2606	highly similar to RNA polymerase (alpha
-2.05	lmo2130	similar to unknown protein
-2.05	lmo0782	smbA
-2.05	lmo1365	TktB; similar to D-1-deoxyxylulose 5-phosphate synthase
-2.05	lmo0620	unknown
-2.05	lmo0699	similar to flagellar switch protein FliM
-2.04	lmo2508	similar to conserved hypothetical protei
-2.04	lmo1848	similar metal cations ABC transporter (permease protein)
-2.04	lmo1689	similar to A/G-specific adenine glycosyl
-2.03	lmo0694	unknown
-2.03	lmo1723	membrane protein, putative
-2.03	lmo1718	similar to putative outer surface protein
-2.03	lmo2033	highly similar to cell-division protein
-2.03	lmo2095	similar to 1-phosphofructokinase
-2.03	lmo0169	similar to a glucose uptake protein
-2.03	lmo1527	similar to protein-export membrane prote
-2.03	lmo2434	highly similar to glutamate decarboxylas
-2.02	lmo1419	conserved hypothetical protein
-2.02	lmo1076	similar to autolysin (EC 3.5.1.28) (N-ac
-2.02	lmo1266	unknown
-2.01	lmo2067	similar to conjugated bile acid hydrolas
-2.01	lmo1581	highly similar to acetate kinase
-2.01	lmo0663	conserved hypothetical proteins
-2.01	lmo1083	similar to dTDP-D-glucose 4,6-dehydratas
-2.01	lmo1455	DNA primase
-2.00	lmo2041	similar to unknown proteins
2.00	lmo2150	unknown
2.00	lmo0149	unknown
2.00	lmo0639	similar to a transcription regulator (surface protein PAg negative regulator par)
2.00	lmo1684	similar to glycerate dehydrogenases
2.01	lmo1220	similar to unknown protein
2.01	lmo0267	similar to other proteins
2.01	lmo1459	similar to glycyl-tRNA synthetase alpha chain
2.01	lmo2763	similar to PTS cellobiose-specific enzym
2.01	lmo1410	unknown
2.01	lmo2407	conserved hypothetical protein
2.02	lmo0355	similar to Flavocytochrome C Fumarate Re
2.02	lmo1514	similar to unknown protein
2.03	lmo2177	similar to unknown protein
2.03	lmo0139/lmo0140	intergenic
2.03	lmo0710	similar to flagellar basal-body rod protein flgB
2.03	lmo2461	SigL, sigma-54 sigma factor
2.03	lmo1053	highly similar to pyruvate dehydrogenase
2.03	lmo0575	similar to transcription regulator GntR

2.04	lmo0483	unknown
2.04	lmo1458	GlyS
2.04	lmo1349	similar to glycine dehydrogenase (decarb
2.04	lmo1348	similar to aminomethyltransferase
2.04	lmo2431	similar to B. subtilis ferrichrome ABC t
2.04	lmo2107	similar to transcriptional regulator (DeoR family)
2.06	lmo0168	similar to B. subtilis transcription reg
2.06	lmo2661	similar to ribulose-5-phosphate 3-epimer
2.06	lmo0711	similar to flagellar basal-body rod prot
2.06	lmo0031	transcriptional regulator LacI family
2.06	lmo2651	similar to mannitol-specific PTS enzyme
2.07	lmo1678	similar to 5-methyltetrahydrofolate-homo
2.07	lmo2664	similar to sorbitol dehydrogenase
2.07	lmo0386	similar to B. subtilis IolD protein, to acetolactate synthase
2.08	lmo0345	similar to sugar-phosphate isomerase
2.09	lmo2370	similar to aminotransferase
2.09	lmo2260	similar to unknown proteins
2.10	lmo2342	similar to 16S pseudouridylate synthase
2.10	lmo0612	similar to transcription regulator MarR family
2.10	lmo1519	AspS
2.10	lmo2816	similar to transport protein
2.10	lmo2392	similar to B. subtilis YuzB protein
2.11	lmo2271	unknown
2.11	lmo0710	similar to flagellar basal-body rod protein flgB
2.12	lmo2714	peptidoglycan anchored protein (LPXTG mo
2.12	lmo1055	highly similar to dihydrolipoamide dehyd
2.13	lmo0639	similar to a transcription regulator (su
2.13	lmo1095	similar to PTS system, cellobiose-specific IIB component (cel A)
2.13	lmo1786	internalin C
2.14	lmo2649	similar to hypothetical PTS enzyme IIC c
2.15	lmo0131	conserved hypothetical protein
2.15	lmo2574	unknown
2.15	lmo0625	putative lipase/acylhydrolase
2.15	lmo2373	similar to phosphotransferase system (PT
2.15	lmo2429	similar to B. subtilis ferrichrome ABC t
2.15	lmo0363	similar to Salmonella typhimurium peptid
2.16	lmo1786	Internalin C
2.17	lmo1919	similar to unknown proteins
2.18	lmo0652/lmo0653	intergenic
2.18	lmo0574	similar to beta-glucosidase
2.18	lmo0483	conserved hypothetical protein
2.19	lmo1740	similar to amino acid (glutamine) ABC tr
2.19	lmo0709	unknown
2.19	lmo0718	unknown
2.19	lmo1508	similar to two-component sensor histidin
2.20	lmo0711	similar to flagellar basal-body rod protein flgC
2.21	lmo2228	similar to unknown protein
2.21	lmo0983	similar to glutathione peroxidase
2.22	lmo1502	similar to unknown proteins
2.22	lmo0078	similar to phosphoglycerate dehydrogenase
2.22	lmo0335	unknown
2.22	No lmo match?	CfpL belongs to the Listeria-specific group of the CRP/FNR-superfamily
2.23	lmo2566	unknown
2.23	lmo2742	SH3 domain protein
2.23	lmo1502	similar to unknown proteins
2.23	lmo1134	similar to regulatory proteins
2.24	lmo2592	similar to oxidoreductase, aldo/keto red
2.24	lmo2647	similar to creatinine amidohydrolase
2.24	lmo2830	similar to thioredoxin
2.24	lmo2593	similar to transcription regulators (MerR family)
2.25	lmo0183	similar to alpha-glucosidase

2.25	lmo2339	conserved hypothetical protein
2.25	lmo0713	similar to flagellar basal-body M-ring p
2.25	lmo0919	similar to ABC transporter ATP-binding p
2.26	lmo2420	unknown
2.26	lmo0562	similar to phosphoribosyl-AMP cyclohydro
2.27	lmo0712	similar to flagellar hook-basal body com
2.28	lmo0963	similar to putative heat shock protein HtpX, Listeria epitope LemB
2.28	lmo1740	similar to amino acid (glutamine) ABC transporter, permease protein
2.28	lmo0916	similar to phosphotransferase system enz
2.29	lmo1407	pyruvate-formate lyase activating enzyme
2.29	lmo0818	similar to cation transporting ATPase
2.30	lmo1507	similar to two-component response regula
2.31	lmo2370	similar to aminotransferase
2.31	lmo0131	conserved hypothetical protein
2.33	lmo2746	conserved hypothetical protein
2.33	lmo2651	similar to mannitol-specific PTS enzyme IIA component
2.34	lmo0720	unknown
2.34	lmo0281	unknown
2.34	lmo0859	similar to putative sugar ABC transporte
2.35	No lmo match?	CfpL belongs to the Listeria-specific group of the CRP/FNR-superfamily
2.35	lmo2646	unknown
2.36	lmo1575	similar to unknown proteins
2.37	lmo2342	similar to 16S pseudouridylate synthase
2.38	lmo2649	similar to hypothetical PTS enzyme IIC component
2.39	lmo2159	similar to oxidoreductase
2.39	lmo0625	unknown
2.39	lmo2666	similar to PTS system galactitol-specifi
2.40	lmo2637	conserved lipoprotein
2.41	lmo0030	conserved hypothetical protein
2.41	lmo1501	similar to unknown proteins
2.42	lmo0486	ribosomal protein L32
2.42	lmo2107	similar to transcriptional regulator (De
2.43	lmo0721	putative fibronectin-binding protein
2.45	lmo2721	similar to glucosamine-6-phosphate isomerase
2.45	lmo1519	aspartyl-tRNA synthetase
2.45	lmo0877	similar to B. subtilis NagB protein (glu
2.45	lmo1349	similar to glycine dehydrogenase (decarboxylating) subunit 1
2.46	lmo0716	similar to H+-transporting ATP synthase
2.46	lmo2388	similar to B. subtilis YwqG protein
2.46	lmo2649	similar to hypothetical PTS enzyme IIC component
2.46	lmo1799	putative peptidoglycan bound protein (LP
2.46	lmo1350	similar to glycine dehydrogenase (decarb
2.47	lmo2418	similar to ABC transporter, permease protein
2.48	lmo2206	similar to endopeptidase Clp ATP-binding
2.49	lmo0180	similar to sugar ABC transporter, permea
2.49	lmo0138	unknown
2.50	lmo0709	unknown
2.50	lmo1799	putative peptidoglycan bound protein (LPXTG motif)
2.50	lmo1244	weakly similar to phosphoglycerate mutase 1
2.51	lmo2650	similar to hypothetical PTS enzyme IIB c
2.53	lmo2581	conserved hypothetical protein
2.53	lmo0983	similar to glutathione peroxidase
2.54	lmo1332	similar to conserved hypothetical proteins
2.54	lmo2392	similar to B. subtilis YuzB protein
2.55	lmo0484	unknown
2.55	lmo2705	conserved hypothetical protein
2.55	lmo1917	similar to pyruvate formate-lyase
2.56	lmo2117	similar to unknown proteins
2.56	lmo1502	similar to unknown proteins
2.58	lmo2159	similar to oxidoreductase
2.59	lmo2257	hypothetical CDS

2.59	lmo0734	similar to transcriptional regulator (La
2.60	lmo1381	unknown
2.61	lmo1244	weakly similar to phosphoglycerate mutase 1
2.62	lmo2418	similar to ABC transporter, permease pro
2.63	lmo2729	similar to unknown proteins
2.63	lmo0391	unknown
2.65	lmo2432	ribosomal small subunit pseudouridine synthase A
2.66	lmo2066	unknown
2.66	lmo1961	similar to oxidoreductases
2.69	lmo1961	similar to oxidoreductases
2.72	lmo1459	similar to glycyl-tRNA synthetase alpha
2.72	lmo1744	similar to unknown proteins
2.73	lmo2210	unknown
2.75	lmo0634	similar to an E. coli putative tagatose
2.75	lmo2792	DNA-binding protein
2.76	lmo1138	similar to ATP-dependent Clp protease pr
2.76	lmo0719	similar to unknown protein
2.76	lmo0261	similar to phospho-beta-glucosidase
2.77	lmo2374	similar to aspartate kinase
2.77	lmo0711	similar to flagellar basal-body rod protein flgC
2.77	lmo2442	unknown
2.77	lmo2817	similar to peptidases
2.77	lmo2819	similar to carboxypeptidase
2.78	lmo2418	similar to ABC transporter, permease protein
2.80	lmo2819	similar to carboxypeptidase
2.80	lmo0278	similar to sugar ABC transporter, ATP-bi
2.80	lmo2417	conserved lipoprotein (putative ABC transporter binding protein)
2.81	lmo0643	similar to putative transaldolase
2.83	lmo1628	highly similar to tryptophan synthase (b
2.85	lmo1459	similar to glycyl-tRNA synthetase alpha chain
2.85	lmo1138	similar to ATP-dependent Clp protease proteolytic component
2.85	lmo2819	similar to carboxypeptidase
2.86	lmo1637	similar to membrane proteins
2.88	lmo1739	similar to amino acid (glutamine) ABC transporter (ATP-binding protein)
2.88	lmo2548	ribosomal protein L31
2.89	lmo0181	similar to sugar ABC transporter, sugar-binding protein
2.90	lmo0383	highly similar to B. subtilis methylmalonate-semialdehyde dehydrogenase IolA
2.94	lmo2660	similar to transketolase
2.95	lmo2419	similar to ABC transporter (ATP-binding
2.95	lmo1636	similar to similar to ABC transporter (A
2.98	lmo0622	hypothetical
3.01	lmo2580	similar to ABC transporter, ATP-binding
3.01	lmo0561	similar to phosphorybosil-AMP-cyclohydro
3.01	lmo0553	unknown
3.03	lmo0919	similar to ABC transporter ATP-binding protein (antibiotic resistance)
3.04	lmo0917	similar to beta-glucosidase
3.04	lmo2156	unknown
3.09	lmo1244	weakly similar to phosphoglycerate mutas
3.10	lmo2417	conserved lipoprotein (putative ABC tran
3.12	lmo0383	highly similar to B. subtilis methylmalonate-semialdehyde dehydrogenase IolA
3.12	lmo2817	similar to peptidases
3.13	lmo0739	similar to 6-phospho-beta-glucosidase
3.15	lmo0181	similar to sugar ABC transporter, sugar-binding protein
3.16	lmo2566/lmo2567	intergenic
3.17	lmo2207	similar to unknown protein
3.22	lmo1298	similar to glutamine synthetase represso
3.24	lmo0180	similar to sugar ABC transporter, permease protein
3.26	lmo2147	similar to unknown proteins
3.27	lmo2659	similar to ribulose-phosphate 3-epimeras
3.27	lmo1257	unknown
3.28	lmo0443	similar to B. subtilis transcription reg

3.31	lmo2818	similar to transmembrane efflux protein
3.32	lmo0181	similar to sugar ABC transporter, sugar-
3.38	lmo2419	similar to ABC transporter (ATP-binding protein)
3.38	lmo0362	similar to conserved hypothetical protei
3.39	lmo2162	similar to unknown proteins
3.39	lmo0392	highly similar to B. subtilis YqfA prote
3.42	lmo1332	similar to conserved hypothetical protei
3.42	lmo0261	similar to phospho-beta-glucosidase
3.42	lmo1406	pyruvate formate-lyase
3.45	lmo0138	unknown
3.47	lmo0536	similar to 6-phospho-beta-glucosidase
3.47	lmo1860	similar to peptidyl methionine sulfoxide
3.47	lmo1636	similar to similar to ABC transporter (ATP-binding protein)
3.54	lmo0361	similar to conserved hypothetical integr
3.55	lmo1960	similar to ferrichrome ABC transporter (ATP-binding protein)
3.55	lmo1859	similar to transcriptional regulator (Pi
3.56	lmo2242	similar to O6-methylguanine-DNA methyltransferase
3.62	lmo2242	similar to O6-methylguanine-DNA methyltr
3.64	lmo1960	similar to ferrichrome ABC transporter (
3.66	lmo0800	similar to B. subtilis YqkB protein
3.66	lmo1637	similar to membrane proteins
3.68	lmo0738	similar to phosphotransferase system (PT
3.72	lmo1630	highly similar to indol-3-glycerol phosphate synthases
3.73	lmo0298	similar to PTS beta-glucoside-specific e
3.73	lmo0623	unknown
3.83	lmo0536	similar to 6-phospho-beta-glucosidase
3.86	lmo1747	similar to ABC transporter (ATP-binding
3.94	lmo1746	similar to ABC transporter (permease)
3.94	lmo1407	PflC, pyruvate-formate lyase activating enzyme
3.99	lmo0737	unknown
4.02	lmo0955	PspA domain, phage-shock protein; represses sigma-54 dependent tx
4.03	lmo1966	halogen_hydrol superfam domain; 5-bromo-4-chloroindolyl phosphate hydrolysis protein
4.03	lmo0393	unknown
4.08	lmo0914	similar to PTS system, IIB component
4.15	lmo1967	similar to toxic ion resistance proteins
4.18	lmo2207	similar to unknown protein
4.23	lmo0393	no conserved domains
4.25	lmo1966	halogen_hydrol superfam domain; 5-bromo-4-chloroindolyl phosphate hydrolysis protein
4.29	lmo2817	similar to peptidases
4.32	lmo1967	similar to toxic ion resistance proteins
4.33	lmo2432	unknown
4.35	lmo0954	unknown
4.41	lmo2385	similar to B. subtilis YuxO protein
4.43	lmo1966	halogen_hydrol superfam domain; 5-bromo-4-chloroindolyl phosphate hydrolysis protein
4.54	lmo0536	similar to 6-phospho-beta-glucosidase
4.59	lmo2261	similar to unknown proteins
4.71	lmo0735	similar to Ribulose-5-Phosphate 3-Epimer
4.73	lmo0485	arsenite oxidase; Nitroreductase-like family which includes NADH oxidase and arsenite oxidiase.
4.87	lmo0301	similar to PTS beta-glucoside-specific e
4.91	lmo0955	PspA domain, phage-shock protein; represses sigma-54 dependent tx
5.13	lmo0485	arsenite oxidase; Nitroreductase-like family which includes NADH oxidase and arsenite oxidiase.
5.18	lmo0300	similar to phospho-beta-glucosidase and
5.23	lmo1630	highly similar to indol-3-glycerol phosp; trpC
5.27	lmo0496	similar to B. subtilis YnzC protein
5.42	lmo2258	unknown; 1TM, coiled coil; no conserved domains
5.51	lmo2258	unknown; 1TM, coiled coil; no conserved domains
5.52	lmo1416	unknown; no subtilis homolog; VanZ-like fold
5.65	lmo1967	similar to toxic ion resistance proteins
5.69	lmo0736	similar to ribose 5-phosphate isomerase

5.70	lmo1631	highly similar to anthranilate phosphori; trpD
5.72	lmo0047	unknown
5.80	lmo0955	PspA domain, phage-shock protein; represses sigma-54 dependent tx
5.93	lmo1629	trpF, phosphoribosyl anthranilate isomerase
6.49	lmo1416	no subtilis homolog; VanZ-like fold
6.68	lmo2186	unknown
6.72	lmo0997	ATP-dependent protease
6.98	lmo0997	clpE; ATP-dependent protease
7.36	lmo1632	highly similar to anthranilate synthase
7.37	lmo2185	unknown; substrate of Sortase B
7.51	lmo1633	TrpE, anthranilate synthase component I; with component II, the glutamine amidotransferase, catalyzes the formation of anthranilate from chorismate and glutamine
8.16	lmo1632	TrpG; with TrpE catalyzes the formation of anthranilate and glutamate from chorismate and glutamine; TrpG provides the glutamine amidotransferase activity
8.86	lmo2487	similar to B. subtilis YvlB protein
9.05	lmo2486	unknown; 1TM, 403aa, coiled coil domain, phage shock protein domain; conserved in E. faecalis
10.52	lmo0485	arsenite oxidase; Nitroreductase-like family which includes NADH oxidase and arsenite oxidiase.
11.08	lmo1007	unknown; 73aa, no TMs or conserved domains
11.71	lmo2567	unknown; 2TM, 66aa
16.42	lmo2567	unknown; 2TM, 66aa
36.28	lmo2568	unknown; 1TM, 107aa, DUF1096; otherwise unique it seems

mRNA from WT and *hpf*::*Himar1* was reverse transcribed, amplified, labeled and hybridized to microarrays for two days. Microarrays contain at least two spots per gene; duplicates were retained to avoid losing differences in regulation between different oligos to the same gene. It should be noted that these microarray data are presented purely for informational purposes, and have not been analyzed for statistical significance.

DISCUSSION

Although ribosomal hibernation has been recognized as a targeted and potentially adaptive behavior in bacteria for more than 20 years, its specific functions remain somewhat unclear. Relatively few biological phenotypes have been associated with hibernation or the inability to hibernate, and none have been associated with hibernation deficiency among bacteria producing a long HPF homolog. Because the bacterial machinery responsible for 100S ribosome formation is highly conserved across many bacterial species and the changes in ribosome configuration in hibernation-deficient bacteria are so striking, the scarcity of obvious phenotypes under standard growth conditions is surprising. It seems likely that the sweeping changes in ribosome complex formation mediated by the hibernation machinery serve a purpose only under specific growth conditions. We reasoned that these conditions might include not only specialized *in vitro* environments, but also the *in vivo* environments occupied by host-associated bacterial pathogens. In addition, we recognized that little is known about the regulation and subcellular functions of long HPFs. For these reasons, we set out to examine the presence, regulation and functional role(s) of hibernation in a relevant human pathogen, *L. monocytogenes*, and to more clearly define the conditions in which the hibernation machinery is expressed and required.

Our first goal was to determine whether ribosomal hibernation occurred in *L. monocytogenes*, and whether the pattern of hibernating ribosomes resembled the patterns already observed in *S. aureus* or *E. coli*. The presence of hibernating ribosomes during exponential growth, as early as four hours after inoculation, more closely resembled the hibernation profile seen in *S. aureus* (Ueta, Wada et al. 2010); several studies have shown that *E. coli* produces essentially no 100S ribosomes until the beginning of stationary phase (Wada, Yamazaki et al. 1990; Yamagishi, Matsushima et al. 1993; Wada, Mikkola et al. 2000). This result was consistent with the only other published hibernation data in an organism producing a long HPF. The presence of large numbers of 100S ribosomes during logarithmic growth suggests that ribosomal hibernation may serve an important purpose even during exponential growth, and that this importance may be common to all long-HPF-producing bacteria (Fig. 3-2). A fundamental difference may exist between bacteria encoding long HPFs and those encoding short HPFs that necessitates additional control over ribosome activity before stationary phase is reached. However, it should be noted that ribosomal hibernation was not apparent during all growth phases in *L. monocytogenes*, as it was in *S. aureus.* Samples isolated two hours after inoculation into fresh media showed little to no 100S ribosome content. Thus, the early stages of *L. monocytogenes* growth in broth appear not to require hibernation.

Ueta et al. speculated that the hibernation behaviors of *S. aureus*, particularly the dropoff in number of 100S ribosomes and the redistribution of saHPF into the 70S pool during post-exponential growth, might correspond to the need for *S. aureus* cells to become coherent and begin expressing virulence factors. Although we did not follow association of HPF with ribosomal complexes over time, our data showed substantially higher association of HPF with 100S than with 70S ribosomes at the transition between logarithmic and stationary phase in *L. monocytogenes*, so any virulence-gene-specific alterations in hibernation at stationary phase may be specific to *S. aureus*. However, the idea that easily dissociated 70S-HPF complexes are responsible for virulence gene expression is intriguing. Further, it is tempting to speculate that

hibernation might serve as a generalized mechanism for preferential translation of only specific messages during times of need or stress. Additional experiments are currently in progress to explore this possibility.

While *rmf* and *hpf* expression and/or translation have both been shown to increase at the entry to stationary phase (Wada, Yamazaki et al. 1990; Maki, Yoshida et al. 2000), it is unclear what specific stimulus causes expression of *hpf* and induction of hibernation during broth growth of *L. monocytogenes*. We observed that the signal stimulating *hpf* transcription during the transition from logarithmic to stationary phase was contained in the growth media, as treatment of mid-log phase bacteria with media conditioned to stationary phase stimulated approximately 100-fold transcriptional upregulation of *hpf* compared to fresh media (Fig. 3-4a). With this in mind, there were three possible changes in the growth media that we believed were most likely to stimulate hibernation. First, it is possible that bacterial conditioning of the media results in accumulation of a bacterial molecule that induces *hpf* transcription. Alternatively, it is possible that bacterial growth depletes the media of some nutrient essential for growth, and that this depletion stimulates hibernation. Lastly, the growth media may change in some other way (such as a shift in pH) that induces *hpf* transcription. Ueta *et al*. showed that the nutrient richness of growth media influenced the extent of ribosome dimerization by *S. aureus*, but did not investigate what components were responsible for induction of hibernation (Ueta, Wada et al. 2010). In addressing these possibilities, we determined that the *hpf* transcription-stimulatory activity was predominantly dependent on glucose depletion; supplementation of conditioned media with glucose restored *hpf* expression to roughly the level seen in fresh media (Fig. 3-4b). Preliminary results also suggest that addition of concentrated conditioned media to fresh media may produce a small difference in transcription, albeit one less important than that induced by glucose supplementation (unpublished results). This suggests that multiple nutritional factors may influence the decision to hibernate.

Stressful conditions in the growth environment also appear to influence *hpf* regulation. We observed ≈10-fold increases in *hpf* expression under NaCl, ethanol, and heat stresses, all of which were ablated in the absence of the stress-responsive sigma factor σ^B (Fig. 3-4c). These observations are in agreement with the published data that σ^B, along with σ^H, is capable of regulating *hpf* expression in *L. monocytogenes* and *B. subtilis* (Drzewiecki, Eymann et al. 1998; Chaturongakul, Raengpradub et al. 2011), and reinforce the possible role for long HPFs in stress tolerance. In contrast with the above expression data, published proteomic analyses of the σ^B regulon in response to various stresses in *L. monocytogenes* have failed to identify HPF as a σ^B-regulated protein (Abram, Starr et al. 2008; Abram, Su et al. 2008; Shin, Kim et al. 2010). In agreement with these results, we observe only a small change in tagged HPF protein level over the course of growth in broth, even during the transition from exponential to stationary phase when a 100-fold increase in transcription occurs (unpublished results). The lack of a direct correspondence between the observed large increase in *hpf* expression and the associated change in HPF protein abundance hints at another layer of post-transcriptional HPF regulation in Gram-positives that has not yet been appreciated.

Despite the striking transcriptional changes discussed above, phenotypic changes caused by HPF deficiency are fairly scarce. One of the few biological phenotypes observed thus far in hibernation-deficient bacteria is the survival defect displayed by RMF mutant bacteria

during growth in nutrient-poor conditions. An *E. coli* RMF mutant displays wild-type viability in culture for approximately two days, then begins to die rapidly and produces 1000-fold fewer CFU after 5 days of incubation (Yamagishi, Matsushima et al. 1993). Similarly, RMF-deficient *P. aeruginosa* deep within biofilms display substantially reduced survival. HPF and YfiA deletions have shown no defects in growth or survival under the same conditions (Williamson, Richards et al. 2012). Despite being completely unable to form 100S ribosomes (similar to an *E. coli* RMF mutant), our *L. monocytogenes* HPF mutant survived post-exponential growth in monoculture comparably to WT. It was only in competitive co-culture that HPF mutant *L. monocytogenes* showed a severe post-exponential survival defect (Fig. 3-5a,b). Because the vast majority of time spent in the environment is likely spent in close association with other bacterial populations, the ability to compete effectively for nutrients is critically important. Finding the cause of this competitive survival defect will provide valuable insight into at least one of the cellular functions of hibernation. The specificity of the *hpf*::*Himar1* competitive defect to autoclave-sterilized media (Fig. 3-5d) suggests that the presence of a toxic compound affects HPF mutant bacteria more strongly than WT. Products of the Maillard reaction, which occurs during heat sterilization of complex media, have been shown to suppress virulence gene expression in *L. monocytogenes* (Sheikh-Zeinoddin, Perehinec et al. 2000), so it is not surprising to observe an additional phenotype that is only revealed in a specific background. The absence of a defect in filtered BHI also argues against the idea that the competitive defect results from a growth defect in *hpf*::*Himar1*. These data, combined with the observation that buffered media slows the appearance of the competitive defect (Fig. 3-5c), lead us to hypothesize that hibernation in *L. monocytogenes* is involved in general stress tolerance during post-exponential growth.

We have demonstrated above the first *in vivo* phenotype for HPF-deficient bacteria: oral infection of mice with a mixture of WT and *hpf*::*Himar1 L. monocytogenes* results in a > 300-fold median defect of *hpf*::*Himar1* in colonization of the MLN. Other tissues tested (liver, spleen, and intestine) each showed ≈10-fold defects in colonization by *hpf*::*Himar1* compared to WT (Fig. 3-6b). To display such a striking defect in the MLN, the HPF mutant strain must either have a defect in reaching the MLN or a defect in growth or survival once there. Research performed in a guinea pig model of infection has shown that there are two main routes of *L. monocytogenes* trafficking to deep tissues. Bacteria can access the hepatic portal vein directly from the intestine, or they can traffic to the MLN through phagocytosis by immune cells sampling the intestinal contents and subsequently spread to deep tissues. Passage from the intestine to the spleen via the MLN appears to present a substantial bottleneck, suggesting that the MLN or some other environment along that pathway is restrictive for *L. monocytogenes* survival (Melton-Witt, Rafelski et al. 2012). One possible explanation of the defect in the MLN is that *hpf*::*Himar1* is especially susceptible to the stress that causes this bottleneck. For instance, a population of immune cells may exist in the MLN that produces reactive oxygen species or antimicrobial peptides that are particularly effective against HPF-deficient *L. monocytogenes*. Alternatively, the lack of HPF might impair passage through the intestinal epithelium, limiting initial colonization of the MLN. Because the number of *hpf*::*Himar1* bacteria in the MLN was actually below the level of detection in some mice, we suggest that a restrictive cell type or milieu between the intestine and the MLN is responsible for the observed defect.

Based on previous bioinformatic analysis, bacteria encoding long HPF homologs do not encode either YfiA or RMF homologs (Ueta, Ohniwa et al. 2008; Ueta, Wada et al. 2010). Since RMF is essential for 100S ribosome formation in *E. coli*, it is unclear how dimerization is accomplished in bacteria that encode long HPF but lack RMF. Ueta *et al.* suggested that perhaps long HPF is a bifunctional protein, and that the ≈90 amino acid C-terminal end of saHPF performs the function that RMF performs in *E. coli*. Homology is quite limited, however, and the overall basicity of RMF (pI=11.3) is not conserved in the C-terminus of saHPF (residues 110-173, calculated pI=3.9). The same is true of *L. monocytogenes* HPF (residues 110-173, calculated pI=4.0). Nonetheless, we sought to investigate the possibility that the two halves of *L. monocytogenes* HPF could be functionally decoupled. We generated tagged and untagged N- and C-terminal truncations of HPF and examined their ability to complement the 100S ribosome phenotype of HPF-deficient *L. monocytogenes*. Unfortunately, neither the N- nor C-terminal fragments rescued ribosome dimerization or post-exponential competition to any significant extent (data not shown). We are currently investigating whether inadequate expression or stability of these fragments may be responsible for the failure to rescue.

We are also interested in the possibility that ribosomal hibernation may be linked to c-di-AMP homeostasis in Gram-positive bacteria. It was recently observed that c-di-AMP is required for optimal growth in rich media, and that c-di-AMP secretion occurs only at the end of exponential growth (Woodward, Iavarone et al. 2010), (J.J. Woodward, unpublished results). In addition, it has been reported that activity of a c-di-AMP-degrading phosphodiesterase in *B. subtilis* is regulated by (p)ppGpp during the stringent response (Rao, See et al. 2010). Combining these observations with the transcriptional data above showing HPF downregulation under conditions favorable for c-di-AMP accumulation, we suggest that hibernation may be one of the responses regulated by c-di-AMP downstream of nutrient sensing. Since (p)ppGpp dependence of RMF expression has also been previously observed (Izutsu, Wada et al. 2001), a link between these two basic bacterial systems seems plausible.

Genome-wide gene expression data may also provide insight into the nature and purpose of ribosomal hibernation. HPF and its homologs were significantly regulated in several published microarrays under a variety of conditions, including σ^B-inducing stress and growth in blood (Toledo-Arana, Dussurget et al. 2009; Chaturongakul, Raengpradub et al. 2011). We carried out whole-genome expression microarray analysis in our HPF-deficient mutant and found that the sets of upregulated and downregulated genes displayed certain functional themes. A large number of ribosomal proteins were transcriptionally regulated, almost all in the downward direction: 24 ribosomal proteins were downregulated, while only two were upregulated. The additional presence of four elongation factors among the downregulated genes strengthens the impression that translation is negatively affected by the absence of HPF. While this behavior initially seems counterintuitive, it may be a transcriptional response to aberrantly high translation. It has been established that bacteria can modulate expression of ribosomal components to bring the overall rate of translation to the desired level, even in the presence of ribosomal mutations that make translation less efficient (Mikkola and Kurland 1991). The absence of HPF during stationary phase likely leads to aberrantly high levels of translation during a time when translational output is normally reduced, causing bacteria to downregulate expression of ribosomal components in response. Based on this explanation, we would predict that overexpression of HPF during logarithmic phase would result in aberrant

overexpression of ribosomal proteins and accessory factors. We are currently in the process of constructing an HPF overexpression vector to test this hypothesis, among others.

The presence of *sigB* and its related regulators in the set of downregulated genes is also thought-provoking. σ^B has been shown to regulate *hpf* expression in both *B. subtilis* and *L. monocytogenes* , but these transcriptional results raise the possibility of a regulatory loop in which HPF, in turn, regulates *sigB*. Several phosphotransferase systems (PTS) were also among the genes up- and downregulated in *hpf*::*Himar1* bacteria. A larger number and array of PTS systems were upregulated, suggesting a net increase in demand for metabolic carbon sources. This observation is in keeping with the data we have presented on glucose-dependent repression of *hpf* expression; bacteria lacking HPF and continuing translation at a high rate during stationary phase are likely to encounter severe carbon limitation.

Despite having been discovered in a screen for altered hemolysis, *hpf*::*Himar1* bacteria did not appear to differentially regulate any genes obviously involved in LLO production or activity. We suspect that the altered hemolytic phenotype of HPF-deficient *L. monocytogenes* results from translational or post-translational changes in LLO regulation that would be difficult to identify by expression microarray analysis. Alternatively, the altered hemolytic activity of *hpf*::*Himar1* may occur indirectly through pathways not specific to LLO regulation.

In summary, we have presented the first observation of ribosomal hibernation in the foodborne pathogen *Listeria monocytogenes*. This is also the first report on the disruption of a long HPF gene and the phenotypic consequences of HPF deficiency in long-HPF-producing bacteria. We showed that HPF is required for production of 100S ribosomes in *L. monocytogenes*, and that the absence of HPF confers competitive disadvantages both *in vitro* and *in vivo*. The *in vivo* defect, a >300-fold median decrease in recoverable *hpf*::*Himar1* CFU from the mesenteric lymph nodes of infected mice, is the first virulence-related phenotype connected to hibernation in the literature. We are excited to continue investigating the role of hibernation in virulence and stress tolerance in *L. monocytogenes*.

MATERIALS AND METHODS

Bacterial Culture Conditions. All culture conditions were as described in the Chapter 2 Materials and Methods, with the following additions. Where use of filtered BHI was specified, BHI powder (Difco, Detroit, MI) was dissolved in MilliQ purified water and sterilized by filtration using 0.22 µm Stericup vacuum filter units (Millipore, Billerica, MA). Sterilized BHI was stored at room temperature. Unless otherwise noted, bacterial cultures used for experiments were started by diluting stationary phase overnight cultures to OD_{600} = 0.02.

Conditioned Media and Stress Treatment Experiments. Conditioned media was generated by inoculating fresh media with WT bacteria as described above and growing at 37°C with shaking for the specified length of time. Bacteria were then removed by centrifugation (10 min @ ≈1700 × g) and filtration (0.22 µm Stericup vacuum filter), and stored at 4°C until use. Conditioned media transcriptional regulation experiments were performed at mid-log phase (OD ≈0.4); bacteria were pelleted and resuspended in conditioned media and incubated for 30 min @ 37°C with shaking before flash freezing and RNA extraction. Stress treatments were also performed at mid-log phase; stress-inducing agents were added to the existing media and bacteria were incubated for 5 min @ 37°C (or 46°C for heat stress treated samples) with shaking before flash freezing and RNA extraction.

Preparation of Crude Ribosomes. Preparation and fractionation of ribosome samples were performed using a protocol adapted from (Ueta, Wada et al. 2010). Cowpea mosaic virus (CPMV) fragments of 68, 95, and 115S were used as sedimentation standards. All buffers were prepared with nuclease-free water and reagent powders. 100 mL cultures of *L. monocytogenes* in BHI were inoculated to an OD_{600} of 0.02 to 0.04 in 500 mL Erlenmeyer flasks and grown at 37°C with shaking until the desired growth phase was reached. Bacteria were harvested by pelleting 10 min @ 3000 × **g** in a tabletop centrifuge, then resuspended in 1.2 mL Ribosome Extraction (RE) buffer (20 mM Tris-HCl pH 7.6, 15 mM Magnesium Acetate, 100 mM Ammonium Acetate, 6 mM 2-mercaptoethanol, 2 mM Phenylmethylsulfonyl Fluoride (PMSF)) per 100 mL of culture. Cell suspensions were transferred to 1.5 mL microcentrifuge tubes along with ≈250 µL of sterile 0.1 mm zirconia/silica beads (BioSpec, Bartlesville, OK) and bacterial cells were disrupted by vortexing 10 min @ 4°C. Bacterial lysates were separated from beads and cell debris was pelleted in a microcentrifuge for 15 min @ 9000 × **g**, 4°C. Supernatants were transferred to separate tubes on ice; pellets were resuspended in 600 µL fresh RE buffer and pelleted again for 15 min @ 9000 × **g**, 4°C. Supernatants from the two spins were combined and layered onto 3 mL pads of 30% sucrose in ribosome fractionation (RF) buffer (20 mM Tris-HCl pH 7.6, 15 mM Magnesium Acetate, 100 mM Ammonium Acetate, 6 mM 2-mercaptoethanol) in 10.4 mL polycarbonate bottles (Beckmann Coulter, Brea, CA). Bottles were very gently filled to the shoulder with RF buffer using a Pipet-Aid and centrifuged in a Type 70.1 Ti rotor (Beckman) in a Beckman XL-70 preparative ultracentrifuge for 2 h @ 65000 RPM (290000 × **g**), 4°C. Supernatants were gently decanted, then pellets were washed with 1 mL RF buffer each and resuspended in 500 µL RF buffer each using a glass pipette. Resuspended crude ribosome (CR) samples were transferred to 1.5 mL microcentrifuge tubes and stored at -20°C until separation on sucrose gradients.

Sucrose Density Gradient Centrifugation. 11 mL, 5-21% sucrose gradients in RF buffer were prepared by progressively layering 21, 17, 13, 9, and 5 percent sucrose-RF buffer solutions

on top of one another in 2.2 mL increments in 12 mL open-top clear ultracentrifuge tubes (Denville Scientific, Metuchen, NJ). Gradients were agitated by gently plunging a sealed glass pipette into each twice, then sealed with parafilm and allowed to equilibrate for 24 to 48 hours at 4°C. CR samples were thawed on ice and nucleic acid content was measured by A_{260}. 150 µg of each sample was diluted to 500 µL total volume in RF buffer and layered gently onto an equilibrated 5-21% gradient. Gradients were centrifuged in an SW41 Ti rotor (Beckman) for 2 h @ 37000 RPM (170000 × g), 4°C in a Beckman XL70 preparative ultracentrifuge. Gradients were analyzed and fractions collected using an ISCO gradient fractionator.

Quantitative Western Blotting. Quantitative Western blots were performed using a LiCor Odyssey scanner (LiCor, Lincoln, NE). Blocking was performed with Odyssey Blocking Buffer (LiCor) mixed 1:1 with PBS (Gibco). Primary staining was performed using either the anti-FLAG M2 antibody (Sigma-Aldrich, St. Louis, MO) at a 1:1000 dilution or the His-Probe (G18) antibody (Santa Cruz Biotechnology, Santa Cruz, CA) at a 1:500 dilution. Secondary staining was performed using IRDye 680 polyclonal goat anti-mouse antibody (LiCor). Blots were analyzed using the LiCor Odyssey scanner.

Broth Competition Assays. Two *L. monocytogenes* strains to be competed with one another were grown separately overnight at 37°C with shaking, then added to 50 mL BHI in a 250 mL Erlenmeyer flask to a final OD_{600} of 0.02 in a 1:1 ratio (as calculated by OD_{600}). OD measurement and plating for CFU were performed immediately, then once every 24 hours thereafter for a period of five to eight days. At each time point, each competitive culture was serially diluted and spread onto LB and LB + erythromycin 1 µg/mL plates. The ratio of (Erm^R CFU) / (Total CFU - Erm^R CFU) was interpreted as the ratio of transposon-carrying bacteria to WT bacteria. Randomly selected colonies were periodically patched from LB plates to LB + Erm 1 µg/mL plates to verify that the above calculation faithfully reflected the number of Erm^R CFU in the culture.

Quantitative RT-PCR. Bacterial RNA was isolated as previously described for microarray analysis (Crimmins, Schelle et al. 2009). DNA contamination was removed using the Turbo DNA*free* kit (Ambion/Life, Carlsbad, CA). Reverse transcription was performed using iScript reverse transcriptase (Bio-Rad, Hercules, CA) and qPCR was performed using SYBR FAST qPCR Master Mix (KAPA Biosystems, Cambridge, MA). Primers to *hpf* (5'-GAAGTAACAGAACCGATTCGAGA-3' and 5'-CTCCACTTGTTTCTTCTGCAC-3') and *bglA* (5'-ATAAGTTGGCATTGCTAGGAC-3' and 5'-ACCTATACCAAGCTGTCCAC-3') were used to detect experimental and control transcripts, respectively. Amplification and detection were performed in an Mx3000P thermal cycler and data were analyzed using the MxPro software (Stratagene, La Jolla, CA).

Competitive Index Assays. Competitive index assays in mice were performed as previously described (Auerbuch, Lenz et al. 2001). Oral infection of mice was accomplished immediately following 16 h of starvation by oral gavage of 200 µL of PBS containing a total of 10^8 *L. monocytogenes* CFU.

LITERATURE CITED

(2011). "Multistate outbreak of listeriosis associated with Jensen Farms cantaloupe--United States, August-September 2011." MMWR Morb Mortal Wkly Rep **60**(39): 1357-1358.

Abram, F., E. Starr, et al. (2008). "Identification of components of the sigma B regulon in Listeria monocytogenes that contribute to acid and salt tolerance." Appl Environ Microbiol **74**(22): 6848-6858.

Abram, F., W. L. Su, et al. (2008). "Proteomic analyses of a Listeria monocytogenes mutant lacking sigmaB identify new components of the sigmaB regulon and highlight a role for sigmaB in the utilization of glycerol." Appl Environ Microbiol **74**(3): 594-604.

Agafonov, D. E., V. A. Kolb, et al. (1999). "A protein residing at the subunit interface of the bacterial ribosome." Proc Natl Acad Sci U S A **96**(22): 12345-12349.

Alouf, J. E. (2001). "Pore-forming bacterial protein toxins: an overview." Curr Top Microbiol Immunol **257**: 1-14.

Apirakaramwong, A., J. Fukuchi, et al. (1998). "Enhancement of cell death due to decrease in Mg2+ uptake by OmpC (cation-selective porin) deficiency in ribosome modulation factor-deficient mutant." Biochem Biophys Res Commun **251**(2): 482-487.

Apirakaramwong, A., K. Kashiwagi, et al. (1999). "Involvement of ppGpp, ribosome modulation factor, and stationary phase-specific sigma factor sigma(S) in the decrease in cell viability caused by spermidine." Biochem Biophys Res Commun **264**(3): 643-647.

Auerbuch, V., L. L. Lenz, et al. (2001). "Development of a competitive index assay to evaluate the virulence of Listeria monocytogenes actA mutants during primary and secondary infection of mice." Infect Immun **69**(9): 5953-5957.

Bishop, D. K. and D. J. Hinrichs (1987). "Adoptive transfer of immunity to Listeria monocytogenes. The influence of in vitro stimulation on lymphocyte subset requirements." J Immunol **139**(6): 2005-2009.

Bubert, A., Z. Sokolovic, et al. (1999). "Differential expression of Listeria monocytogenes virulence genes in mammalian host cells." Mol Gen Genet **261**(2): 323-336.

Bubunenko, M., T. Baker, et al. (2007). "Essentiality of ribosomal and transcription antitermination proteins analyzed by systematic gene replacement in Escherichia coli." J Bacteriol **189**(7): 2844-2853.

Camilli, A., A. Portnoy, et al. (1990). "Insertional mutagenesis of Listeria monocytogenes with a novel Tn917 derivative that allows direct cloning of DNA flanking transposon insertions." J Bacteriol **172**(7): 3738-3744.

Camilli, A., L. G. Tilney, et al. (1993). "Dual roles of plcA in Listeria monocytogenes pathogenesis." Mol Microbiol **8**(8388529): 143-157.

Camilli, A., L. G. Tilney, et al. (1993). "Dual roles of plcA in Listeria monocytogenes pathogenesis." Mol Microbiol **8**(1): 143-157.

Cao, M., A. P. Bitar, et al. (2007). "A mariner-based transposition system for Listeria monocytogenes." Appl Environ Microbiol **73**(8): 2758-2761.

Chakraborty, T., M. Leimeister-Wachter, et al. (1992). "Coordinate regulation of virulence genes in Listeria monocytogenes requires the product of the prfA gene." J Bacteriol **174**(2): 568-574.

Chan, K., C. C. Kim, et al. (2005). "Microarray-based detection of Salmonella enterica serovar Typhimurium transposon mutants that cannot survive in macrophages and mice." Infect Immun **73**(9): 5438-5449.

Chatterjee, S. S., H. Hossain, et al. (2006). "Intracellular gene expression profile of Listeria monocytogenes." Infect Immun **74**(2): 1323-1338.

Chaturongakul, S., S. Raengpradub, et al. (2011). "Transcriptomic and phenotypic analyses identify coregulated, overlapping regulons among PrfA, CtsR, HrcA, and the alternative sigma factors sigmaB, sigmaC, sigmaH, and sigmaL in Listeria monocytogenes." Appl Environ Microbiol **77**(1): 187-200.

Cheng, L. W. and D. A. Portnoy (2003). "Drosophila S2 cells: an alternative infection model for Listeria monocytogenes." Cell Microbiol **5**(12): 875-885.

Clausen, T., C. Southan, et al. (2002). "The HtrA family of proteases: implications for protein composition and cell fate." Mol Cell **10**(3): 443-455.

Cossart, P., M. F. Vicente, et al. (1989). "Listeriolysin O is essential for virulence of Listeria monocytogenes: direct evidence obtained by gene complementation." Infect Immun **57**(11): 3629-3636.

Crimmins, G. T., M. W. Schelle, et al. (2009). "Listeria monocytogenes 6-Phosphogluconolactonase mutants induce increased activation of a host cytosolic surveillance pathway." Infect Immun **77**(7): 3014-3022.

Datta, A. R. and M. H. Kothary (1993). "Effects of glucose, growth temperature, and pH on listeriolysin O production in Listeria monocytogenes." Appl Environ Microbiol **59**(10): 3495-3497.

Decatur, A. L. and D. A. Portnoy (2000). "A PEST-like sequence in listeriolysin O essential for Listeria monocytogenes pathogenicity." Science **290**(11062133): 992-995.

Decatur, A. L. and D. A. Portnoy (2000). "A PEST-like sequence in listeriolysin O essential for Listeria monocytogenes pathogenicity." Science **290**(5493): 992-995.

Doan, T. and S. Aymerich (2003). "Regulation of the central glycolytic genes in Bacillus subtilis: binding of the repressor CggR to its single DNA target sequence is modulated by fructose-1,6-bisphosphate." Mol Microbiol **47**(6): 1709-1721.

Domann, E., J. Wehland, et al. (1992). "A novel bacterial virulence gene in Listeria monocytogenes required for host cell microfilament interaction with homology to the proline-rich region of vinculin." EMBO J **11**(5): 1981-1990.

Donat, S., K. Streker, et al. (2009). "Transcriptome and functional analysis of the eukaryotic-type serine/threonine kinase PknB in Staphylococcus aureus." J Bacteriol **191**(13): 4056-4069.

Drzewiecki, K., C. Eymann, et al. (1998). "The yvyD gene of Bacillus subtilis is under dual control of sigmaB and sigmaH." J Bacteriol **180**(24): 6674-6680.

Echenique, J., A. Kadioglu, et al. (2004). "Protein serine/threonine kinase StkP positively controls virulence and competence in Streptococcus pneumoniae." Infect Immun **72**(15039376): 2434-2437.

Echenique, J., A. Kadioglu, et al. (2004). "Protein serine/threonine kinase StkP positively controls virulence and competence in Streptococcus pneumoniae." Infect Immun **72**(4): 2434-2437.

El-Sharoud, W. M. and G. W. Niven (2007). "The influence of ribosome modulation factor on the survival of stationary-phase Escherichia coli during acid stress." Microbiology **153**(Pt 1): 247-253.

Eymann, C. and M. Hecker (2001). "Induction of sigma(B)-dependent general stress genes by amino acid starvation in a spo0H mutant of Bacillus subtilis." FEMS Microbiol Lett **199**(2): 221-227.

Farber, J. M. and P. I. Peterkin (1991). "Listeria monocytogenes, a food-borne pathogen." Microbiol Rev **55**(3): 476-511.

Fegatella, F., J. Lim, et al. (1998). "Implications of rRNA operon copy number and ribosome content in the marine oligotrophic ultramicrobacterium Sphingomonas sp. strain RB2256." Appl Environ Microbiol **64**(11): 4433-4438.

Fenwick, M. L. (1968). "The effect of ribonuclease on polysomes and ribosomes of bacteria and animal cells." Biochem J **107**(4): 481-489.

Folio, P., P. Chavant, et al. (2004). "Two-dimensional electrophoresis database of Listeria monocytogenes EGDe proteome and proteomic analysis of mid-log and stationary growth phase cells." Proteomics **4**(10): 3187-3201.

Gaidenko, T. A., T.-J. Kim, et al. (2002). "The PrpC serine-threonine phosphatase and PrkC kinase have opposing physiological roles in stationary-phase Bacillus subtilis cells." J Bacteriol **184**(12399479): 6109-6114.

Gaidenko, T. A., T. J. Kim, et al. (2002). "The PrpC serine-threonine phosphatase and PrkC kinase have opposing physiological roles in stationary-phase Bacillus subtilis cells." J Bacteriol **184**(22): 6109-6114.

Gaillard, J. L., P. Berche, et al. (1991). "Entry of L. monocytogenes into cells is mediated by internalin, a repeat protein reminiscent of surface antigens from gram-positive cocci." Cell **65**(7): 1127-1141.

Gaillard, J. L., P. Berche, et al. (1987). "In vitro model of penetration and intracellular growth of Listeria monocytogenes in the human enterocyte-like cell line Caco-2." Infect Immun **55**(11): 2822-2829.

Gaillard, J. L., P. Berche, et al. (1986). "Transposon mutagenesis as a tool to study the role of hemolysin in the virulence of Listeria monocytogenes." Infect Immun **52**(1): 50-55.

Garay-Arroyo, A., J. M. Colmenero-Flores, et al. (2000). "Highly hydrophilic proteins in prokaryotes and eukaryotes are common during conditions of water deficit." J Biol Chem **275**(8): 5668-5674.

Garsin, D. A., J. Urbach, et al. (2004). "Construction of an Enterococcus faecalis Tn917-mediated-gene-disruption library offers insight into Tn917 insertion patterns." J Bacteriol **186**(21): 7280-7289.

Gedde, M. M., D. E. Higgins, et al. (2000). "Role of listeriolysin O in cell-to-cell spread of Listeria monocytogenes." Infect Immun **68**(2): 999-1003.

Gedde, M. M., D. E. Higgins, et al. (2000). "Role of listeriolysin O in cell-to-cell spread of Listeria monocytogenes." Infect Immun **68**(10639481): 999-991003.

Glaser, P., L. Frangeul, et al. (2001). "Comparative genomics of Listeria species." Science **294**(5543): 849-852.

Glomski, I. J., A. L. Decatur, et al. (2003). "Listeria monocytogenes mutants that fail to compartmentalize listerolysin O activity are cytotoxic, avirulent, and unable to evade host extracellular defenses." Infect Immun **71**(14638761): 6754-6765.

Glomski, I. J., A. L. Decatur, et al. (2003). "Listeria monocytogenes mutants that fail to compartmentalize listerolysin O activity are cytotoxic, avirulent, and unable to evade host extracellular defenses." Infect Immun **71**(12): 6754-6765.

Glomski, I. J., M. M. Gedde, et al. (2002). "The Listeria monocytogenes hemolysin has an acidic pH optimum to compartmentalize activity and prevent damage to infected host cells." J Cell Biol **156**(11901168): 1029-1038.

Glomski, I. J., M. M. Gedde, et al. (2002). "The Listeria monocytogenes hemolysin has an acidic pH optimum to compartmentalize activity and prevent damage to infected host cells." J Cell Biol **156**(6): 1029-1038.

Gray, M. J., N. E. Freitag, et al. (2006). "How the bacterial pathogen Listeria monocytogenes mediates the switch from environmental Dr. Jekyll to pathogenic Mr. Hyde." Infect Immun **74**(5): 2505-2512.

Grundling, A., L. S. Burrack, et al. (2004). "Listeria monocytogenes regulates flagellar motility gene expression through MogR, a transcriptional repressor required for virulence." Proc Natl Acad Sci U S A **101**(33): 12318-12323.

Grundling, A., M. D. Gonzalez, et al. (2003). "Requirement of the Listeria monocytogenes broad-range phospholipase PC-PLC during infection of human epithelial cells." J Bacteriol **185**(21): 6295-6307.

Hartl, D. L., A. R. Lohe, et al. (1997). "Modern thoughts on an ancyent marinere: function, evolution, regulation." Annu Rev Genet **31**: 337-358.

Harty, J. T., A. R. Tvinnereim, et al. (2000). "CD8+ T cell effector mechanisms in resistance to infection." Annu Rev Immunol **18**: 275-308.
Ho, S. N., H. D. Hunt, et al. (1989). "Site-directed mutagenesis by overlap extension using the polymerase chain reaction." Gene **77**(1): 51-59.
Hodgson, D. A. (2000). "Generalized transduction of serotype 1/2 and serotype 4b strains of Listeria monocytogenes." Mol Microbiol **35**(2): 312-323.
Hyyrylainen, H. L., A. Bolhuis, et al. (2001). "A novel two-component regulatory system in Bacillus subtilis for the survival of severe secretion stress." Mol Microbiol **41**(5): 1159-1172.
Izutsu, K., A. Wada, et al. (2001). "Expression of ribosome modulation factor (RMF) in Escherichia coli requires ppGpp." Genes Cells **6**(8): 665-676.
Jacobs, M., J. B. Andersen, et al. (1993). "Bacillus subtilis PrsA is required in vivo as an extracytoplasmic chaperone for secretion of active enzymes synthesized either with or without pro-sequences." Mol Microbiol **8**(5): 957-966.
Jain, V., M. Kumar, et al. (2006). "ppGpp: stringent response and survival." J Microbiol **44**(1): 1-10.
Jin, H. and V. Pancholi (2006). "Identification and biochemical characterization of a eukaryotic-type serine/threonine kinase and its cognate phosphatase in Streptococcus pyogenes: their biological functions and substrate identification." J Mol Biol **357**(5): 1351-1372.
Jones, S. and D. A. Portnoy (1994). "Characterization of Listeria monocytogenes pathogenesis in a strain expressing perfringolysin O in place of listeriolysin O." Infect Immun **62**(7960143): 5608-5613.
Jones, S. and D. A. Portnoy (1994). "Characterization of Listeria monocytogenes pathogenesis in a strain expressing perfringolysin O in place of listeriolysin O." Infect Immun **62**(12): 5608-5613.
Jones, S. and D. A. Portnoy (1994). "Small plaque mutants." Methods Enzymol **236**: 526-531.
Joshi, S. M., A. K. Pandey, et al. (2006). "Characterization of mycobacterial virulence genes through genetic interaction mapping." Proc Natl Acad Sci U S A **103**(31): 11760-11765.
Kang, C. M., D. W. Abbott, et al. (2005). "The Mycobacterium tuberculosis serine/threonine kinases PknA and PknB: substrate identification and regulation of cell shape." Genes Dev **19**(14): 1692-1704.
Kathariou, S., P. Metz, et al. (1987). "Tn916-induced mutations in the hemolysin determinant affecting virulence of Listeria monocytogenes." J Bacteriol **169**(3): 1291-1297.
Kato, T., H. Yoshida, et al. (2010). "Structure of the 100S ribosome in the hibernation stage revealed by electron cryomicroscopy." Structure **18**(6): 719-724.
Kocks, C., E. Gouin, et al. (1992). "L. monocytogenes-induced actin assembly requires the actA gene product, a surface protein." Cell **68**(3): 521-531.
Kolter, R., D. A. Siegele, et al. (1993). "The stationary phase of the bacterial life cycle." Annu Rev Microbiol **47**: 855-874.
Kontinen, V. P. and M. Sarvas (1993). "The PrsA lipoprotein is essential for protein secretion in Bacillus subtilis and sets a limit for high-level secretion." Mol Microbiol **8**(4): 727-737.
Kristich, C. J., C. L. Wells, et al. (2007). "A eukaryotic-type Ser/Thr kinase in Enterococcus faecalis mediates antimicrobial resistance and intestinal persistence." Proc Natl Acad Sci U S A **104**(9): 3508-3513.
Lampe, D. J., B. J. Akerley, et al. (1999). "Hyperactive transposase mutants of the Himar1 mariner transposon." Proc Natl Acad Sci U S A **96**(20): 11428-11433.
Lampe, D. J., M. E. Churchill, et al. (1996). "A purified mariner transposase is sufficient to mediate transposition in vitro." Embo J **15**(19): 5470-5479.
Larsson, J. T., A. Rogstam, et al. (2007). "YjbH is a novel negative effector of the disulphide stress regulator, Spx, in Bacillus subtilis." Mol Microbiol **66**(3): 669-684.
Lauer, P., M. Y. Chow, et al. (2002). "Construction, characterization, and use of two Listeria monocytogenes site-specific phage integration vectors." J Bacteriol **184**(15): 4177-4186.

Lawley, T. D., K. Chan, et al. (2006). "Genome-wide screen for Salmonella genes required for long-term systemic infection of the mouse." PLoS Pathog **2**(2): e11.
Leimeister-Wachter, M., W. Goebel, et al. (1989). "Mutations affecting hemolysin production in Listeria monocytogenes located outside the listeriolysin gene." FEMS Microbiol Lett **53**(1-2): 23-29.
Lety, M. A., C. Frehel, et al. (2002). "Critical role of the N-terminal residues of listeriolysin O in phagosomal escape and virulence of Listeria monocytogenes." Mol Microbiol **46**(2): 367-379.
Lety, M. A., C. Frehel, et al. (2001). "Identification of a PEST-like motif in listeriolysin O required for phagosomal escape and for virulence in Listeria monocytogenes." Mol Microbiol **39**(5): 1124-1139.
Lou Y, Y. A., Ed. (1999). Characteristics of *Listeria monocytogenes* important to food processors. Listeria, listeriosis, and food safety. New York, NY, Marcel Dekker Inc.
Ludwig, H., G. Homuth, et al. (2001). "Transcription of glycolytic genes and operons in Bacillus subtilis: evidence for the presence of multiple levels of control of the gapA operon." Mol Microbiol **41**(2): 409-422.
Mackaness, G. B. (1962). "Cellular resistance to infection." J Exp Med **116**: 381-406.
Mackaness, G. B. (1969). "The influence of immunologically committed lymphoid cells on macrophage activity in vivo." J Exp Med **129**(5): 973-992.
Madec, E., A. Laszkiewicz, et al. (2002). "Characterization of a membrane-linked Ser/Thr protein kinase in Bacillus subtilis, implicated in developmental processes." Mol Microbiol **46**(12406230): 571-586.
Madec, E., A. Laszkiewicz, et al. (2002). "Characterization of a membrane-linked Ser/Thr protein kinase in Bacillus subtilis, implicated in developmental processes." Mol Microbiol **46**(2): 571-586.
Maki, Y., H. Yoshida, et al. (2000). "Two proteins, YfiA and YhbH, associated with resting ribosomes in stationary phase Escherichia coli." Genes Cells **5**(12): 965-974.
Mandin, P., H. Fsihi, et al. (2005). "VirR, a response regulator critical for Listeria monocytogenes virulence." Mol Microbiol **57**(5): 1367-1380.
Marles-Wright, J. and R. J. Lewis (2007). "Stress responses of bacteria." Curr Opin Struct Biol **17**(6): 755-760.
Marquis, H., V. Doshi, et al. (1995). "The broad-range phospholipase C and a metalloprotease mediate listeriolysin O-independent escape of Listeria monocytogenes from a primary vacuole in human epithelial cells." Infect Immun **63**(11): 4531-4534.
Martin, P. and R. A. Macleod (1984). "Observations on the distinction between oligotrophic and eutrophic marine bacteria." Appl Environ Microbiol **47**(5): 1017-1022.
McLauchlin, J. (1990). "Human listeriosis in Britain, 1967-85, a summary of 722 cases. 1. Listeriosis during pregnancy and in the newborn." Epidemiol Infect **104**(2): 181-189.
McLauchlin, J. (1990). "Human listeriosis in Britain, 1967-85, a summary of 722 cases. 2. Listeriosis in non-pregnant individuals, a changing pattern of infection and seasonal incidence." Epidemiol Infect **104**(2): 191-201.
Mechold, U., G. Fang, et al. (2007). "YtqI from Bacillus subtilis has both oligoribonuclease and pAp-phosphatase activity." Nucleic Acids Res **35**(13): 4552-4561.
Melton-Witt, J. A., S. M. Rafelski, et al. (2012). "Oral infection with signature-tagged Listeria monocytogenes reveals organ-specific growth and dissemination routes in guinea pigs." Infect Immun **80**(2): 720-732.
Miki, K. and G. B. Mackaness (1964). "The Passive Transfer of Acquired Resistance to Listeria Monocytogenes." J Exp Med **120**: 93-103.
Mikkola, R. and C. G. Kurland (1991). "Evidence for demand-regulation of ribosome accumulation in E coli." Biochimie **73**(12): 1551-1556.

Milohanic, E., P. Glaser, et al. (2003). "Transcriptome analysis of Listeria monocytogenes identifies three groups of genes differently regulated by PrfA." Mol Microbiol **47**(6): 1613-1625.
Nakano, S., E. Kuster-Schock, et al. (2003). "Spx-dependent global transcriptional control is induced by thiol-specific oxidative stress in Bacillus subtilis." Proc Natl Acad Sci U S A **100**(23): 13603-13608.
Niven, G. W. (2004). "Ribosome modulation factor protects Escherichia coli during heat stress, but this may not be dependent on ribosome dimerisation." Arch Microbiol **182**(1): 60-66.
North, R. J. (1970). "The relative importance of blood monocytes and fixed macrophages to the expression of cell-mediated immunity to infection." J Exp Med **132**(3): 521-534.
North, R. J. (1978). "The concept of the activated macrophage." J Immunol **121**(3): 806-809.
Okada, Y., S. Makino, et al. (2002). "Cloning of rel from Listeria monocytogenes as an osmotolerance involvement gene." Appl Environ Microbiol **68**(4): 1541-1547.
Park, S. F. and G. S. Stewart (1990). "High-efficiency transformation of Listeria monocytogenes by electroporation of penicillin-treated cells." Gene **94**(1): 129-132.
Pinner, R. W., A. Schuchat, et al. (1992). "Role of foods in sporadic listeriosis. II. Microbiologic and epidemiologic investigation. The Listeria Study Group." JAMA **267**(15): 2046-2050.
Plasterk, R. H., Z. Izsvak, et al. (1999). "Resident aliens: the Tc1/mariner superfamily of transposable elements." Trends Genet **15**(8): 326-332.
Poncet, S., E. Milohanic, et al. (2009). "Correlations between carbon metabolism and virulence in bacteria." Contrib Microbiol **16**: 88-102.
Port, G. C. and N. E. Freitag (2007). "Identification of novel Listeria monocytogenes secreted virulence factors following mutational activation of the central virulence regulator, PrfA." Infect Immun **75**(12): 5886-5897.
Portnoy, D. A., P. S. Jacks, et al. (1988). "Role of hemolysin for the intracellular growth of Listeria monocytogenes." J Exp Med **167**(4): 1459-1471.
Portnoy, D. A., P. S. Jacks, et al. (1988). "Role of hemolysin for the intracellular growth of Listeria monocytogenes." J Exp Med **167**(2833557): 1459-1471.
Provoda, C. J. and K. D. Lee (2000). "Bacterial pore-forming hemolysins and their use in the cytosolic delivery of macromolecules." Adv Drug Deliv Rev **41**(2): 209-221.
Quisel, J. D., W. F. Burkholder, et al. (2001). "In vivo effects of sporulation kinases on mutant Spo0A proteins in Bacillus subtilis." J Bacteriol **183**(22): 6573-6578.
Rajagopal, L., A. Clancy, et al. (2003). "A eukaryotic type serine/threonine kinase and phosphatase in Streptococcus agalactiae reversibly phosphorylate an inorganic pyrophosphatase and affect growth, cell segregation, and virulence." J Biol Chem **278**(16): 14429-14441.
Rajagopal, L., A. Clancy, et al. (2003). "A eukaryotic type serine/threonine kinase and phosphatase in Streptococcus agalactiae reversibly phosphorylate an inorganic pyrophosphatase and affect growth, cell segregation, and virulence." J Biol Chem **278**(12562757): 14429-14441.
Rao, F., R. Y. See, et al. (2010). "YybT is a signaling protein that contains a cyclic dinucleotide phosphodiesterase domain and a GGDEF domain with ATPase activity." J Biol Chem **285**(1): 473-482.
Ripio, M. T., K. Brehm, et al. (1997). "Glucose-1-phosphate utilization by Listeria monocytogenes is PrfA dependent and coordinately expressed with virulence factors." J Bacteriol **179**(22): 7174-7180.
Ripio, M. T., K. Brehm, et al. (1997). "Glucose-1-phosphate utilization by Listeria monocytogenes is PrfA dependent and coordinately expressed with virulence factors." J Bacteriol **179**(9371468): 7174-7180.
Robertson, H. M. and D. J. Lampe (1995). "Recent horizontal transfer of a mariner transposable element among and between Diptera and Neuroptera." Mol Biol Evol **12**(5): 850-862.
Rogstam, A., J. T. Larsson, et al. (2007). "Mechanisms of adaptation to nitrosative stress in Bacillus subtilis." J Bacteriol **189**(8): 3063-3071.

Rubin, E. J., B. J. Akerley, et al. (1999). "In vivo transposition of mariner-based elements in enteric bacteria and mycobacteria." Proc Natl Acad Sci U S A **96**(4): 1645-1650.
Samuel Raj, V., C. Full, et al. (2002). "Decrease in cell viability in an RMF, sigma(38), and OmpC triple mutant of Escherichia coli." Biochem Biophys Res Commun **299**(2): 252-257.
Sarvas, M., C. R. Harwood, et al. (2004). "Post-translocational folding of secretory proteins in Gram-positive bacteria." Biochim Biophys Acta **1694**(1-3): 311-327.
Saskova, L., L. Novakova, et al. (2007). "Eukaryotic-type serine/threonine protein kinase StkP is a global regulator of gene expression in Streptococcus pneumoniae." J Bacteriol **189**(11): 4168-4179.
Sassetti, C. M., D. H. Boyd, et al. (2001). "Comprehensive identification of conditionally essential genes in mycobacteria." Proc Natl Acad Sci U S A **98**(22): 12712-12717.
Sassetti, C. M., D. H. Boyd, et al. (2003). "Genes required for mycobacterial growth defined by high density mutagenesis." Mol Microbiol **48**(1): 77-84.
Schmid, F. X. (2001). "Prolyl isomerases." Adv Protein Chem **59**: 243-282.
Schmid, F. X., L. M. Mayr, et al. (1993). "Prolyl isomerases: role in protein folding." Adv Protein Chem **44**: 25-66.
Schnupf, P., J. Hofmann, et al. (2006). "Regulated translation of listeriolysin O controls virulence of Listeria monocytogenes." Mol Microbiol **61**(4): 999-1012.
Schnupf, P., J. Hofmann, et al. (2006). "Regulated translation of listeriolysin O controls virulence of Listeria monocytogenes." Mol Microbiol **61**(16859495): 999-991012.
Schnupf, P. and D. A. Portnoy (2007). "Listeriolysin O: a phagosome-specific lysin." Microbes Infect **9**(10): 1176-1187.
Schnupf, P. and D. A. Portnoy (2007). "Listeriolysin O: a phagosome-specific lysin." Microbes Infect **9**(17720603): 1176-1187.
Schnupf, P., D. A. Portnoy, et al. (2006). "Phosphorylation, ubiquitination and degradation of listeriolysin O in mammalian cells: role of the PEST-like sequence." Cell Microbiol **8**(2): 353-364.
Schnupf, P., D. A. Portnoy, et al. (2006). "Phosphorylation, ubiquitination and degradation of listeriolysin O in mammalian cells: role of the PEST-like sequence." Cell Microbiol **8**(16441444): 353-364.
Schuchat, A., B. Swaminathan, et al. (1991). "Epidemiology of human listeriosis." Clin Microbiol Rev **4**(2): 169-183.
Schuerch, D. W., E. M. Wilson-Kubalek, et al. (2005). "Molecular basis of listeriolysin O pH dependence." Proc Natl Acad Sci U S A **102**(35): 12537-12542.
Scortti, M., H. J. Monzo, et al. (2007). "The PrfA virulence regulon." Microbes Infect **9**(10): 1196-1207.
Shah, I. M. and J. Dworkin (2010). "Induction and regulation of a secreted peptidoglycan hydrolase by a membrane Ser/Thr kinase that detects muropeptides." Mol Microbiol **75**(5): 1232-1243.
Shah, I. M., M.-H. Laaberki, et al. (2008). "A eukaryotic-like Ser/Thr kinase signals bacteria to exit dormancy in response to peptidoglycan fragments." Cell **135**(18984160): 486-496.
Shah, I. M., M. H. Laaberki, et al. (2008). "A eukaryotic-like Ser/Thr kinase signals bacteria to exit dormancy in response to peptidoglycan fragments." Cell **135**(3): 486-496.
Sheikh-Zeinoddin, M., T. M. Perehinec, et al. (2000). "Maillard reaction causes suppression of virulence gene expression in Listeria monocytogenes." Int J Food Microbiol **61**(1): 41-49.
Shen, A. and D. E. Higgins (2005). "The 5' untranslated region-mediated enhancement of intracellular listeriolysin O production is required for Listeria monocytogenes pathogenicity." Mol Microbiol **57**(16102013): 1460-1473.
Shen, A. and D. E. Higgins (2005). "The 5' untranslated region-mediated enhancement of intracellular listeriolysin O production is required for Listeria monocytogenes pathogenicity." Mol Microbiol **57**(5): 1460-1473.
Shin, J. H., J. Kim, et al. (2010). "sigmaB-dependent protein induction in Listeria monocytogenes during vancomycin stress." FEMS Microbiol Lett **308**(1): 94-100.

Skalka, B., J. Smola, et al. (1982). "Routine test for in vitro differentiation of pathogenic and apathogenic Listeria monocytogenes strains." J Clin Microbiol **15**(3): 503-507.
Smith, G. A., H. Marquis, et al. (1995). "The two distinct phospholipases C of Listeria monocytogenes have overlapping roles in escape from a vacuole and cell-to-cell spread." Infect Immun **63**(11): 4231-4237.
Smith, K. and P. Youngman (1992). "Use of a new integrational vector to investigate compartment-specific expression of the Bacillus subtilis spoIIM gene." Biochimie **74**(1391050): 705-711.
Smith, K. and P. Youngman (1992). "Use of a new integrational vector to investigate compartment-specific expression of the Bacillus subtilis spoIIM gene." Biochimie **74**(7-8): 705-711.
Smyth, C. J. and J. L. Duncan (1978). Thiol-activated (oxygen-labile cytolysins). Bacterial Toxins and Cell Membranes. J. Jelaszewicz and T. Wadström. New York, Academic Press, Inc.**:** 129-183.
Squeglia, F., R. Marchetti, et al. (2011). "Chemical basis of peptidoglycan discrimination by PrkC, a key kinase involved in bacterial resuscitation from dormancy." J Am Chem Soc **133**(51): 20676-20679.
Stack, H. M., R. D. Sleator, et al. (2005). "Role for HtrA in stress induction and virulence potential in Listeria monocytogenes." Appl Environ Microbiol **71**(8): 4241-4247.
Sun, A. N., A. Camilli, et al. (1990). "Isolation of Listeria monocytogenes small-plaque mutants defective for intracellular growth and cell-to-cell spread." Infect Immun **58**(2172168): 3770-3778.
Sun, A. N., A. Camilli, et al. (1990). "Isolation of Listeria monocytogenes small-plaque mutants defective for intracellular growth and cell-to-cell spread." Infect Immun **58**(11): 3770-3778.
Suzuki, H. and W. W. Kilgore (1967). "Decomposition of ribosomal particles in Escherichia coli treated with mitomycin C." J Bacteriol **94**(3): 666-676.
Tavazoie, S. and G. M. Church (1998). "Quantitative whole-genome analysis of DNA-protein interactions by in vivo methylase protection in E. coli." Nat Biotechnol **16**(6): 566-571.
Thedieck, K., T. Hain, et al. (2006). "The MprF protein is required for lysinylation of phospholipids in listerial membranes and confers resistance to cationic antimicrobial peptides (CAMPs) on Listeria monocytogenes." Mol Microbiol **62**(5): 1325-1339.
Tilney, L. G. and D. A. Portnoy (1989). "Actin filaments and the growth, movement, and spread of the intracellular bacterial parasite, Listeria monocytogenes." J Cell Biol **109**(4 Pt 1): 1597-1608.
Tjalsma, H., A. Bolhuis, et al. (2000). "Signal peptide-dependent protein transport in Bacillus subtilis: a genome-based survey of the secretome." Microbiol Mol Biol Rev **64**(3): 515-547.
Toledo-Arana, A., O. Dussurget, et al. (2009). "The Listeria transcriptional landscape from saprophytism to virulence." Nature **459**(7249): 950-956.
Tweten, R. K. (2005). "Cholesterol-dependent cytolysins, a family of versatile pore-forming toxins." Infect Immun **73**(10): 6199-6209.
Ueta, M., R. L. Ohniwa, et al. (2008). "Role of HPF (hibernation promoting factor) in translational activity in Escherichia coli." J Biochem **143**(3): 425-433.
Ueta, M., C. Wada, et al. (2010). "Formation of 100S ribosomes in Staphylococcus aureus by the hibernation promoting factor homolog SaHPF." Genes Cells **15**(1): 43-58.
Ueta, M., H. Yoshida, et al. (2005). "Ribosome binding proteins YhbH and YfiA have opposite functions during 100S formation in the stationary phase of Escherichia coli." Genes Cells **10**(12): 1103-1112.
Vazquez-Boland, J. A., C. Kocks, et al. (1992). "Nucleotide sequence of the lecithinase operon of Listeria monocytogenes and possible role of lecithinase in cell-to-cell spread." Infect Immun **60**(1): 219-230.
Vazquez-Boland, J. A., C. Kocks, et al. (1992). "Nucleotide sequence of the lecithinase operon of Listeria monocytogenes and possible role of lecithinase in cell-to-cell spread." Infect Immun **60**(1309513): 219-230.

Vazquez-Boland, J. A., M. Kuhn, et al. (2001). "Listeria pathogenesis and molecular virulence determinants." Clin Microbiol Rev **14**(11432815): 584-640.
Vazquez-Boland, J. A., M. Kuhn, et al. (2001). "Listeria pathogenesis and molecular virulence determinants." Clin Microbiol Rev **14**(3): 584-640.
Vila-Sanjurjo, A., B. S. Schuwirth, et al. (2004). "Structural basis for the control of translation initiation during stress." Nat Struct Mol Biol **11**(11): 1054-1059.
Wada, A., K. Igarashi, et al. (1995). "Ribosome modulation factor: stationary growth phase-specific inhibitor of ribosome functions from Escherichia coli." Biochem Biophys Res Commun **214**(2): 410-417.
Wada, A., R. Mikkola, et al. (2000). "Growth phase-coupled changes of the ribosome profile in natural isolates and laboratory strains of Escherichia coli." J Bacteriol **182**(10): 2893-2899.
Wada, A., Y. Yamazaki, et al. (1990). "Structure and probable genetic location of a "ribosome modulation factor" associated with 100S ribosomes in stationary-phase Escherichia coli cells." Proc Natl Acad Sci U S A **87**(7): 2657-2661.
Way, S. S., L. J. Thompson, et al. (2004). "Characterization of flagellin expression and its role in Listeria monocytogenes infection and immunity." Cell Microbiol **6**(3): 235-242.
Weiss, D. S., A. Brotcke, et al. (2007). "In vivo negative selection screen identifies genes required for Francisella virulence." Proc Natl Acad Sci U S A **104**(14): 6037-6042.
Westers, H., L. Westers, et al. (2006). "The CssRS two-component regulatory system controls a general secretion stress response in Bacillus subtilis." Febs J **273**(16): 3816-3827.
Whitman, W. B., D. C. Coleman, et al. (1998). "Prokaryotes: the unseen majority." Proc Natl Acad Sci U S A **95**(12): 6578-6583.
Williamson, K. S., L. A. Richards, et al. (2012). "Heterogeneity in Pseudomonas aeruginosa biofilms includes expression of ribosome hibernation factors in the antibiotic tolerant subpopulation and hypoxia induced stress response in the metabolically active population." J Bacteriol.
Wilson, D. N. and K. H. Nierhaus (2007). "The weird and wonderful world of bacterial ribosome regulation." Crit Rev Biochem Mol Biol **42**(3): 187-219.
Wilson, R. L., L. L. Brown, et al. (2006). "Listeria monocytogenes 10403S HtrA is necessary for resistance to cellular stress and virulence." Infect Immun **74**(1): 765-768.
Wonderling, L. D. and D. O. Bayles (2004). "Survival of Listeria monocytogenes strain H7762 and resistance to simulated gastric fluid following exposure to frankfurter exudate." J Food Prot **67**(6): 1170-1176.
Woodward, J. J., A. T. Iavarone, et al. (2010). "c-di-AMP secreted by intracellular Listeria monocytogenes activates a host type I interferon response." Science **328**(5986): 1703-1705.
Woodward, J. J., N. I. Martin, et al. (2007). "An Escherichia coli expression-based method for heme substitution." Nat Methods **4**(1): 43-45.
Yamagishi, M., H. Matsushima, et al. (1993). "Regulation of the Escherichia coli rmf gene encoding the ribosome modulation factor: growth phase- and growth rate-dependent control." EMBO J **12**(2): 625-630.
Yeung, P. S., N. Zagorski, et al. (2005). "The metalloprotease of Listeria monocytogenes controls cell wall translocation of the broad-range phospholipase C." J Bacteriol **187**(8): 2601-2608.
Yoshida, H., Y. Maki, et al. (2002). "The ribosome modulation factor (RMF) binding site on the 100S ribosome of Escherichia coli." J Biochem **132**(6): 983-989.
Yoshida, H., H. Yamamoto, et al. (2004). "RMF inactivates ribosomes by covering the peptidyl transferase centre and entrance of peptide exit tunnel." Genes Cells **9**(4): 271-278.
Zemansky, J. (2009). Development of a *mariner* based transposon and identification of *Listeria monocytogenes* determinants, including the peptidyl-prolyl isomerase PrsA2, that contribute ot

its hemolytic phenotype. Molecular and Cell Biology. Berkeley, CA, University of California, Berkeley. **Ph.D.**

Zemansky, J., B. C. Kline, et al. (2009). "Development of a mariner-based transposon and identification of Listeria monocytogenes determinants, including the peptidyl-prolyl isomerase PrsA2, that contribute to its hemolytic phenotype." J Bacteriol **191**(12): 3950-3964.

Zhang, R., H. Y. Ou, et al. (2004). "DEG: a database of essential genes." Nucleic Acids Res **32**(Database issue): D271-272.